Aus dem Zentrum für Innere Medizin der Universität zu Köln
Klinik und Poliklinik für Innere Medizin I
Direktor: Universitätsprofessor Dr. med. M. Hallek

Patterns of micro-RNAs, their target pathways, and non-canonical functions of miR regulating proteins in T-prolymphocytic leukemia

Inaugural-Dissertation zur Erlangung der Doktorwürde
der Medizinischen Fakultät
der Universität zu Köln

vorgelegt von
Till Jonas Braun
aus Kempen

promoviert am 26. April 2023

Gedruckt mit Genehmigung der Medizinischen Fakultät der Universität zu Köln
Druckjahr 2023

Dekanin/Dekan: Universitätsprofessor Dr. med. G. R. Fink

1. Gutachterin oder Gutachter: Privatdozent Dr. med. M. Herling
2. Gutachterin oder Gutachter: Universitätsprofessor Dr. med. Dr. nat. med. R. T. Ullrich

Erklärung

Ich erkläre hiermit, dass ich die vorliegende Dissertationsschrift ohne unzulässige Hilfe Dritter und ohne Benutzung anderer als der angegebenen Hilfsmittel angefertigt habe; die aus fremden Quellen direkt oder indirekt übernommenen Gedanken sind als solche kenntlich gemacht.

Bei der Auswahl und Auswertung des Materials sowie bei der Herstellung des Manuskriptes habe ich keine Unterstützungsleistungen erhalten.

Weitere Personen waren an der Erstellung der vorliegenden Arbeit nicht beteiligt. Insbesondere habe ich nicht die Hilfe einer Promotionsberaterin/eines Promotionsberaters in Anspruch genommen. Dritte haben von mir weder unmittelbar noch mittelbar geldwerte Leistungen für Arbeiten erhalten, die im Zusammenhang mit dem Inhalt der vorgelegten Dissertationsschrift stehen.

Die Dissertationsschrift wurde von mir bisher weder im Inland noch im Ausland in gleicher oder ähnlicher Form einer anderen Prüfungsbehörde vorgelegt.

In den für diese kumulative Promotionen zugrundeliegenden Publikationen[1,2] wurde die wesentliche Arbeit zur Fertigstellung der beiden Manuskripte durch mich geleistet. Insbesondere die konzeptionelle Gestaltung, die Projektkoordination, die inhaltlichen Datenanalysen und die Manuskripterstellung wurden von mir unter Betreuung von Frau Dr. Alexandra Schrader, Herrn Prof. Dr. Stefan Hüttelmaier und Herrn PD Dr. Marco Herling eigenständig durchgeführt. Herr Prof. Dr. Hallek sorgte für die Bereitstellung der räumlichen sowie strukturellen Ressourcen, die diese Promotion ermöglichten.

Der Beitrag der Koautoren umfasste mRNA/miR-Sequenzierungsanalysen als Teil einer bezahlten Dienstleistung von Herrn Marek Franitza und Frau Dr. Janine Altmüller an der hiesigen Core Facility. Unterstützung bei der IT-Datenverarbeitung wurde von Herr Dr. Markus Glass und Herr Linus Wahnschaffe geleistet. Die abschließenden Datenanalysen und Visualisierungen wurden von mir durchgeführt.

Herr Linus Wahnschaffe war für das klinische Datenmanagement und die Datenerfassung zuständig. Klinische Korrelationen, die auf der Grundlage der erfassten Datensätze ausgewertet wurden, wurden von mir berechnet.

Die in den Manuskripten gezeigten *in-vitro* Experimente wurden weitgehend unabhängig von mir durchgeführt, mit einer Ausnahme, nämlich den immunhistochemischen Studien, die von Dr. Nadine Bley an der Martin-Luther Universität Halle/Wittenberg durchgeführt wurden. In der Arbeitsgruppe von PD Dr. Marco Herling wurden die Experimente von Herrn Dr. Sebastian Oberbeck, Frau Johanna Stachelscheid, Frau Petra Mayer, Herrn Dr. Tony Müller und Herrn Moritz Otte technisch angeleitet und unterstützt.

Frau Katharina Ommer und Frau Prof. Birgit Gathof (UKK, Institut für Transfusionsmedizin) halfen mit der Bereitstellung von Proben gesunder Spender. Die weitere experimentelle Bearbeitung dieser Proben wurde von Till Braun durchgeführt.

Die *in-silico* Modellierung der AGO2-ZAP70 Interaktionen wurde von Dr. Daniel Auguin (FRA) in enger Abstimmung mit mir durchgeführt.

Die Verfassung der ersten Manuskript-Version, der Revisions-Schrift sowie des finalen Manuskriptes erfolgte durch mich.

Erklärung zur guten wissenschaftlichen Praxis:

Ich erkläre hiermit, dass ich die Ordnung zur Sicherung guter wissenschaftlicher Praxis und zum Umgang mit wissenschaftlichem Fehlverhalten (Amtliche Mitteilung der Universität zu Köln AM 132/2020) der Universität zu Köln gelesen habe und verpflichte mich hiermit, die dort genannten Vorgaben bei allen wissenschaftlichen Tätigkeiten zu beachten und umzusetzen.

Köln, den 15. August 2022

Unterschrift: 

Till Jonas Braun

Danksagung

An diesem Punkt möchte ich gerne meinen größten Dank an Herrn PD Dr. Marco Herling ausdrücken, der mir die Möglichkeit gegeben hat, in seinem Labor für Lymphozytäres Signaling und Onkoproteom zu promovieren. Danke für all die Unterstützung, das Öffnen so vieler Türen und die zahlreichen Möglichkeiten, an spannenden wissenschaftlichen Projekten mitzuwirken.

Ebenso geht mein Dank an Herrn Prof. Dr. Michael Hallek für seine Unterstützung sowie die Ressourcen, die er als Kliniksdirektor für dieses Projekt zur Verfügung gestellt hat.

Besonders bedanken möchte ich mich bei Frau Dr. Alexandra Schrader für ihre großartige Supervision, ihren unbändigen Optimismus sowie die zahlreichen, unschätzbaren Diskussionen. Ich habe so vieles lernen dürfen.

Danke an all meine Kolleginnen und Kollegen für die so freundschaftliche Atmosphäre. Die Arbeit mit Euch hat unfassbar viel Freude bereitet. Ein besonderes Danke geht an Herrn Dr. Sebastian Oberbeck für die Geduld, aber auch den Spaß beim Anlernen neuer Methodiken.

Mein tiefster Dank geht auch an meine Eltern, meine Schwester Clara, sowie meinen Schwager Jan. Ohne Eure Unterstützung, Euer Verständnis, aber auch Euer Interesse wäre diese Promotion nicht möglich gewesen. Ein großes Danke möchte ich auch an meine Freunde ausrichten. Danke für Eure Unterstützung und danke für Eure Ablenkung in den richtigen Situationen.

Table of contents

List of abbreviations

AGO2	argonaute RISC catalytic component 2
AKT	protein kinase B
ATM	ataxia telangiectasia mutated
BCL2	B-cell lymphoma 2
BCR	B-cell receptor
C. elegans	Caenorhabditis elegans
CAR	chimeric antigen receptor
CDK	cyclin-dependent kinas
CHOP	cyclophosphamide, vincristine, doxuribucin, prednisone
chr	chromosome
CLL	chronic lymphocytic leukemia
CNA	copy number alteration
CTLA4	cytotoxic T-lymphocyte-associated protein 4
DANN	desoxyribonucleic acid
del	deleted
DGCR8	DiGeorge critical region 8
DLBCL	diffuse large B-cell lymphoma
dn	double-negative
dp	double-positive
dsRBP	double-stranded RNA-binding protein
EGFR	epidermal growth factor receptor
EMA	European Medicines Agency
ERK	extracellular-signal regulated kinase
EZH2	enhancer of zeste homolog 2
FDA	Food and Drug Administration
FISH	fluorescence in situ hybridization
GEP	gene expression profiles
GRB2	growth factor receptor-bound protein 2
inv	inversion
ITAM	immunoreceptor tyrosine-based activation motifs
ITK2	interleukine-2-inducible T-cell k
JAK1	janus kinase 1
JAK3	janus kinase 3
KMT	lysine methyltransferase
KRAS	Kirsten rat sarcoma virus
LAT	linker for activation of T-cells
LATS	large tumor suppressor kinase
LCK	lymphocyte-specific protein tyrosine kinase
MAPK	mitogen-activated protein kinase
MAR	minimally amplified region
MDM2	mouse double minute 2 homolog
MHC	major histocompatibility complex

miR	microRNA
MTCP1	mature T-cell proliferation 1
mut	mutated
NHL	non-Hodgkin's lymphoma
OS	overall survival
PB	peripheral blood
PI3K	phosphoinositide 3-kinase
PLCγ1	phospholipase C gamma 1
pre-miRs	precursor microRNAs
pr	promotor
pri-miRs	pimary microRNAs
PTCL	peripheral T-cell lymphoma
PTM	post-translational modifications
RAS	rat sarcoma
RISC	RNA-induced silencing complex
RNA Pol II	RNA polymerase II
RNAi	RNA interference
STAT5	signal transducer and activator of transcription 5
t	translocation
tg	transgenic
T-ALL	T-cell acute lymphoblastic leukemia
T-PLL	T-cell prolymphocytic leukemia
TCL1A	TCL1 family AKT coactivator A
TCR	T-cell receptor
TET2	tet methylcytosine dioxygenase 2
TGFB1	transforming growths factor beta 1
TRA	T-cell receptor alpha
TRBP	trans-activation-responsive RNA-binding protein
Tyr	Tyrosine
WHO	World Health Organization
ZAP70	zeta-associated proteinase 70

1. Zusammenfassung

Die T-Prolymphozytenleukämie (T-PLL) ist eine aggressive und refraktäre, reifzellige T-Zell-Neoplasie mit derzeit sehr begrenzten therapeutischen Möglichkeiten. Das Krankheitskonzept basiert auf einer kooperativen Störung von TCL1A und ATM, die zu einer verstärkten T-Zell-Rezeptor (TZR) Aktivierung sowie zu aberranten DNA-Reparaturmechanismen beiträgt. Wir haben kürzlich wiederkehrende Amplifikationen auf Chromosom 8q beschrieben, die häufig das AGO2-Gen betreffen. Bei einer Reihe von Malignomen wurde AGO2 eine onkogene Rolle zugeschrieben, indem es zu einer dysregulierten Verarbeitung von microRNAs (miRs) kommt. Hier stellen wir einen integrierten Mehrebenen-Datensatz von 46 T-PLL-Patienten vor, der eine Überexpression von AGO2 in der Mehrheit der T-PLL Fälle zeigt. Diese Überexpression war mit einer größeren Tumorlast sowie einer höheren Proliferationsfähigkeit *in vitro* verbunden, was auf eine onkogene Rolle von AGO2 bei der Leukämogenese der T-PLL hinweist. Zusätzlich zu pro-onkogenen miR-om/Transkriptom-Netzwerken, die von AGO2 bestimmt werden, zeigen wir eine bisher unbeschriebene Beziehung zwischen dem TZR-Signalweg und AGO2. *In-vitro* Systeme mit transient modulierter AGO2-Proteinexpression zeigten eine verstärkende Rolle von AGO2 bei der Phospho-Aktivierung der TCR-Kinasen ZAP70, PLCγ1 und LAT. Diese Effekte wurden durch direkte Protein-Protein-Interaktionen vermittelt, wie Interaktionen mit LCK und ZAP70 in Massenspektrometrie-Analysen und Proximity Ligation Assays in TCR-aktivierten Zellen zeigten. Nachfolgend postulierte Modelle drei-dimensionaler Strukturen dieser Interaktionen sagen eine membranöse Proteinkomplexbildung, die eine post-transkriptionelle Modifikation von AGO2 durch LCK erfordert, voraus. Zusätzlich zu einer globalen Störung des "miR-Master-Regulators" AGO2 zeigen wir ein T-PLL-spezifisches miR-Expressionsprofil mit 34 signifikant deregulierten miRs. Wichtig ist, dass diese miR-Signaturen den Einfluss der konstitutiven TCR-Aktivierung aufzeigen. Vor allem wurden zwei große Untergruppen von T-PLL-Fällen durch die Expression der miR-141- und miR-200c-Cluster definiert. Darüber hinaus waren aggressivere Formen bzw. Phasen der T-PLL mit einer erhöhten Expression von miR-223-3p und einer reduzierten Expression von miR-21 sowie des miR-29 Clusters assoziiert. Mit einem integrativen Ansatz der miR- und mRNA-Sequenzierung konnten wir regulatorische Netzwerke aufdecken, die hauptsächlich die DNA-Schadensreaktion und Überlebenswege beeinflussen. Schließlich haben wir einen kombinatorischen miR-basierten Prognose-Score zum Gesamtüberleben entwickelt, der die pathobiologischen Auswirkungen von AGO2- und miR-Störungen auf die T-PLL weiter verdeutlicht.

2. Summary

T-prolymphocytic leukemia (T-PLL) is an aggressive and refractory mature T-cell neoplasm with currently very limited therapeutic options. The current disease concept is centered around cooperative perturbations of TCL1A and ATM, leading to enhanced T-cell receptor signaling as well as aberrant DNA repair mechanisms. We recently described recurrent gains on chromosome 8q, that frequently involve the *AGO2* gene. In a variety of malignancies, AGO2 was assigned an oncogenic role by mediating microRNA (miR) processing. Here, we present an integrated multi-level dataset of 46 T-PLL patients, demonstrating overexpression of AGO2 in a majority of T-PLL cases. This overexpression was associated with a larger tumor burden as well as a higher proliferation capacity *in vitro*, indicating an oncogenic role of AGO2 in the leukemogenesis of T-PLL. In addition to pro-oncogenic miR-ome/transcriptome networks shaped by AGO2, we demonstrate a previously undescribed relationship between TCR signaling and AGO2. *In-vitro* systems of transiently modulated AGO2 protein expression demonstrated an enhancing role of AGO2 on the phosphor-activation of the TCR upstream-kinases ZAP70, PLCγ1, and LAT. Notably, these effects were mediated by direct protein-protein interactions, as shown by interactions with LCK and ZAP70 in global mass-spectrometry analysis and proximity ligation assays in TCR-activated cells. Subsequent models of three-dimensional structures revealed a membranous protein complex formation, requiring post-transcriptional modifications of AGO2 by LCK. In addition to a global perturbation of the 'miR-master regulator' AGO2, we showed a T-PLL specific miR expression signature, consisting of 34 miRs, which presented a differential expression in T-PLL compared to pan T-cells of age-matched healthy donors. Importantly, these miR signatures revealed the influence of constitutive TCR activation. Most prominently, two major subgroups of T-PLL cases were defined by the expression of the miR-141 and miR-200c cluster. In addition, more aggressive presentations of T-PLL were associated with increased expression of miR-223-3p and reduced expression of miR-21 as well as the miR-29 cluster. In an integrative approach of miR as well as mRNA sequencing, we were able to uncover regulatory networks, mainly shaping DNA damage response and survival pathways. We, finally, developed a combinatorial miR-based overall survival score, further highlighting the pathobiological impact of AGO2 and miR-ome perturbations.

3. Introduction

According to the global cancer statistics of the World Health Organization (WHO), 19.3 million new cancer cases and 10 million cancer deaths were estimated for 2020,[3] representing a leading cause of disability and premature death worldwide.[4] Notably, cancer incidences have not reached their maximum: Estimations predict 30.2 million new cancer cases in 2040 (**Figure 1**),[3] mainly due to ongoing epidemiological and demographic changes. The growing and aging world population, accompanied by cancer-supporting influences like unhealthy lifestyle (e.g. smoking, drinking, physical inactivity) or harmful environmental influences (e.g. fine dust pollution), represent the key driving forces.[5] However, while the cancer incidence is currently rising, a reduction in cancer-associated mortality is observable.[3] This is, on the one hand, based on treatment advances but, on the other hand, a great success of early detection programs.[6] As the diverse spectrum of neoplastic diseases, all summarized under the label 'cancer', originate from distinct molecular mechanisms, there will not be a single cure for all entities. In order to further reduce mortality rates, the development of therapies suitable for the whole spectrum of cancer entities is one of the main tasks of our time.

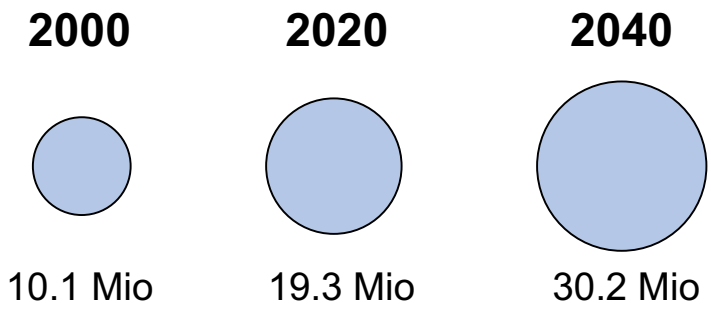

Figure 1: The incidence of cancer is rapidly rising, hence presenting a leading cause of disability and premature death in the 21st century.
Pie chart presenting the estimated amount of new cancer cases in 2000, 2020, and 2040, according to the global cancer statistic of the WHO.[3,7] Circle sizes are calculated relative to the presented cases. Notably, ongoing epidemiological and demographic transitions result in a rapid increase of new cancer diagnoses.

Among the 19.3 million new cancer cases in 2020, around 600,000 lymphoma cases and 500,000 leukemia cases were diagnosed.[3] Lymphomas are defined as tumors of the immune systems and are classified into two main categories: Hodgkin lymphoma, encountering for about 10% of all lymphoma diagnoses, and non-Hodgkin lymphoma (~90%, NHL). NHLs represent a heterogenous group of malignancies arising from the lymphoid system with a broad range of histological, clinical, and biological features. Most of the NHLs arise from B-lymphocytes (~85-90%), the remainder originates from T- or NK-lymphocytes.[8] The main representatives of the group of B-NHLs are diffuse large B-cell lymphoma (DLBCL), chronic lymphocytic

leukemia (CLL), and follicular lymphoma.[8] Among the NHL that belong to the T-cell counterpart, peripheral T-cell lymphoma (PTCL) is the most common subtype (~10-15% of all NHLs).[9] PTCLs encompass a clinically heterogeneous group of uncommon but mainly highly aggressive diseases.[10] The WHO further classifies PTCLs into four categories (nodal, extranodal, cutaneous, and primarily leukemic; **Figure 2**).[11] Within the spectrum of leukemic PTCLs, T-prolymphocytic leukemia (T-PLL) emerges as the most prevalent subtype.[12]

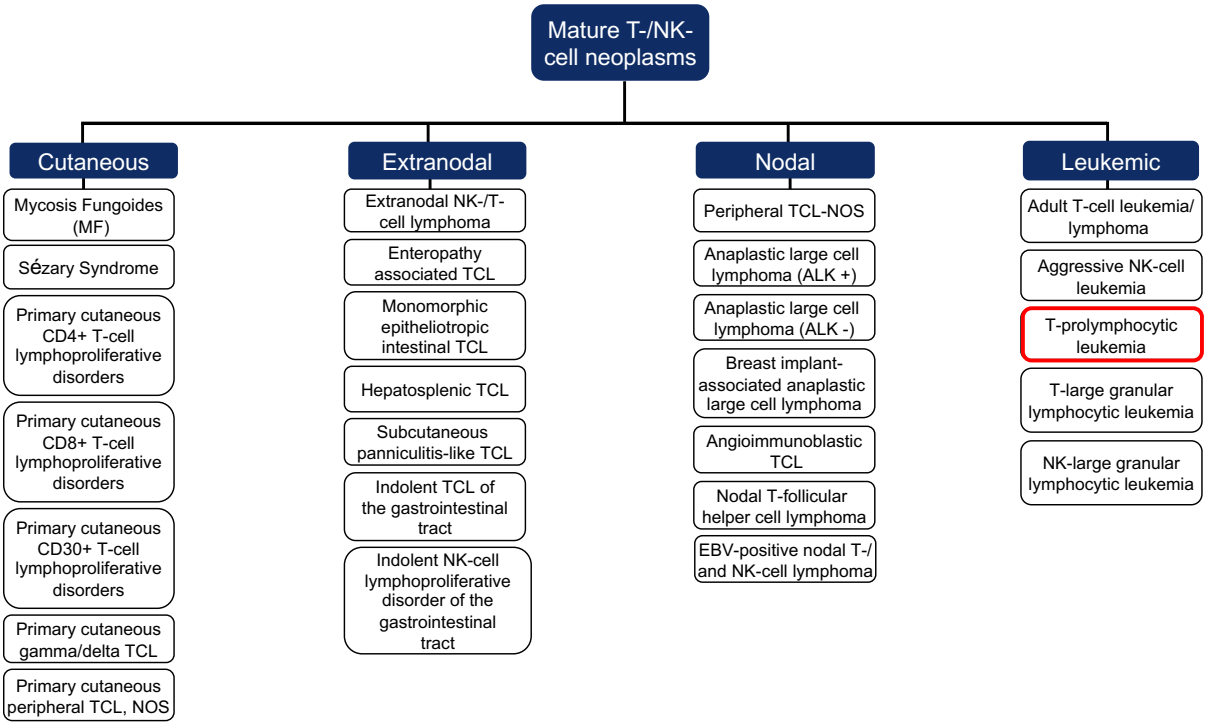

Figure 2: World Health Organization 2022 classification of mature T-cell lymphomas: peripheral T-cell lymphomas.
ALK: anaplastic lymphoma kinase, EBV: Epstein-Barr virus, TCL: T-cell lymphoma, NK: natural killer, NOS: not otherwise specified, MF: Mycosis Fungoides. The presented thesis concentrates on T-cell prolymphocytic leukemia (red box). Adapted from Alaggio *et al.*[13]

3.1 The clinical characteristics of T-prolymphocytic leukemia

According to the WHO classification, T-PLL represents an aggressive T-cell leukemia. T-PLL cells are small- to medium-sized prolymphocytes, presenting a post-thymic phenotype.[11] The disease was first described as a distinct entity in 1973 by Catovsky *et al.*.[14] With approximately 1-2 new cases per 1 million persons per year, T-PLL is very rare.[15] Nevertheless, it is the most common primary leukemic form of peripheral T-cell neoplasms in Europe and North America.[15]

3.1.1. Clinical presentation

T-PLL in its predominant sporadic form is a disease of older age, with a median age of onset of ~65 years.[12,16] However, initial diagnoses occur in a wide range between the age of 40 and 90 years. Males are more frequently affected than females (ratio: ~1.3).[12,17]

The characteristic lymphocytosis of T-PLL at diagnosis is above 100,000/µl blood in approximately 75% of patients and increases rapidly, often exponentially.[12,16] At this stage of the disease, nonspecific constitutive symptoms, such as tendency to infection and bleeding, fatigue, and B-symptoms are often present.[12,18] In addition, bone marrow infiltration is usually observable. Further symptoms include splenomegaly (~80% of cases), small-node generalized lymphadenopathy (~45-50%), thrombocytopenia (<100,000/µl in ~45-50%), hepatomegaly (~35-40%), anemia (<10g/dl, ~25%), skin infiltration (~25%), and malignant effusions (pleura, pericardium, ascites, ~10-15%).[12,18] Central nervous system involvement is extremely rare.[16] Notably, in approximately 10-15% of patients, the diagnosis is made based on incidental findings in peripheral blood of asymptomatic patients.[19] The period of this so-called indolent disease stage can last for a variable period of time, which can be up to several years. However, disease progression into an 'active' T-PLL disease is inevitable.[16,19]

3.1.2. Diagnostic criteria

In 2019, Staber *et al.* published consensus criteria for the diagnosis, staging, and treatment response assessment in T-PLL,[20] in order to facilitate clinical decision making and comparison from clinical trials. For the first time, criteria for the diagnosis of T-PLL were established, utilizing distinctive morphologic, immunophenotypic, cytogenetic, and molecular features of the leukemic cell.[15,20] The three main criteria were defined as: (*i*) monoclonal lymphocytosis in peripheral blood (>5x10^3/µl) with a mature T-cell immunophenotype, (*ii*) evidence of a chromosomal aberration involving loci 14q32.1 (*TCL1 family AKT coactivator A (TCL1A)*) or Xq28 (*mature T-cell proliferation 1 (MTCP1)*), and (*iii*) detection of T-cell specific expression of TCL1A or p13MTCP1 protein in flow cytometry or immunohistochemistry.[20,21] Criterium (*i*), and (*ii*) or (*iii*) must be fulfilled for the diagnosis of T-PLL. T-PLL cases, which do not show overexpression of TCL1A, TCL1B, or p13MTCP1, are classified as 'TCL1-family negative T-PLL'.

In addition, two out of the following secondary criteria have to be met: (*i*) rapidly (exponentially) increasing blood lymphocyte counts with doubling times less than 6 months, (*ii*) additional detection of chromosomal aberrations with gains on 8q or a del11q22 or a complex aberrant karyotype, (*iii*) presence of (hepato-)splenomegaly or effusions, and (*iv*) prolymphocytic morphology in blood smear.[20] As important differential diagnoses, reactive T-cell expansions (e.g. in the context of viral infections), as well as other mature T-cell malignancies with leukemic presentation (e.g. Sézary Syndrome, T-large granular lymphocyte leukemia), must be taken into account.[17,18]

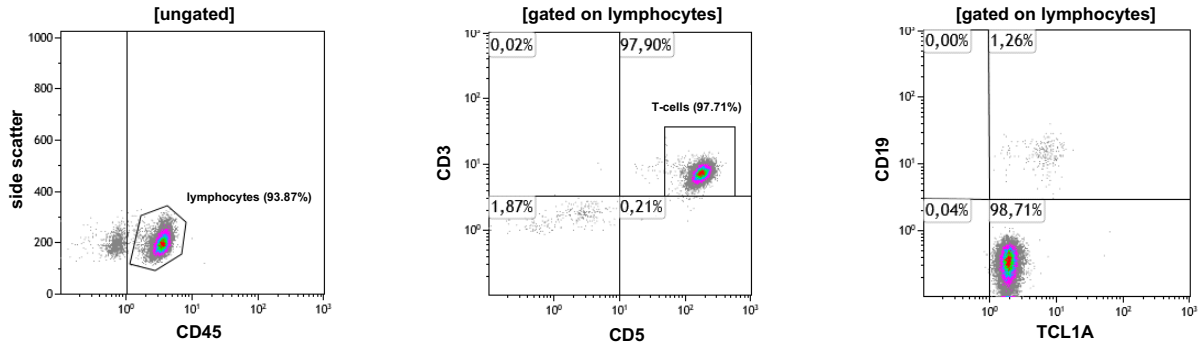

Figure 3: TCL1A protein expression is defined as a main criterium of T-PLL.
Flow cytometrical analyses of one exemplarily T-PLL patient using peripheral blood. a) Staining for the pan-lymphocyte marker CD45 reveals a distinct and pure lymphocyte population. b) Staining for the pan T-cell markers CD3 and CD5 present a pure T-cell population. c) Intracellular staining for TCL1A reveals the presence of this protein in 99% of lymphocytes.

3.1.3. Currently limited treatment options

Overall, T-PLL is an aggressive and chemotherapy-refractory disease with currently very limited therapeutic options,[19] resulting in a median overall survival (OS) of less than three years.[18] The chemotherapy-refractory behavior of T-PLL cells is reflected by low response rates towards the treatment with alkylators, anthracyclines, purine analogs, or combination chemotherapies like CHOP (cyclophosphamide, vincristine, doxorubicin, prednisone).[12,22–25] Furthermore, these rare responses are usually of short duration (~3 months) and do not extend the median OS of T-PLL patients.

The therapeutic implementation of monoclonal antibodies presented a milestone in the treatment of T-PLL. As virtually all T-PLL cases express the surface CD52 antigen,[26] the humanized monoclonal anti-CD52 antibody alemtuzumab induces high remission rates (>80%, when given as first-line treatment).[24,25,27,28] Up to now, alemtuzumab represents the best treatment for T-PLL patients. Nevertheless, in virtually all patients, the disease recurs at median after 12 months. At this stage of relapsed disease, treatment options are scarce. Long-term remission for longer than 5 years can only be accomplished in less than 20% of patients, eligible for allogeneic stem cell transplantation.[17,19]

All in all, the main challenge in treating T-PLL is to reach long-term disease-free survival.[19] Therefore, an improved understanding of molecular dependencies in T-PLL is indispensable. The investigation of these molecular vulnerabilities, that are exploitable for the development of novel targeted treatment approaches, should be forced in the research field of this rare disease.

3.2 The current pathogenetic understanding of T-PLL

Over the last years, genomic as well as epigenomic studies have remarkably extended our understanding of T-PLL's leukemogenesis. DNA damage repair mechanisms, apoptosis regulation, as well as alterations of cytokine signaling and epigenetic regulation were identified as

hallmarks of this orphan disease, besides already established genomic lesions around TCL1 family members.[29] In the following, the current understanding of T-PLL's pathophysiology is summarized.

3.2.1. TCL1-family activation and ATM deficiencies as initiating lesions

Chromosomal rearrangements (e.g. translocations, inversions) are recognized as the initial event of malignant transformation or are associated with tumor progression in the majority of human leukemias and lymphomas.[30,31] In human B- and T-cells, chromosomal imbalances often occur as a consequence of mistakes during the recombination process of genes, encoding for immunoglobulins or T-cell receptors (TCRs).[32] Thereby, cellular proto-oncogenes are juxtaposed to enhancer elements, leading to deregulated expression of these proto-oncogenes.[33,34] Likewise, rearrangements of the *T cell receptor alpha locus* (*TRA*) are recognized as a molecular hallmark of T-PLL's leukemogenesis.[35] These *inversions* (*inv*) or *translocations* (*t*) lead to juxtaposition of the *TCL1A* locus (*inv(14)(q11;q32); t(14;14)(q11;q32*) or the *MTCP1* locus (*t(X;14)*) to highly active *TRA* gene enhancer elements, preventing the physiological silencing of the expression of these TCL1 family members at the CD4/CD8 double-positive thymocyte stage.[34] While the expression of TCL1A is observable in the majority of T-PLL cases (>80%), rearrangements affecting the *MTCP1* locus are present only in a minority of cases (<20%).[12,35,36] Notably, the oncogenic role of both members of the TCL1 family has been formally proven in transgenic mouse models.[37,38] Furthermore, high TCL1A expression is associated with genomic instability, forming the basis for additional genomic aberrations.[36] Since these rearrangements are already present in preleukemic T-cell expansions, they are understood as the initial step of T-PLL's leukemogenesis.[29]

TCL1 family-activating lesions are then followed by dysregulation of the tumor suppressor *ataxia telangiectasia mutated* (*ATM*).[39] *ATM* is either affected by genomic deletions (11q22.3) or mutations.[36,40,41] Remarkably, genomic aberrations of *ATM* belong to the small fraction of mutations in T-PLL that present variant allele fractions of higher than 80%, suggesting an early acquisition of this lesion.[36,42] This unique combination of overrepresented TCL1A expression and dysfunctional ATM forms the basis of neoplastic transformation by preventing the execution of safeguarding mechanisms upon DNA damage.[36]

3.2.2. T-cell receptor signaling as a central pro-leukemogenic pathway

T-PLL cells show a mature, memory-spectrum phenotype, revealing antigen experience. Expression of the TCR was found in 80% of T-PLL cases and is associated with poor patient survival and a hyper-proliferative phenotype.[15] Moreover, gene expression profiles showing prominent signatures of T-cell activation further point towards TCR involvement in T-PLL´s pathophysiology.[36]

In general, TCR signaling is a major determinant of T-cell fate by shaping T-cell development, differentiation, activation, homeostasis, and immune tolerance.[43,44] The extracellular TCR complex represents a glycosylated heterodimer on the surface of human T cells, composed of TCRα and β subunits.[45] These TCRα and β subunits are generated by somatic V(D)J recombination during the thymic T-cell development, resulting in variable and constant regions, which are covalently linked by disulfide bonds.[46] Hydrophobic interactions associate the TCR to invariant CD3 proteins, consisting of γ, δ, ε, and ζ chains.[45] In the first step of TCR activation, the antigen is presented through antigen-presenting cells (e.g. macrophages, B-cells, or dendritic cells) via MHC molecules (**Figure 4**). Then, the lymphocyte-specific protein tyrosine kinase (Lck) phosphorylates tyrosines in immunoreceptor tyrosine-based activation motifs (ITAMs) of CD3ζ, which are responsible for the transmission of intracellular TCR signals.[47] The subsequent signaling cascade includes zeta-associated proteinase 70 (ZAP70), as well as the linker for activation of T-cells (LAT).[48] In the next step, LAT recruits the phospholipase C gamma 1 (PLCγ1), activating Ca^{2+} signaling pathways, as well as the growth factor receptor-bound protein 2 (GRB2), triggering rat sarcoma (RAS) and mitogen-activated protein kinase (MAPK) pathways.[49,50] In the context of CD28-mediated co-stimulation, the TCR additionally recruits phosphoinositide 3-kinase (PI3K)-protein kinase B (AKT) signaling, which is essential for the regulation of cell growth and proliferation, metabolism, survival, and apoptosis.[44,51]

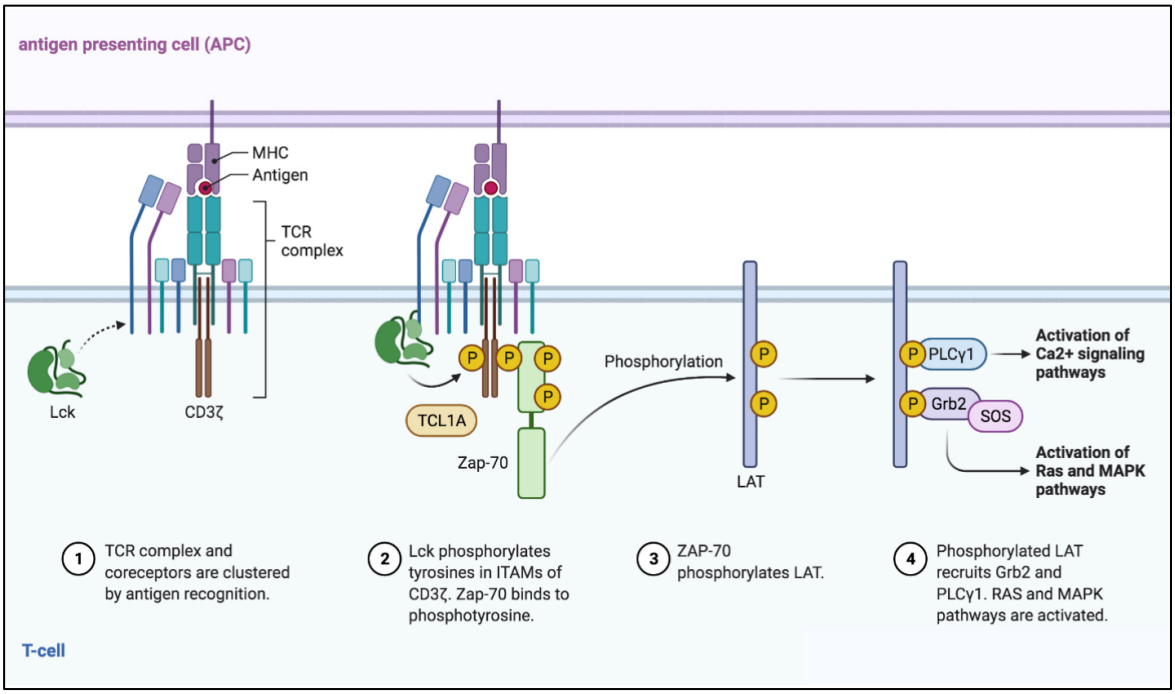

Figure 4: T-cell receptor activation and associated downstream signaling
The antigen is presented through antigen-presenting cells, leading to phosphorylation of tyrosines in immunoreceptor tyrosine-based activation motifs (ITAMs) of CD3ζ. Following, ZAP70 binds to phosphotyrosine and then phosphorylates LAT. The phosphorylated LAT recruits PLCγ1, leading to activation of Ca^{2+} signaling pathways, as well as GRB2, activating the RAS and MAPK pathway. In T-PLL, TCL1A enhances phospho-activation of TCR kinases. The figure was created in biorender, by adapting the template of A. Iwasaki and R. Medzhitov.

In PTCL, several subgroups, presenting specific patterns of TCR activation, were described:[44] (*i*) Entities with functionally intact TCR signaling and oncogenic enhancer elements, (*ii*) entities with autonomous, constitutive TCR signaling, and (*iii*) entities with a complete replacement of the TCR by functional stand-ins.[44]

T-PLL belongs to the first described group: The illegitimate expression of TCL1A lowers the threshold for TCR activation, driving the shift of naïve T cells into a rising pool of memory T cells.[52] This step of T-PLL's leukemogenesis represents the origin of final T-PLL outgrowth. Increased autonomy of T-PLL cells is further entertained by impaired control mechanisms (e.g. downregulation of CTLA4).[36] TCL1A was also shown to interact with AKT, further enhancing TCR signaling.[15]

3.2.3. Identification of secondary hallmarks

Besides TCL1/ATM perturbations in combination with an increased autonomy via sustained (TCR) activation, further genomic aberrations are acquired during the exponential outgrowth of the expanding pool of T cells. Exemplarily, 62% of T-PLL patients present gain-of-function mutations, activating the Janus kinase (JAK)/signal transducer and activator of transcription (STAT) signaling pathway.[36,41,42,53] Predominantly, *JAK3* (26% of T-PLL) and *STAT5B* (19%) are affected, followed by *JAK1* (6%), all mainly showing missense mutations in the SH2 or pseudokinase domains.[54] Besides mutations of *JAK*/*STAT* genes, negative regulators of this pathway are frequently affected by genomic losses, potentially further enhancing JAK/STAT signaling[54]. Additionally, mutations of epigenetic regulators are frequently observed in T-PLL (e.g. *enhancer of zeste homolog 2* (*EZH2*), *tet methylcytosine dioxygenase 2* (*TET2*), or *lysine methyltransferase* (*KMTs*)).[36,41,42,53] In line, first data revealed an altered epigenetic reprogramming of T-PLL cells, as shown in a small cohort of six patients.[55]

Importantly, these (secondary) hallmarks of T-PLL cells are currently being explored as potential target pathways. In **Figure 5**, these novel therapeutic approaches, we well as clinically often used substances (e.g. alkylating agents, purine analogues, alemtuzumab) are displayed. Interestingly, virtually all therapeutic approaches are centered around the incapability of the T-PLL cell, to exert p53-mediated responses upon genotoxic stress.

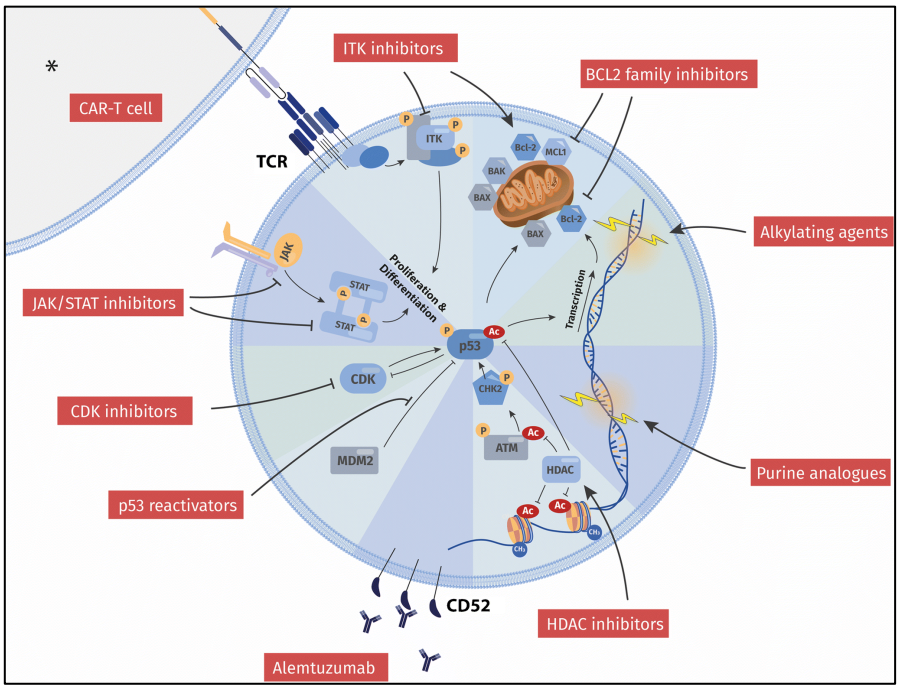

Figure 5: Overview of treatment strategies in T-PLL.
The current treatment concept is centered around a (chemo-)immunotherapeutic approach, by the usage of the CD52 antibody alemtuzumab as well as of alkylating agents and purine analogs. The incapability of T-PLL cells to execute adequate p53-mediated responses upon genotoxic stress was translated into pre-clinical approaches, e.g. by reactivating p53 via MDM2, by inhibition of cyclin-dependent kinases (CDK), by inhibition of (histone) deacetylases (HDAC), or by targeting of BCL2 family members. Further strategies concentrate on the interruption of vital growth factors (JAK/STAT inhibitors, interleukin-2-inducible kinase (ITK) inhibitors). In addition, novel treatment approaches utilizing immunogenic cell death (e.g. CAR T-cell therapies) are also under development. However, there is no approved drug (FDA or EMA) for T-PLL up to date, underlining the need for new active substances in this rare disease. Adapted from Braun *et al.*.[19]

3.2.4. Gains at chromosome 8q underly *AGO2* amplifications

Furthermore, cytogenetic analyzes revealed recurrent amplifications at chromosome (chr.) 8q in T-PLL cells (53%[12]-77%[41] of T-PLL cases, depending on the cohort and type of analysis). These overrepresentations of chr.8q were mainly attributed to a trisomy 8q, resulting out of isochromosomes (8)(q10).[35] Recently, our research group defined the minimally amplified region (MAR), which was predominantly affected by this hotspot aberration at chr. 8q.[36] As a control, patient-derived germlines were used. Contrary to the current theory that *MYC* defines the chr.8 associated gains, we identified *argonaute RISC catalytic component* 2 (*AGO2*) as the primary target of this MAR: While all cases harboring chr.8 associated gains presented *AGO2* amplifications, *MYC* gains were only present in around 70% of these cases.[36] In addition, the miRs-1206/1207/1208 were involved in this MAR.[36] AGO2 associated gains were further validated using fluorescence *in situ* hybridization (FISH) probes (**Figure 6**). Interestingly, we identified an association between AGO2 amplifications and more complex karyotypes.[36] Given the frequent genetic amplification of the miR-master regulator AGO2, a global perturbation of T-PLL's miR-ome is most likely, however, no systematic assessment of the expression

of small RNAs in a large cohort of T-PLL patients (n>25) has been performed to date. Furthermore, the pathogenetic impact of AGO2 on T-PLL's leukemogenesis remains elusive.

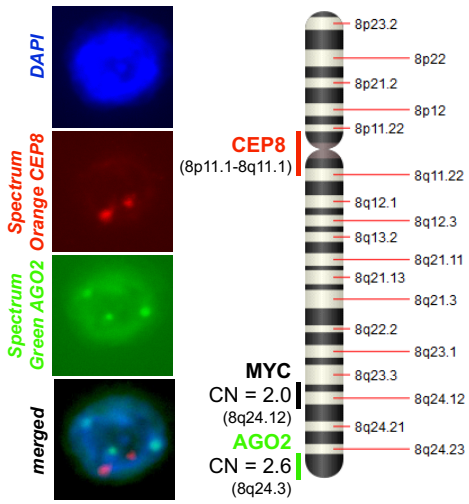

Figure 6: AGO2 defines the minimally amplified region of chromosome 8q. Exemplarily fluorescence in situ-hybridization (scale bar=5µm) of one T-PLL patient harboring a chr. 8q associated gain. While *MYC* was not affected by this MAR, we identified an amplification of *AGO2*. Adapted from Braun *et al.*.[1]

3.3 RNA interference

As AGO2 is the central regulator of miRs, primarily affecting RNA interference, detailed information on these processes as well as known alterations of this machinery in leukemia is provided in the following.

3.3.1. Canonical microRNA biogenesis

RNA interference (RNAi) describes a natural mechanism of eukaryotic cells for the targeted silencing of genes, based on an interaction of miRs with the genetic information-transmitting mRNA and by utilizing several enzyme complexes.[56] RNAi involves several pathways, with the canonical pathway being the best studied and described in detail below (**Figure 7**).

In the genome, miRs are either encoded as individual genes or as a cluster of up to several hundred miRs, regularly embedded in introns of protein-coding genes.[56,57] In general, the canonical mechanism of miR biogenesis can be divided into four distinct phases: In a first step, the miRs are transcribed by the RNA polymerase II (RNA Pol II) as primary miRs (pri-miRs).[58] The transcribed pri-miRs are capped as well as polyadenylated and the 20-25 nucleotides of the mature miR are now located in the stem of a hairpin.[58] In the next step, the pri-miRs are cut into single hairpins, which are called precursor miRs (pre-miRs).[59] This step of miR biogenesis is executed by a nuclear protein complex called microprocessor, containing the RNase III enzyme Drosha, the double-stranded RNA (dsRNA)-binding protein (dsRBP), the DiGeorge critical region 8 (DGCR8), and other less well-studied proteins (e.g.p27).[56,59] After the export of the pre-miRs into the cytoplasm via the export receptor exportin 5,[60] the pre-miRs are

cleaved into a dsRNA of 20-25 nucleotides length by the RNase III-type enzyme Dicer.[61] During this process, Dicer is accompanied by the dsRBP trans-activation-responsive RNA-binding protein (TRBP).[56,61] In a final step the dsRNA is incorporated into the so-called RNA-induced silencing complex (RISC).[62] Within this complex, the dsRNA is cleaved into single strands. Thereby, AGO2 selects one strand to become the mature miR (guide strand), while the other strand (passenger strand) is abandoned.[56] Besides this well-established way of canonical miR biogenesis, several other routes of miR processing are described, being independent of the microprocessor or Dicer.[56]

Ultimately, the incorporated guide strand can activate the RISC complex to cleave an mRNA, which is complementary to the sequence of the guide strand.[56] In this way, the guide strand determines which mRNA is degraded by the RISC complex. Alternatively, the enzyme complex can block the function of an mRNA complementary to the guide strand, leading to an inhibition of translation without cleavage.[63,64] Both ways lead to a suppression of the conversion of genetic information and, thereby, to silencing of genes.

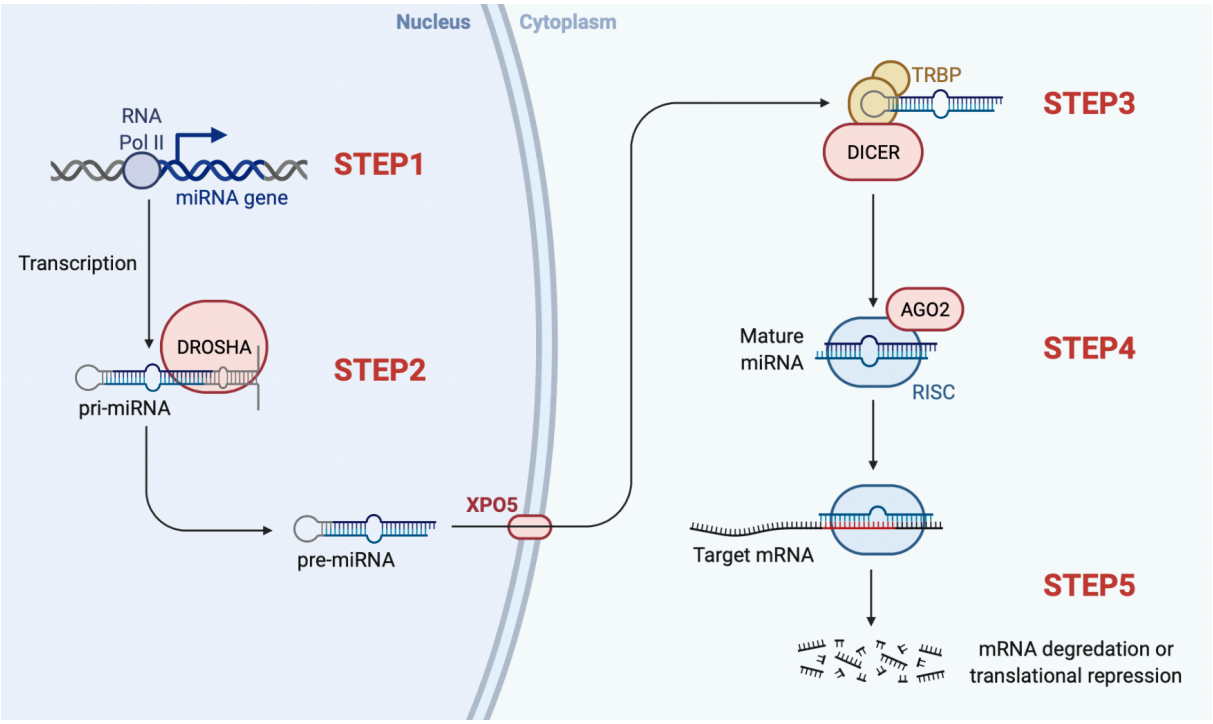

Figure 7: AGO2 is involved in the canonical pathway of miR biogenesis.
STEP 1: Transcription of the pri-miR by the RNA polymerase II (RNA Pol II).[58] STEP 2: Processing of the pri-miR into single hairpins (pre-miR) by the microprocessor (nuclear protein complex containing Drosha).[59] STEP 3: After exportation in the cytoplasm utilizing exporting 5 (XP05),[60] the pre-miR is cleaved into dsRNA by Dicer (in complex with the dsRBP trans-activation-responsive RNA-binding protein TRBP).[61] STEP 4: Cleavage of the dsRNA into single strands within the RNA-induced silencing complex (RISC) containing AGO2.[62] STEP5: Finally, the RISC binds to a target mRNA, leading to either repression of translation or decay of mRNA.[56] The figure was created in biorender.

3.3.2. AGO2 and its role in cancer

AGO2 belongs to the Argonaute family, which is evolutionarily highly conserved in mammals.[65] As described above, the members of this family play an important role in RNAi as crucial members of the RISC.[56] Notably, AGO2 is the only member of this family, presenting an endonuclease activity.[66] The authors around N. T. Schirle revealed four core domains of this protein: The N domain of AGO2 is essential for the unwinding of the dsRNA during the RISC assembly, presenting a rate-limiting step of RNAi.[67] However, for the subsequent steps of gene silencing (e.g. mRNA loading or subsequent slicing), the N terminal is not required. The second component of AGO2, the PAZ domain, binds the 2-nucleotide 3' overhang of the guide strand during the formation of the RISC complex.[68] Likewise, Dicer carries a comparable PAZ domain.[68] In line with the function of the PAZ motif, AGO2 presenting a dysfunctional PAZ domain is incapable to form the RISC complex. The third domain of AGO2 is called the MID. This motif is responsible for the 5' overhang binding of the guide strand. In addition, the MID domain carries an adjacent binding pocket for the cooperative binding of the cap of the target mRNA. The fourth domain, the so-called PIWI domain, executes the catalytic activity of AGO2, by carrying an enduring RNase H-like endonucleolytic activity.[69] Additionally, the PIWI motif is essential for the recruitment of GW182 family of scaffolding proteins, which are part of the miR-mediated gene silencing machinery.[70] The PIWI domain is further required for the interaction between the MID domain and the respective mRNA, by stabilizing this interaction.[71] Conclusively, AGO2 is characterized by the architecture of two lobes, with the N terminal and PAZ domain as one lobe and the MID and PIWI domain as the other lobe, connected by two linkers (**Figure 8**).[66]
Besides the above-outlined function of AGO2 in mRNA decay and repression of translation, additional modes of AGO2's action were recently identified, making AGO2 a multifaceted player in gene silencing.[69] Exemplarily, the stability of miRs seems to be dependent on the expression of AGO2, as shown by reduced half-lives of multiple endogenous miRs in a cellular system lacking AGO2.[72] Furthermore, a Dicer-independent way of miR biogenesis was postulated, with AGO2 replacing the function of Dicer in cleaving the pre-miRs.[73]
The function of AGO2, regulating the miR processing machinery, can be influenced by post-translational modifications (PTMs), predominantly induced by extracellular stimuli. These PTMs lead to a specific loading of the RISC with a distinct repertoire of miRs, establishing cell- and state-specific patterns of gene expression.[56] The best-understood mechanism is the phosphorylation of AGO2 at Tyrosine 393 (Tyr^{393}) by the epidermal growth factor receptor (EGFR).[74] Under hypoxic conditions, AGO2 gets phosphorylated, leading to an inhibition of its interaction with Dicer, hence impairing the loading of the RISC with a specific subset of miRs.[74]

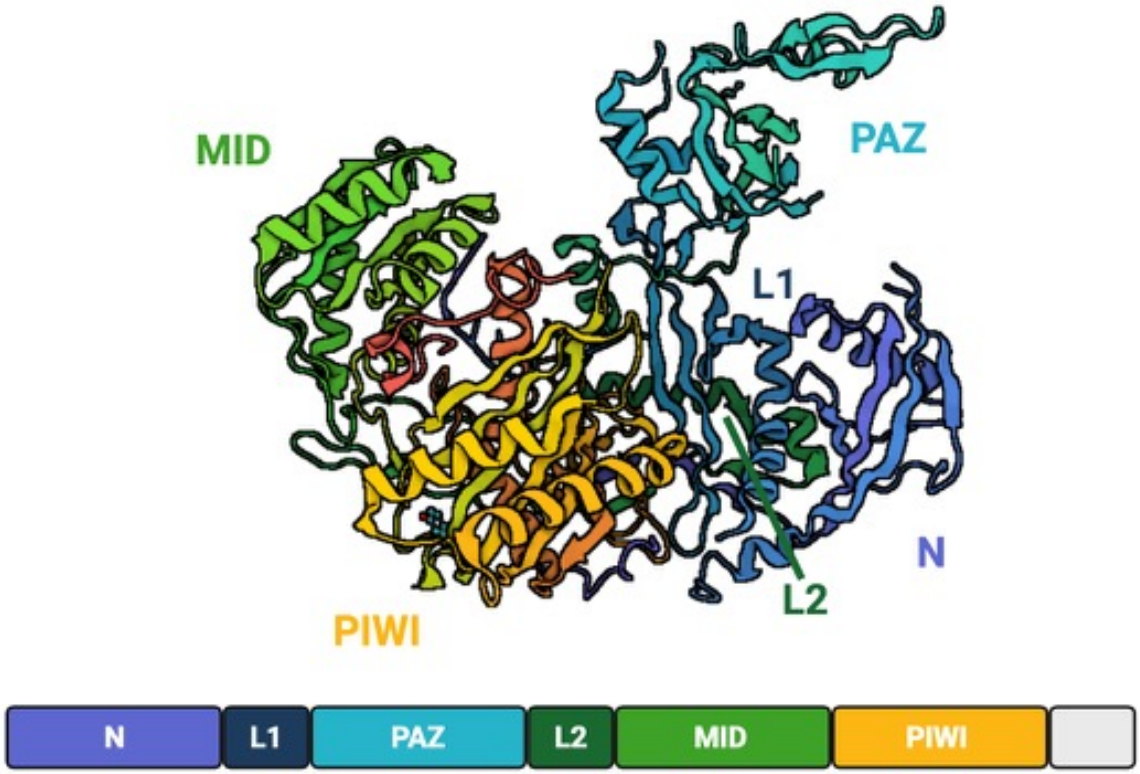

Figure 8: AGO2 consists of four distinct domains, resulting in a bi-lobed architecture. Crystal structure of AGO2, as revealed by Schirle *et al.*.[66] AGO2 presents a bi-lobed structure, presenting four core domains: N terminal (responsible for RNA unwinding), PAZ domain (3' overhang binding of the guide strand), MID (mainly 5' overhang binding of the guide strand), and PIWI domain (mainly catalytic activity). The four core domains are connected by two linkers.

Besides its many roles in small RNA induced gene silencing, AGO2 is frequently overexpressed in several malignant tumors and has recently been described as an oncogenic factor.[69] Elevated expression of AGO2 has been shown for solid (e.g. colon carcinoma,[75] ovarian carcinoma[76]), as well as leukemic malignancies (e.g. myeloma[77]). Its oncogenic functions have been demonstrated to work by two distinct mechanisms: Either by selecting a subset of defined miRs, that target mRNAs of tumor-suppressive molecules,[74] or by interacting with well-established tumor factors (e.g. with RAD51 upon DNA double-strand breaks).[69,78]

In T-PLL, AGO2 is the primary target of recurrently occurring gains of chr. 8q.[36] However, systematic analyzes of AGO2 mRNA and protein expression as well as the impact of genomic amplification on those, have not been performed in T-PLL. Furthermore, investigations deciphering the potential pathogenetic impact of AGO2 on T-PLL's leukemogenesis have not been conducted.

3.3.3. MicroRNAs and their role in cancer

MiRs are short, highly conserved, non-coding RNAs, with a size of around 21-23 nucleotides.[79] As major interactors in gene silencing, miRs guide the AGO proteins to the 3' untranslated region of the target mRNA, hence leading to mRNA decay or inhibition of translation of the

respective mRNA.[80] The first description of a miR goes back to the year 1993, in which Ambros *et al.* described the expression of the miR lin-1 in *Caenorhabditis elegans* (*C. elegans*), affecting the development of *C. elegans* by regulating the expression of the protein lin-14.[81] Since then, a large variety of new miRs has been discovered. In 2021, the miR repository miRbase lists 1,917 distinct pre-miRs, as well as 2,654 mature miRs in Homo sapiens.[82] Strikingly, virtually every cellular process is dependent on miR expression.[79] In line, mouse models lacking the miR biogenesis machinery (e.g. Dicer knockout) show lethality during the embryonic period[83]. Furthermore, computational predictions reveal hundreds of mRNA targets for each miR species with a rapidly growing knowledge on specific interactions and modes of miR (dys)regulations.[84,85]

Generally, deregulation of miR expression is a feature of most cancers.[86] The first evidence of a role of miRs on leukemogenesis was provided by the team around C. Croce, identifying deletions of the miR-15a/miR-16-1 locus at chromosome 13q14 in chronic lymphocytic leukemia (CLL).[87] Deletion of this miR-15/16/dleu2 locus in mice induced the development of a CLL-like disease,[88] supporting the hypothesis of a tumor-suppressive role of miR-15a/miR-16-1. Strikingly, the anti-apoptotic protein *B-cell lymphoma 2* (*BCL2*) was identified as the primary target of this miR cluster.[89]

While oncogenic TCL1A expression is mainly caused by genomic aberrations in T-PLL, downregulation of TCL1A-targeting miRs is thought to contribute to TCL1A overexpression in CLL.[90] Besides the well-established TCL1A-targeting miRs-29, -181, and -34b/c,[90,91] our research group established a disturbed regulatory axis of EVI1-miR484 mediated TCL1A repression in CLL.[92]

Furthermore, the involvement of certain miRs in the pathogenesis of various mature T-cell entities has been described. Exemplarily, the miR-155 was shown to be overexpressed in cutaneous T-cell lymphoma (CTCL), transcriptionally activated by STAT5.[93,94] This STAT5/miR-155 pathway promoted proliferation in T cells *in vitro.*[94] In addition, overexpression of miR-122 was demonstrated in CTCL, leading to inhibition of p53 and, thereby, inhibited apoptosis of malignant T cells induced by chemotherapy.[95] Notably, a systematic analysis of deregulations of the ‘miR-ome’ in T-PLL has not been reported.

3.4 Objectives

Overall, we strive to identify new molecular dependencies in T-PLL that are exploitable for the development of novel targeted treatment approaches. Our preliminary data strongly implicate deregulations of AGO2 as well as miRs at various levels, potentially contributing to the malignant phenotype of T-PLL cells. Therefore, we aim to enhance our existing profiling data sets by global miR signatures.

Aim 1 - "AGO2": AGO2 is genomically gained and overexpressed in T-PLL. Therefore, we (*i*) aim to characterize the expression of AGO2 protein in a large cohort of T-PLL and to correlate this expression with the respective copy numbers and mRNA expression. To further analyze the function and role of elevated AGO2 in T-PLL, we aim to (*ii*) compare clinical characteristics as well as gene expression profiles (GEP) of patients with normally expressed and overexpressed AGO2 protein. Additional investigations aim at (*iii*) evaluations of AGO2´s effect on proliferation capacity, as well as TCR activation, in cell line systems and primary T-PLL cells. Finally, we strive to (*iv*) characterize the interactome of AGO2, identifying potential interactors of AGO2 mediating the discovered effects.

Aim 2 - "miR-ome": As we observe a deregulation of the "miR-master regulator" AGO2, T-PLL cells likely harbor a skewed global miR-profile. Therefore, we (*i*) aim at identifying global profiles of miR expression via miR sequencing, supplementing our existing transcriptome and whole exome data sets. Primary samples, isolated from peripheral blood (PB) of 46 treatment-naïve T-PLL patients, will be analyzed. For these cases, high throughput profiling platform data and comprehensive clinical data are available. Complementary transcriptome sequencing will be available for all cases. T cells from PB of 6 age-matched healthy donors will be included as controls. To investigate, whether T-PLL's miR-ome resembles those of TCR-stimulated or unstimulated healthy T-cells, we will additionally sequence TCR-activated T cells derived from healthy donors.

Furthermore, we (*ii*) aim at performing analyses of functional clusters of miRs and at predicting evolutionally conserved miR-mRNA regulatory networks. As miR-mediated regulation of cellular processes is based on the induction of low-level changes of mRNA abundancies affecting a larger cohort of genes rather than one single factor [2], we will perform gene set enrichment analysis on miR-associated mRNAs. We (*iii*) will further conduct *in-silico* predictions of evolutionally conserved miR-binding sites of target sequences using respective software tools and align these data with miR-mRNA correlation data utilizing our data set.

Moreover, we will associate the identified miR alterations with clinical and prognostic features. In addition, we (*iv*) aim at developing the first survival score in T-PLL, in order to improve current clinical stratifications. We, therefore, will build multivariate scores, utilizing miRs that were associated with overall survival in our training cohort. Finally, we will validate this combinatorial miR-based score in an independent test cohort.

4. Material and Methods

Material and methods that were used to produce the results discussed below are published in my first-author publications.[1,2]

5. Results

The results discussed below are published in my first-author publications.[1,2]

6. Discussion

Here, we present overexpression of the miR master regulator AGO2 in a large cohort of T-PLL cases, on the floor of genomic aberrations of chr. 8q. This overexpression was associated with a higher tumor burden as well as a higher proliferation capacity *in vitro*, indicating an oncogenic role of AGO2 in the leukemogenesis of T-PLL. In addition to miR-ome/transcriptome networks shaped by AGO2, we demonstrate a previously undescribed relationship between TCR signaling and AGO2: AGO2 augments TCR signaling strength through direct protein-protein interactions, as part of a complex with the TCR kinases LCK and ZAP70. In addition to a global perturbation of the 'miR-master regulator' AGO2, T-PLL cells present a specific miR-ome consisting of 34 miRs, which show a differential expression compared to pan T cells of age-matched healthy donors. Importantly, these miR signatures revealed the influence of constitutive TCR activation. In an integrative approach of miR as well as mRNA sequencing, we were able to uncover regulatory networks, mainly shaping DNA damage response and survival pathways. We finally developed a combinatorial miR-based overall survival score, further highlighting the pathobiological impact of AGO2 and miR-ome perturbations.

6.1 Independence of AGO2 protein overexpression from genomic aberrations

At the outset, we recapitulated our observation of genomic gains on chromosome 8q, as analyzed by SNP arrays and being observed in around 30% of T-PLL cases.[36] Importantly, these copy number alterations (CNA) were predominantly defined by the locus of *AGO2* (involved in 100% of cases) and, in second place, by the locus of the proto-oncogene *MYC* (around 70% of cases). As a central piece of this study, we present an integrated multi-level dataset derived from a cohort of 46 well-annotated T-PLL cases, assessing the association between the previously identified amplifications of *AGO2* and the expression of AGO2 mRNA and protein. Here, we detected a significant correlation between AGO2 CN and mRNA expression in T-PLL cells, however, AGO2 protein expression was not associated with the copy number. This finding points towards distinct modes of AGO2 upregulation, besides the recently described copy number gains. Exemplarily, regulation of AGO2 protein stability by the availability of miRs is conceivable, as shown in a murine model.[96] Further modes of regulation of AGO2 protein stability include post-translational modifications, like prolyl 4-hydroxylation.[97] None of these mechanisms has yet been investigated in T-PLL, might however explain the observed discrepancy of CN-protein association.

6.2 TCR signal augmentation as a novel non-canonical function of AGO2

In line with the canonical function of AGO2, we identified AGO2-specific transcriptome modifications mediated by miR dysregulations. These transcriptomes were mainly associated with enhanced survival signaling, accelerated cell cycle transition, as well as impaired DNA damage responses.

In addition to AGO2's canonical miR-mediated effects, we unravel a novel, non-conventional mode of action of AGO2 as a major finding of the presented work: TCR signal strength of the TCR was enhanced upon AGO2 upregulation. This effect was mainly mediated by direct protein-protein interactions with upstream-located TCR signaling kinases. In detail, AGO2 interacted with the kinases LCK and ZAP70, as shown by mass spectrometric analyses. Subsequent *in-silico* modeling further revealed a membranous complex formation of the respective proteins as well as post-translational modifications of AGO2 by ZAP70. This non-canonical mode of action adds on the current understanding of non-conventional oncogenic roles of AGO2. Exemplarily, an interaction between AGO2 and the recombinase RAD51 was shown, mediating the accumulation of RAD51 at DNA double-strand breaks.[78] Furthermore, an interaction between AGO2 and KRAS, leading to fastened tumor progression in a non-small cell lung cancer model, represents another mode of action of AGO2, mediated by protein-protein interactions.[98] In our *in-silico* model, phosphorylation of AGO2's residue Tyr^{529} was predicted to be necessary for the interaction of AGO2 with ZAP70. In line, phosphorylation of AGO2's residue Tyr^{529} was shown to correlate with diminished binding of small RNAs, which further supports our hypothesis of a novel, non-canonical function of AGO2, when phosphorylated at Tyr^{529}.[99]

Besides AGO2's non-conventional oncogenic roles, AGO2 was described as a pro-tumorigenic factor in various malignancies through disturbed RNAi. In hepatocellular carcinoma, *MYC* mRNA stability was dependent on AGO2 expression and associated with poor prognosis.[100] In lung cancer, acetylation of AGO2 led to enhanced miR-19b biogenesis, again associated with poor prognosis.[101] In summary, AGO2 can be characterized as a potential oncogene that exerts its functions through both RNAi-independent and canonical, RNAi-dependent mechanisms.

6.3 The TCR-signaling shaped miR-ome

In line with AGO2's enhancing effect on TCR signaling, a TCR-hyperactivated phenotype is frequently observed in T-PLL cells.[52] Global gene expression signatures of T-PLL cells further resemble those of T-cell activation.[36] Besides the impact of AGO2 on TCR signaling, TCL1A was shown to act as a catalytic enhancer of important TCR kinases (e.g. ERK and AKT).[15] In addition, genomic losses of negative regulators of T-cell activation (e.g. CTLA4) are regularly observed in T-PLL,[36] further leading to enhanced TCR signaling. These findings emphasize the important role of this pathway in the leukemogenesis of T-PLL. In line, more activated phenotypes of T-PLL cells were associated with a shortened overall survival.[52]

Besides the influence of alterations of the RNAi machinery on TCR activation, we identified a T-PLL-specific miR-ome that resembles patterns also found in TCR-activated T cells from healthy donors. For this, we utilized miR sequencing, assessing expression profiles in TCR-activated T cells of age-matched healthy donors. We were the first to identify a specific

remodeling of miR expression signatures upon TCR stimulation. Besides previously described miRs (miR-17-5p or miR-150-5p), we identified yet unknown miRs to be regulated in dependence on TCR signals (e.g. upregulation of miR-18a-5p). Comparable effects on the miR-ome of B-cells were reported in response to B-cell receptor (BCR) stimuli.[102] Conclusively, we identified a reciprocal shaping of the RNAi machinery and TCR signaling: While AGO2, as well as miRs, influenced the TCR signaling capacity, TCR signaling itself shaped the expression of certain miRs and AGO2.

6.4 miR-based regulatory networks in T-PLL

As a central part of this work, we report 34 miRs to be differentially expressed in T-PLL cells, as compared to T cells derived from age-matched healthy donors, representing the first description of T-PLL's miR-ome. Subsequently, Erkeland *et al.*[103](n=31 T-PLL cases, n=35 differentially expressed miRs) and Patil *et al.*[104] (n=7 T-PLL cases, n=111 differentially expressed miRs) have published descriptions of the miR-ome of T-PLL cells. However, our cohort still represents the biggest cohort analyzed for small RNA expression. Notably, as we[2] and Patil *et al.*[104] identified up- as well as downregulation of certain miR clusters, Erkeland *et al.*[103] only detected overexpression of miRs. The observed differences between the published data are mainly influenced by methodological variations (small RNA sequencing vs. array-based approaches) as well as cohort sizes and patient selection. Exemplarily, the proportion of untreated T-PLL patients differed among the cohorts. As the impact of different lines of therapy on the miR-ome is unclear, this may have contributed to the divergent results.

Combining all three data sets, the miR-200c/141 cluster, the miR-29 family, miR-21, and miR-223-3p emerge as hallmarks of the miR-ome of T-PLL cells. Previous reports postulated a role of these miRs either as onco-miRs or tumor suppressive miRs in other B- and T-cell malignancies.[105–108] In addition, we identified potential target genes, which likely arbitrate the pro-oncogenic effects of the respective miRs. Deregulations of the respective miRs were further associated with an activated phenotype or a more aggressive clinical course.

By analyzing the miR-omes and transcriptomes of primary T-PLL cells in an integrated fashion, we highlight a strong impact of miRs as post-transcriptional regulators on anti-apoptotic signaling and DNA damage repair mechanisms. Perturbations of these pathways are built on the basis of TCL1A overexpression and dysfunctional ATM aberrations.[36] We, here, postulate that the miR-ome of T-PLL cells forms regulatory networks, that substantially contribute to enhanced survival signaling and impaired DNA-damage repair mechanisms. Comparable networks were postulated for T-cell acute lymphoblastic leukemia (T-ALL) as well as CLL.[109,110]

Exemplarily, the miR-200c/141 cluster stood out as one of the most differentially expressed miR family in all three cohorts. For miR-200c and miR-141, both located on chromosome 12.p13, cell-type-specific functions have been postulated. While cancer progression was associated with high miR-200c/141 expression in ovarian cancer,[111] a diminished proliferation

capacity upon miR-200c/141 upregulation was observed in breast cancer.[112] In T-PLL, Erkeland and colleagues postulate a correlation of high miR-200c/141 expression with a shortened OS,[103] which we could not validate in our cohort. Potential target genes of this cluster, mediating a pro-oncogenic role in T-PLL, involve the cytokine *transforming growths factor beta 1* (*TGFB1*)[103] and the *large tumor suppressor kinase 1/2* (*LATS1/2*).

In summary, the identification of the recurrent genomic aberrations, involving the small RNA-binding protein AGO2, and of a T-PLL-specific gene expression signature, adds on the current understanding of T-PLL's leukemogenesis.[29] Based on *TCL1A* activating aberrations and perturbations of *ATM*, leading to enhanced TCR activation and reduced DNA repair capacities, a pre-leukemic T-PLL cell arises. Further leukemic outgrowth is mediated by the here identified overexpression of AGO2 and dysregulations of miRs, exemplarily represented by the upregulation of the miR-200c/141 cluster, besides JAK/STAT-activating lesions as well as epigenetic alterations (**Figure 9**).

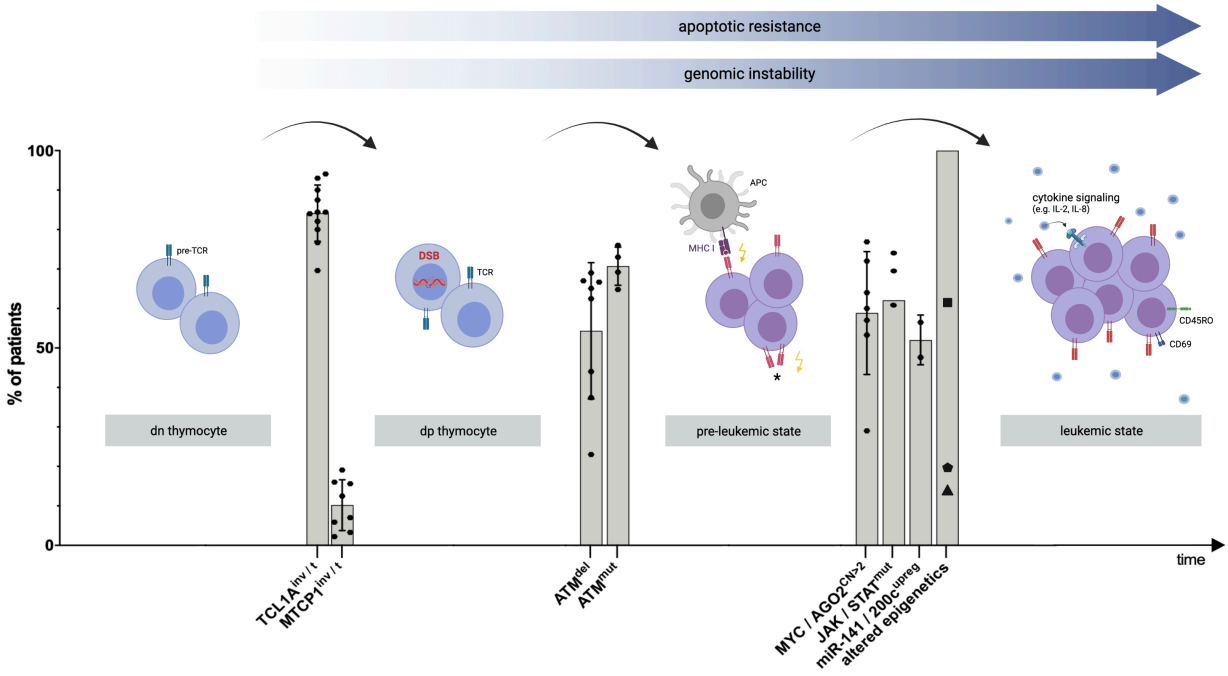

Figure 9: AGO2 overexpression and miR deregulations drive the transition of pre-leukemic T cells to the leukemic T-PLL state.
Schematic model of the clonal evolution of T-PLL cells, based on genomic profiling and corresponding functional analyses. X-axis: Timeline presenting the chronology of the most recurrent genomic aberrations. Y-axis: Percentage of T-PLL cases showing the respective genomic lesion (median ± standard deviation). The underlying publications can be found in [29]. *(i)* During the transition from double-negative (dn) thymocytes to the double-positive (dp) thymocyte stage, *translocations (t)* and *inversions (inv)* of chromosome 14 take place, leading to constitutive expression of the TCL1 family members *TCL1A* or *MTCP1*. *(ii)* Next, *deletions (del)* and *mutations (mut)* of *ATM* occur, resulting in an inability of the T-PLL cell, to undergo safeguarding mechanisms upon DNA damage. In addition, the TCR signaling threshold is lowered by overexpression of TCL1A. *(iii)* The final leukemic outgrowth of the T-PLL cell, resulting in an exponential proliferation, is mediated by a variety of genomic aberrations. Besides previously described activating lesions of the JAK/STAT signaling pathways and alterations of epigenetic

regulators, we identified overexpression of AGO2, resulting in enhanced TCR signaling activity, and miR deregulations, forming regulatory networks involved in survival signaling and DNA damage repair pathways, as major driving forces of the final leukemic outgrowth. Adapted from Braun *et al.*.[29]

6.5 Clinical implications

Highlighting the pathobiological impact of deregulations of RNA-binding proteins and miR deregulations, we established the first prognostic score, predicting the outcome of T-PLL patients. A potential application of the so-called miROS-T-PLL survival score is the differentiation between indolent and aggressive phases of T-PLL and, therefore, might help with the decision on therapeutic strategies ('watch and wait' vs. treatment indication). Notably, this score was validated in an independent test cohort.

A T-PLL-specific miR expression signature further implicates miR-based approaches as a new therapeutic strategy in the treatment of T-PLL. Both, miR-mimics for tumor suppressive miRs as well as anti-sense miRs directed against onco-miRs, are conceivable roads to be explored towards a therapy in T-PLL.[113] Exemplarily, an anti-sense inhibitor of miR-155 is currently under investigation in a phase-2 clinical trial for patients with CTCL (NCT03713320).

Moreover, the novel, non-canonical function of AGO2, leading to enhanced TCR signaling activity of T-PLL cells by interacting with ZAP70 and LCK, emphasizes the use of TCR signaling kinases as therapeutic targets in TPLL. For example, we recently presented data on first-generation inhibitors of the interleukine-2-inducible T-cell kinase (ITK2) in the treatment of T-PLL. Although the cell viability was not affected, we detected a diminished TCR activation upon treatment with these inhibitors.[114] In addition, a recent clinical trial tested the combination of the kinase inhibitor ibrutinib in combination with venetoclax,[115] however, the first evaluation did not present promising results (NCT03873493), further underlining the need for novel clinical trials.

6.6 Outlook

Although we present novel data on miR deregulations and the functional impact of the overexpression of the 'miR-master regulator' AGO2, our studies present several limitations, which have to be addressed in the future:

(i) Although we observed overexpression of AGO2 in almost every T-PLL case, this cannot always be explained by genomic aberrations, as shown by a lack of correlation between *AGO2* copy number and protein expression. Further regulatory mechanisms, such as the regulation of AGO2 protein stability by the availability of individual miRs,[96] need to be addressed in the future. In addition, the underlying mechanisms of miR deregulations we detected here, remain elusive, besides the identified influence of constitutive TCR activation. Mutations and CNAs of miR encoding genes as well as epigenetic mechanisms potentially contribute to the T-PLL specific miR-ome, as T-PLL cells are characterized by genomic instability and high burdens of

reactive oxygen species (ROS).[36] However, a systematic assessment of mutations and CNAs of miRs has not been performed in T-PLL.

(ii) The interaction of AGO2 with ZAP70 that was demonstrated *in vitro* as well as *in silico* requires further investigations, addressing the biochemical specifics of this interaction. In detail, the issue of distinguishing indirect miR-mediated ('canonical') vs. direct RNAi-independent ('non-canonical') mechanisms entails fundamental methodological challenges. As one approach, a model of an AGO2 mutant cell system that retains its catalytic domain but cannot interact with TCR kinases is conceivable. However, a genetically modified cell system as described before could generate an artificial cellular system, so that results would have to be interpreted with caution.[116] Another demanding approach addressing this question is to modify the phosphorylation of AGO2 at Tyr^{529}, which was essential for the binding of ZAP70 in our *in-silico* model. Nevertheless, the immediate recruitment of AGO2 at the activated TCR signaling complex strongly implicates a miR-independent function of AGO2.

(iii) Although we show seminal correlations of differentially expressed miRs with clinical parameters as well as potential target mRNAs, functional analyses of these miR alterations are pending. Experiments currently underway are investigating the impact of the miR-200c/141 cluster on the proliferative capacity of T-PLL cells, utilizing stably overexpressing miR-200c/141 T-cell lymphoma cell lines. In addition, we acquired first hints of further functions of AGO2 besides its role in TCR activation, as implicated by antibody-based phospho-kinase arrays. Exemplarily, the role of AGO2 on p27 deregulations should be a task of future research.

(iv) Having identified a TCR-shaping role of AGO2 in T-PLL, it remains unclear, in which phase of leukemogenesis this is of functional relevance (early vs. overt leukemia). It is conceivable that the described effect on TCR signaling capacity is particularly relevant in early phases of disease development and is replaced in later phases by autocrine signaling pathways and the loss of negative regulators. In addition, less is known about the phase-specific expression of the miR-ome and its functional consequences. To study these questions, the T-PLL-like *LCK^{pr}-$hTCL1A^{tg}$* mouse model[37] has to be utilized, as early disease stages or precursor cells are rarely diagnosed in humans. In this model, a phase-specific analysis of miR, as well as AGO2 expression, and their functional impacts is worth striving for.

7. Bibliography

1 Braun T, Stachelscheid J, Bley N, *et al.* Noncanonical Function of AGO2 Augments T-cell Receptor Signaling in T-cell Prolymphocytic Leukemia. *Cancer Research* 2022; **82**: 1818–31.

2 Braun T, Glass M, Wahnschaffe L, *et al.* Micro-RNA networks in T-cell prolymphocytic leukemia reflect T-cell activation and shape DNA damage response and survival pathways. *Haematologica* 2020; **107(1):**187-200.

3 Sung H, Ferlay J, Siegel RL, *et al.* Global Cancer Statistics 2020: GLOBOCAN Estimates of Incidence and Mortality Worldwide for 36 Cancers in 185 Countries. *CA: A Cancer Journal for Clinicians* 2021; **71**: 209–49.

4 Bray F, Laversanne M, Weiderpass E, Soerjomataram I. The ever-increasing importance of cancer as a leading cause of premature death worldwide. *Cancer* 2021; **n/a**.

5 Rahib L, Wehner MR, Matrisian LM, Nead KT. Estimated Projection of US Cancer Incidence and Death to 2040. *JAMA Network Open* 2021; **4**: e214708–e214708.

6 Hashim D, Boffetta P, La Vecchia C, *et al.* The global decrease in cancer mortality: trends and disparities. *Annals of Oncology* 2016; **27**: 926–33.

7 Parkin DM. Global cancer statistics in the year 2000. *The Lancet Oncology* 2001; **2**: 533–43.

8 Ninkovic S, Lambert J. Non-Hodgkin lymphoma. *Medicine* 2017; **45**: 297–304.

9 Macon WR. Peripheral T-Cell Lymphomas. *Hematology/Oncology Clinics of North America* 2009; **23**: 829–42.

10 Foss FM, Zinzani PL, Vose JM, Gascoyne RD, Rosen ST, Tobinai K. Peripheral T-cell lymphoma. *Blood* 2011; **117**: 6756–67.

11 Swerdlow SH, Campo E, Pileri SA, *et al.* The 2016 revision of the World Health Organization classification of lymphoid neoplasms. *Blood* 2016; **127**: 2375–90.

12 Matutes E, Brito-Babapulle V, Swansbury J, *et al.* Clinical and laboratory features of 78 cases of T-prolymphocytic leukemia. *Blood* 1991; **78**: 3269–74.

13 Alaggio R, Amador C, Anagnostopoulos I, *et al.* The 5th edition of the World Health Organization Classification of Haematolymphoid Tumours: Lymphoid Neoplasms. *Leukemia* 2022; **36**: 1720–48.

14 Catovsky D, Galetto J, Okos A, Galton DA, Wiltshaw E, Stathopoulos G. Prolymphocytic leukaemia of B and T cell type. *Lancet* 1973; **2**: 232–4.

15 Herling M, Patel KA, Teitell MA, *et al.* High TCL1 expression and intact T-cell receptor signaling define a hyperproliferative subset of T-cell prolymphocytic leukemia. *Blood* 2008; **111**: 328–37.

16 Dearden C. How I treat prolymphocytic leukemia. *Blood* 2012; **120**: 538–51.

17 Cross M, Dearden C. B and T cell prolymphocytic leukaemia. *Best Practice & Research Clinical Haematology* 2019; **32**: 217–28.

18 Jain P, Aoki E, Keating M, *et al.* Characteristics, outcomes, prognostic factors and treatment of patients with T-cell prolymphocytic leukemia (T-PLL). *Annals of Oncology* 2017; **28**: 1554–9.

19 Braun T, von Jan J, Wahnschaffe L, Herling M. Advances and Perspectives in the Treatment of T-PLL. *Curr Hematol Malig Rep* 2020; **15**: 113–24.

20 Staber PB, Herling M, Bellido M, *et al.* Consensus criteria for diagnosis, staging, and treatment response assessment of T-cell prolymphocytic leukemia. *Blood* 2019; **134**: 1132–43.

21 Herling M, Khoury JD, Washington LT, Duvic M, Keating MJ, Jones D. A systematic approach to diagnosis of mature T-cell leukemias reveals heterogeneity among WHO categories. *Blood* 2004; **104**: 328–35.

22 Mercieca J, Matutes E, Dearden C, MacLennan K, Catovsky D. The role of pentostatin in the treatment of T-cell malignancies: analysis of response rate in 145 patients according to disease subtype. *J Clin Oncol* 1994; **12**: 2588–93.

23 Weidmann E, Hess G, Chow KU, *et al.* A phase II study of alemtuzumab, fludarabine, cyclophosphamide, and doxorubicin (Campath-FCD) in peripheral T-cell lymphomas. *Leukemia and Lymphoma* 2010; **51**: 447–55.

24 Hopfinger G, Busch R, Pflug N, *et al.* Sequential chemoimmunotherapy of fludarabine, mitoxantrone, and cyclophosphamide induction followed by alemtuzumab consolidation is effective in T-cell prolymphocytic leukemia. *Cancer* 2013; **119**: 2258–67.

25 Pflug N, Cramer P, Robrecht S, *et al.* New lessons learned in T-PLL: results from a prospective phase-II trial with fludarabine–mitoxantrone–cyclophosphamide–alemtuzumab induction followed by alemtuzumab maintenance. *Leukemia & Lymphoma* 2019; **60**: 649–57.

26 Ginaldi L, De Martinis M, Matutes E, *et al.* Levels of expression of CD52 in normal and leukemic B and T cells: Correlation with in vivo therapeutic responses to Campath-1H. *Leukemia Research* 1998; **22**: 185–91.

27 Keating MJ, Cazin B, Coutré S, *et al.* Campath-1H Treatment of T-Cell Prolymphocytic Leukemia in Patients for Whom at Least One Prior Chemotherapy Regimen Has Failed. *Journal of Clinical Oncology* 2002; **20**: 205–13.

28 Dearden CE, Khot A, Else M, *et al.* Alemtuzumab therapy in T-cell prolymphocytic leukemia: comparing efficacy in a series treated intravenously and a study piloting the subcutaneous route. *Blood* 2011; **118**: 5799–802.

29 Braun T, Dechow A, Friedrich G, Seifert M, Stachelscheid J, Herling M. Advanced Pathogenetic Concepts in T-Cell Prolymphocytic Leukemia and Their Translational Impact. *Front Oncol* 2021; **11**: 775363.

30 Pegoraro L, Palumbo A, Erikson J, *et al.* A 14;18 and an 8;14 chromosome translocation in a cell line derived from an acute B-cell leukemia. *Proc Natl Acad Sci U S A* 1984; **81**: 7166–70.

31 Rabbitts TH. Translocations, master genes, and differences between the origins of acute and chronic leukemias. *Cell* 1991; **67**: 641–4.

32 Williams ME, Innes DJ, Borowitz MJ, *et al.* Immunoglobulin and T Cell Receptor Gene Rearrangements in Human Lymphoma and Leukemia. *Blood* 1987; **69**: 79–86.

33 Virgilio L, Narducci MG, Isobe M, *et al.* Identification of the TCL1 gene involved in T-cell malignancies. *Proc Natl Acad Sci U S A* 1994; **91**: 12530–4.

34 Patil P, Cieslak A, Bernhart SH, *et al.* Reconstruction of rearranged T-cell receptor loci by whole genome and transcriptome sequencing gives insights into the initial steps of T-cell prolymphocytic leukemia. *Genes Chromosomes Cancer* 2020; **59**: 261–7.

35 Maljaei SH, Brito-Babapulle V, Hiorns LR, Catovsky D. Abnormalities of Chromosomes 8, 11, 14, and X in T-Prolymphocytic Leukemia Studied by Fluorescence In Situ Hybridization. *Cancer Genetics and Cytogenetics* 1998; **103**: 110–6.

36 Schrader A, Crispatzu G, Oberbeck S, *et al.* Actionable perturbations of damage responses by TCL1/ATM and epigenetic lesions form the basis of T-PLL. *Nature Communications* 2018; **9**: 697.

37 Virgilio L, Lazzeri C, Bichi R, *et al.* Deregulated expression of TCL1 causes T cell leukemia in mice. *Proc Natl Acad Sci U S A* 1998; **95**: 3885–9.

38 Gritti C, Dastot H, Soulier J, *et al.* Transgenic mice for MTCP1 develop T-cell prolymphocytic leukemia. *Blood* 1998; **92**: 368–73.

39 Stilgenbauer S, Schaffner C, Litterst A, *et al.* Biallelic mutations in the ATM gene in T-prolymphocytic leukemia. *Nat Med* 1997; **3**: 1155–9.

40 Stengel A, Kern W, Zenger M, *et al.* Genetic characterization of T-PLL reveals two major biologic subgroups and *JAK3* mutations as prognostic marker. *Genes, Chromosomes and Cancer* 2016; **55**: 82–94.

41 Kiel MJ, Velusamy T, Rolland D, *et al.* Integrated genomic sequencing reveals mutational landscape of T-cell prolymphocytic leukemia. *Blood* 2014; **124**: 1460–72.

42 Johansson P, Klein-Hitpass L, Choidas A, *et al.* SAMHD1 is recurrently mutated in T-cell prolymphocytic leukemia. *Blood Cancer Journal* 2018; **8(1)**: 11.

43 Pollizzi KN, Powell JD. Integrating canonical and metabolic signalling programmes in the regulation of T cell responses. *Nat Rev Immunol* 2014; **14**: 435–46.

44 Warner K, Weit N, Crispatzu G, Admirand J, Jones D, Herling M. T-cell receptor signaling in peripheral T-cell lymphoma - a review of patterns of alterations in a central growth regulatory pathway. *Curr Hematol Malig Rep* 2013; **8**: 163–72.

45 Gorentla BK, Zhong X-P. T cell Receptor Signal Transduction in T lymphocytes. *J Clin Cell Immunol* 2012; **2012**: 5.

46 Bassing CH, Swat W, Alt FW. The mechanism and regulation of chromosomal V(D)J recombination. *Cell* 2002; **109 Suppl**: S45-55.

47 Letourneur F, Klausner RD. Activation of T cells by a tyrosine kinase activation domain in the cytoplasmic tail of CD3 epsilon. *Science* 1992; **255**: 79–82.

48 Chan AC, Desai DM, Weiss A. The role of protein tyrosine kinases and protein tyrosine phosphatases in T cell antigen receptor signal transduction. *Annu Rev Immunol* 1994; **12**: 555–92.

49 Braiman A, Barda-Saad M, Sommers CL, Samelson LE. Recruitment and activation of PLCgamma1 in T cells: a new insight into old domains. *EMBO J* 2006; **25**: 774–84.

50 Jang IK, Zhang J, Chiang YJ, *et al.* Grb2 functions at the top of the T-cell antigen receptor–induced tyrosine kinase cascade to control thymic selection. *Proceedings of the National Academy of Sciences* 2010; **107**: 10620 LP – 10625.

51 Porta C, Paglino C, Mosca A. Targeting PI3K/Akt/mTOR Signaling in Cancer. *Front Oncol* 2014; **4**: 64.

52 Oberbeck S, Schrader A, Warner K, *et al.* Non-canonical effector functions of the T-memory-like T-PLL cell are shaped by cooperative TCL1A and TCR signaling. *Blood* 2020; **136**: 2786–2802.

53 López C, Bergmann AK, Paul U, *et al.* Genes encoding members of the JAK-STAT pathway or epigenetic regulators are recurrently mutated in T-cell prolymphocytic leukaemia. *British Journal of Haematology* 2016; **173**: 265–73.

54 Wahnschaffe L, Braun T, Timonen S, *et al.* JAK/STAT-Activating Genomic Alterations Are a Hallmark of T-PLL. *Cancers (Basel)* 2019; **11**: 1833.

55 Tian S, Zhang H, Zhang P, *et al.* Epigenetic alteration contributes to the transcriptional reprogramming in T-cell prolymphocytic leukemia. *Scientific Reports* 2021; **11**: 8318.

56 Treiber T, Treiber N, Meister G. Regulation of microRNA biogenesis and its crosstalk with other cellular pathways. *Nature Reviews Molecular Cell Biology* 2019; **20**: 5–20.

57 Ha M, Kim VN. Regulation of microRNA biogenesis. *Nat Rev Mol Cell Biol* 2014; **15**: 509–24.

58 Lee Y, Kim M, Han J, *et al.* MicroRNA genes are transcribed by RNA polymerase II. *EMBO J* 2004; **23**: 4051–60.

59 Lee Y, Ahn C, Han J, *et al.* The nuclear RNase III Drosha initiates microRNA processing. *Nature* 2003; **425**: 415–9.

60 Lund E, Güttinger S, Calado A, Dahlberg JE, Kutay U. Nuclear export of microRNA precursors. *Science* 2004; **303**: 95–8.

61 Grishok A, Pasquinelli AE, Conte D, *et al.* Genes and mechanisms related to RNA interference regulate expression of the small temporal RNAs that control C. elegans developmental timing. *Cell* 2001; **106**: 23–34.

62 Kobayashi H, Tomari Y. RISC assembly: Coordination between small RNAs and Argonaute proteins. *Biochim Biophys Acta* 2016; **1859**: 71–81.

63 Djuranovic S, Nahvi A, Green R. miRNA-mediated gene silencing by translational repression followed by mRNA deadenylation and decay. *Science* 2012; **336**: 237–40.

64 Bazzini AA, Lee MT, Giraldez AJ. Ribosome profiling shows that miR-430 reduces translation before causing mRNA decay in zebrafish. *Science* 2012; **336**: 233–7.

65 Swarts DC, Makarova K, Wang Y, *et al.* The evolutionary journey of Argonaute proteins. *Nat Struct Mol Biol* 2014; **21**: 743–53.

66 Schirle NT, MacRae IJ. The crystal structure of human Argonaute2. *Science* 2012; **336**: 1037–40.

67 Kwak PB, Tomari Y. The N domain of Argonaute drives duplex unwinding during RISC assembly. *Nat Struct Mol Biol* 2012; **19**: 145–51.

68 Ma J-B, Ye K, Patel DJ. Structural basis for overhang-specific small interfering RNA recognition by the PAZ domain. *Nature* 2004; **429**: 318–22.

69 Ye Z, Jin H, Qian Q. Argonaute 2: A Novel Rising Star in Cancer Research. *J Cancer* 2015; **6**: 877–82.

70 Braun JE, Huntzinger E, Izaurralde E. The role of GW182 proteins in miRNA-mediated gene silencing. *Adv Exp Med Biol* 2013; **768**: 147–63.

71 Girard A, Sachidanandam R, Hannon GJ, Carmell MA. A germline-specific class of small RNAs binds mammalian Piwi proteins. *Nature* 2006; **442**: 199–202.

72 Winter J, Diederichs S. Argonaute proteins regulate microRNA stability: Increased microRNA abundance by Argonaute proteins is due to microRNA stabilization. *RNA Biol* 2011; **8**: 1149–57.

73 Cheloufi S, Dos Santos CO, Chong MMW, Hannon GJ. A dicer-independent miRNA biogenesis pathway that requires Ago catalysis. *Nature* 2010; **465**: 584–9.

74 Shen J, Xia W, Khotskaya YB, *et al.* EGFR modulates microRNA maturation in response to hypoxia through phosphorylation of AGO2. *Nature* 2013; **497**: 383–7.

75 Li L, Yu C, Gao H, Li Y. Argonaute proteins: potential biomarkers for human colon cancer. *BMC Cancer* 2010; **10**: 38.

76 Vaksman O, Hetland TE, Trope' CG, Reich R, Davidson B. Argonaute, Dicer, and Drosha are up-regulated along tumor progression in serous ovarian carcinoma. *Hum Pathol* 2012; **43**: 2062–9.

77 Wu S, Yu W, Qu X, *et al.* Argonaute 2 promotes myeloma angiogenesis via microRNA dysregulation. *J Hematol Oncol* 2014; **7**: 40.

78 Gao M, Wei W, Li MM, *et al.* Ago2 facilitates Rad51 recruitment and DNA double-strand break repair by homologous recombination. *Cell Research* 2014; **24(5)**: 532-41.

79 Gebert LFR, MacRae IJ. Regulation of microRNA function in animals. *Nature Reviews Molecular Cell Biology* 2019; **20**: 21–37.

80 Mardani R, Jafari Najaf Abadi MH, Motieian M, *et al.* MicroRNA in leukemia: Tumor suppressors and oncogenes with prognostic potential. *Journal of Cellular Physiology* 2019; **234**: 8465–86.

81 Lee RC, Feinbaum RL, Ambros V. The C. elegans heterochronic gene lin-4 encodes small RNAs with antisense complementarity to lin-14. *Cell* 1993; **75**: 843–54.

82 Kozomara A, Birgaoanu M, Griffiths-Jones S. miRBase: from microRNA sequences to function. *Nucleic Acids Res* 2019; **47**: D155–62.

83 Bernstein E, Kim SY, Carmell MA, *et al.* Dicer is essential for mouse development. *Nat Genet* 2003; **35**: 215–7.

84 Rajewsky N, Socci ND. Computational identification of microRNA targets. *Dev Biol* 2004; **267(2)**: 529-35.

85 Bartel DP. MicroRNAs: target recognition and regulatory functions. *Cell* 2009; **136**: 215–33.

86 Peng Y, Croce CM. The role of MicroRNAs in human cancer. *Signal Transduction and Targeted Therapy* 2016; **1**: 15004.

87 Calin GA, Dumitru CD, Shimizu M, *et al.* Frequent deletions and down-regulation of micro- RNA genes miR15 and miR16 at 13q14 in chronic lymphocytic leukemia. *Proc Natl Acad Sci U S A* 2002; **99**: 15524–9.

88 Klein U, Lia M, Crespo M, *et al.* The DLEU2/miR-15a/16-1 cluster controls B cell proliferation and its deletion leads to chronic lymphocytic leukemia. *Cancer Cell* 2010; **17**: 28–40.

89 Cimmino A, Calin GA, Fabbri M, *et al.* miR-15 and miR-16 induce apoptosis by targeting BCL2. *Proc Natl Acad Sci U S A* 2005; **102**: 13944–9.

90 Pekarsky Y, Santanam U, Cimmino A, *et al.* Tcl1 Expression in Chronic Lymphocytic Leukemia Is Regulated by miR-29 and miR-181. *Cancer Research* 2006; **66**: 11590–3.

91 Cardinaud B, Moreilhon C, Marcet B, *et al.* miR-34b/miR-34c: a regulator of TCL1 expression in 11q− chronic lymphocytic leukaemia? *Leukemia* 2009; **23**: 2174.

92 Vasyutina E, Boucas JM, Bloehdorn J, *et al.* The regulatory interaction of EVI1 with the TCL1A oncogene impacts cell survival and clinical outcome in CLL. *Leukemia* 2015; **29**: 2003.

93 Kopp KL, Ralfkiaer U, Nielsen BS, *et al.* Expression of miR-155 and miR-126 in situ in cutaneous T-cell lymphoma. *APMIS* 2013; **121**: 1020–4.

94 Kopp KL, Ralfkiaer U, Gjerdrum LMR, *et al.* STAT5-mediated expression of oncogenic miR-155 in cutaneous T-cell lymphoma. *Cell Cycle* 2013; **12**: 1939–47.

95 Manfè V, Biskup E, Rosbjerg A, *et al.* miR-122 Regulates p53/Akt Signalling and the Chemotherapy-Induced Apoptosis in Cutaneous T-Cell Lymphoma. *PLOS ONE* 2012; **7**: e29541.

96 Smibert P, Yang J-S, Azzam G, Liu J-L, Lai EC. Homeostatic control of Argonaute stability by microRNA availability. *Nat Struct Mol Biol* 2013; **20**: 789–95.

97 Qi HH, Ongusaha PP, Myllyharju J, *et al.* Prolyl 4-hydroxylation regulates Argonaute 2 stability. *Nature* 2008; **455**: 421–4.

98 Tien JC-Y, Chugh S, Goodrum AE, *et al.* AGO2 promotes tumor progression in KRAS-driven mouse models of non–small cell lung cancer. *Proceedings of the National Academy of Sciences* 2021; **118**: e2026104118.

99 Rüdel S, Wang Y, Lenobel R, *et al.* Phosphorylation of human Argonaute proteins affects small RNA binding. *Nucleic Acids Res* 2011; **39**: 2330–43.

100 Zhang K, Pomyen Y, Barry AE, *et al.* AGO2 Mediates MYC mRNA Stability in Hepatocellular Carcinoma. *Mol Cancer Res* 2020; **18**: 612–22.

101 Zhang H, Wang Y, Dou J, *et al.* Acetylation of AGO2 promotes cancer progression by increasing oncogenic miR-19b biogenesis. *Oncogene* 2019; **38**: 1410–31.

102 Yeh Y-Y, Ozer HG, Lehman AM, *et al.* Characterization of CLL exosomes reveals a distinct microRNA signature and enhanced secretion by activation of BCR signaling. *Blood* 2015; **125**: 3297–305.

103 Erkeland SJ, Stavast CJ, Schilperoord-Vermeulen J, *et al.* The miR-200c/141-ZEB2-TGFβ axis is aberrant in human T-cell prolymphocytic leukemia. *Haematologica* 2021; **107(1):** 143-153.

104 Patil P, Hillebrecht S, Chteinberg E, *et al.* T-cell prolymphocytic leukemia is associated with deregulation of oncogenic microRNAs on transcriptional and epigenetic level. *Genes, Chromosomes and Cancer* 2022; **61**: 432–6.

105 Pekarsky Y, Croce CM. Is miR-29 an oncogene or tumor suppressor in CLL? *Oncotarget* 2010; **1**: 224–7.

106 Feng YH, Tsao CJ. Emerging role of microRNA-21 in cancer (Review). Biomedical Reports. 2016; : 5(4): 395–402.

107 Pomari E, Lovisa F, Carraro E, *et al.* Clinical impact of miR-223 expression in pediatric T-Cell lymphoblastic lymphoma. *Oncotarget* 2017; **8**: 107886–98.

108 Humphries B, Yang C. The microRNA-200 family: small molecules with novel roles in cancer development, progression and therapy. *Oncotarget* 2015; **6**: 6472–98.

109 Mavrakis KJ, Van Der Meulen J, Wolfe AL, *et al.* A cooperative microRNA-tumor suppressor gene network in acute T-cell lymphoblastic leukemia (T-ALL). *Nature Genetics* 2011; **43**: 673–8.

110 Li J, Qin Y, Zhang H. Identification of key miRNA-gene pairs in chronic lymphocytic leukemia through integrated analysis of mRNA and miRNA microarray. *Oncol Lett* 2018; **15**: 361–7.

111 Ankasha SJ, Shafiee MN, Abdul Wahab N, Raja Ali RA, Mokhtar NM. Oncogenic Role of miR-200c-3p in High-Grade Serous Ovarian Cancer Progression via Targeting the 3'-Untranslated Region of DLC1. *Int J Environ Res Public Health* 2021; **18**: 5741.

112 Schickel R, Park S-M, Murmann AE, Peter ME. miR-200c regulates induction of apoptosis through CD95 by targeting FAP-1. *Mol Cell* 2010; **38**: 908–15.

113 Fuertes T, Ramiro AR, de Yebenes VG. miRNA-Based Therapies in B Cell Non-Hodgkin Lymphoma. *Trends in Immunology* 2020; **41**: 932–47.

114 Dondorf S, Schrader A, Herling M. Interleukin-2-inducible T-cell kinase (ITK) targeting by BMS-509744 does not affect cell viability in T-cell prolymphocytic leukemia (T-PLL). *J Biol Chem* 2015; **290**: 10568–9.

115 Kornauth CF, Herbaux C, Boidol B, *et al.* The combination of venetoclax and ibrutinib is effective in relapsed/refractory T-prolymphocytic leukemia and influences BCL-2-family member dependencies. *Hematological Oncology* 2019; **37**: 482–4.

116 Yang J-S, Lai EC. Alternative miRNA biogenesis pathways and the interpretation of core miRNA pathway mutants. *Mol Cell* 2011; **43**: 892–903.

8. Appendix

8.1 List of figures

9. Vorabveröffentlichungen von Ergebnissen

Braun T, Stachelscheid J, Bley N, *et al.* Noncanonical Function of AGO2 Augments T-cell Receptor Signaling in T-cell Prolymphocytic Leukemia. *Cancer Research* 2022; **82**: 1818–31.

Braun T, Glass M, Wahnschaffe L, *et al.* Micro-RNA networks in T-cell prolymphocytic leukemia reflect T-cell activation and shape DNA damage response and survival pathways. *Haematologica* 2020; **107(1):**187-200.

Noncanonical Function of AGO2 Augments T-cell Receptor Signaling in T-cell Prolymphocytic Leukemia

Till Braun[1], Johanna Stachelscheid[1], Nadine Bley[2], Sebastian Oberbeck[1], Moritz Otte[1], Tony Andreas Müller[1], Linus Wahnschaffe[1], Markus Glaß[2], Katharina Ommer[3], Marek Franitza[4], Birgit Gathof[3], Janine Altmüller[4], Michael Hallek[1], Daniel Auguin[5,6], Stefan Hüttelmaier[2], Alexandra Schrader[1], and Marco Herling[1,7]

ABSTRACT

T-cell prolymphocytic leukemia (T-PLL) is a chemotherapy-refractory T-cell malignancy with limited therapeutic options and a poor prognosis. Current disease concepts implicate TCL1A oncogene-mediated enhanced T-cell receptor (TCR) signaling and aberrant DNA repair as central perturbed pathways. We discovered that recurrent gains on chromosome 8q more frequently involve the *argonaute RISC catalytic component 2 (AGO2)* gene than the adjacent *MYC* locus as the affected minimally amplified genomic region. AGO2 has been understood as a protumorigenic key regulator of miRNA (miR) processing. Here, in primary tumor material and cell line models, AGO2 overrepresentation associated (i) with higher disease burden, (ii) with enhanced *in vitro* viability and growth of leukemic T cells, and (iii) with miR-omes and transcriptomes that highlight altered survival signaling, abrogated cell-cycle control, and defective DNA damage responses. However, AGO2 elicited also immediate, rather non–RNA-mediated, effects in leukemic T cells. Systems of genetically modulated AGO2 revealed that it enhances TCR signaling, particularly at the level of ZAP70, PLCγ1, and LAT kinase phosphoactivation. In global mass spectrometric analyses, AGO2 interacted with a unique set of partners in a TCR-stimulated context, including the TCR kinases LCK and ZAP70, forming membranous protein complexes. Models of their three-dimensional structure also suggested that AGO2 undergoes posttranscriptional modifications by ZAP70. This novel TCR-associated noncanonical function of AGO2 represents, in addition to TCL1A-mediated TCR signal augmentation, another enhancer mechanism of this important deregulated growth pathway in T-PLL. These findings further emphasize TCR signaling intermediates as candidates for therapeutic targeting.

Significance: The identification of AGO2-mediated activation of oncogenic T cells through signal amplifying protein–protein interactions advances the understanding of leukemogenic AGO2 functions and underlines the role of aberrant TCR signaling in T-PLL.

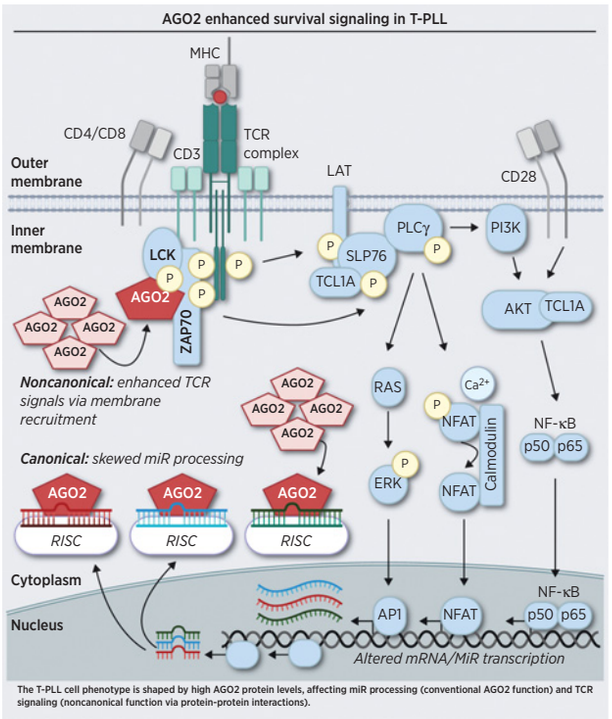

The T-PLL cell phenotype is shaped by high AGO2 protein levels, affecting miR processing (conventional AGO2 function) and TCR signaling (noncanonical function via protein-protein interactions).

Introduction

T-cell prolymphocytic leukemia (T-PLL) is a rare peripheral T-cell neoplasm, yet it represents the most common form of mature T-cell leukemias in the United States and Europe. It is characterized by an aggressive and chemotherapy-refractory course with currently very limited therapeutic options (1, 2). The median overall survival of patients is 20–36 months (3). Patients with T-PLL typically present

[1]Department I of Internal Medicine, Center for Integrated Oncology, Aachen-Bonn-Cologne-Duesseldorf, Excellence Cluster for Cellular Stress Response and Aging-Associated Diseases, Center for Molecular Medicine Cologne, University of Cologne, Cologne, Germany. [2]Institute of Molecular Medicine, Section for Molecular Cell Biology, Faculty of Medicine, Martin Luther University Halle-Wittenberg, Charles Tanford Protein Center, Halle, Germany. [3]Institute of Transfusion Medicine, University of Cologne, Cologne, Germany. [4]Cologne Center for Genomics, Center for Molecular Medicine Cologne, University of Cologne, Cologne, Germany. [5]University of d'Orléans, INRA, USC1328, Orléans, France. [6]Structural Motility, Institut Curie, CNRS, UMR 144, Paris, France. [7]Department of Hematology and Cellular Therapy, University of Leipzig, Leipzig, Germany.

Note: Supplementary data for this article are available at Cancer Research Online (http://cancerres.aacrjournals.org/).

S. Hüttelmaier, A. Schrader, and M. Herling contributed equally to this article.

Corresponding Author: Marco Herling, Hematology, Cell Therapy, Hemostaseology, University of Leipzig, Liebigstraße 22, Leipzig, Saxony 04103, Germany. Phone: 49-341-9713846; E-mail: marco.herling@medizin.uni-leipzig.de

Cancer Res 2022;82:1818–31

doi: 10.1158/0008-5472.CAN-21-1908

with exponentially rising lymphocyte counts and with bone marrow infiltration accompanied by marked (hepato)splenomegaly. Patients do not respond well to standard multiagent chemotherapies. Long-term remissions of >5 years can be accomplished in <20% of patients, but only if they undergo an allogeneic stem cell transplantation in first remission (2, 4). Such otherwise short-lived remissions are usually induced by the anti-CD52 anitibody alemtuzumab.

T-PLL cells are postthymic, antigen-experienced T lymphocytes (5, 6). Expression and functional competence of the T-cell receptor (TCR) is found in 80% of T-PLL cases, which is associated with a poor-prognostic hyperproliferative phenotype (6, 7). Moreover, global gene expression signatures in T-PLL resemble those of T-cell activation, further pointing toward a prominent role of TCR signals in T-PLL pathophysiology (8). However, despite these advances, novel rational treatment designs are urgently needed and these would tremendously benefit from a refined understanding of T-PLL's biology.

As one molecular hallmark and a central initiating lesion, >90% of T-PLL harbor chromosomal aberrations, that is *inv14* or *t(14;14)*, which lead to constitutive expression of the proto-oncogene *T-cell leukemia 1A* (*TCL1A*). This adapter molecule amplifies TCR signals via enhanced kinase activation in leukemic precursors and in tumor cells of T-PLL. In a threshold-lowering fashion, the aberrant TCL1A expression allows the (pre)leukemic memory-type T cell to drive on low-level (autonomous) TCR input and both signals, by TCL1A and by engaged TCR, cooperate toward T-PLL development (6–8). Additional recurrent genomic alterations in T-PLL target the *ataxia telangiectasia–mutated* tumor suppressor gene through deletions and damaging mutations as well as the *STAT5B/JAK1/JAK3* genes through gain-of-function mutations (8, 9).

In genome-wide analyses of somatic copy-number alterations (CNA) we previously identified gains on chromosome 8q in approximately 30% of T-PLL cases. Importantly, we discovered that these always (100%) involve the locus of *argonaute RISC catalytic component 2 (AGO2)*, and at lower frequencies (∼70%) the *MYC* proto-oncogene and the miRNAs (miR)-1206/1207/1208 (8). Recent descriptions of miR profiles in T-PLL revealed resemblance with those of TCR-activated T cells and integration with transcriptome data highlight regulatory networks of survival signaling and DNA damage responses, but the underlying causes of these changes in the leukemic miR-ome remained to be uncovered (10).

miRs assume crucial roles in cancer initiation and progression. Their deregulated levels are mostly attributable to genetic or epigenetic alterations that affect components of the miR processing machinery, such as *AGO2*, *DROSHA*, *XPO5*, or *DICER* (11). *AGO2* encodes for a component of the RNA-induced silencing complex (RISC) that is responsible for the inhibition of mRNA transcription upon miR binding and is, therefore, classified as the central mediator of miR processing (12). Among the four mammalian argonaute proteins, AGO2 is the only member that is endowed with a catalytic domain. Its endonuclease activity is essential for cleavage of the miR/siRNA passenger strand as well as of the RNA that is targeted by the miRs/siRNAs.

In the current study, we demonstrate a generally elevated AGO2 expression in primary T-PLL samples. Highest levels were associated with more aggressive disease parameters such as tumor burden, with a proproliferative cell phenotype, and with specific changes in miR-omes and transcriptomes. Further characterizing the potential oncogenic function of AGO2 in T-PLL, we describe AGO2 interactomes in the context of TCR activation and discover protein–protein interactions of AGO2, that is, with the ζ-chain–associated protein kinase 70 (ZAP70) that, at least in part, underlie the AGO2-dependent TCR hyperactivation in T-PLL.

Materials and Methods

Patient material and clinical data

Peripheral blood (PB)-derived T-cell isolates were obtained from 56 patients with T-PLL and from 8 age-matched healthy donors. The majority of samples ($n = 47/56$; 83.9%) were from treatment-naïve patients. The median age of the cohort was 68 years (range from 32–88 years) and 48.2% of patients were females (summarized data in Supplementary Table S1).

Details on isolation of PB mononuclear cells and magnetic bead–based cell enrichment of pan-$CD3^+$ T cells are presented in the Supplementary Materials and Methods. Patients with T-PLL fulfilling the consensus criteria for the diagnosis of T-PLL (2) were included in the study. We did not define exclusion criteria for this study and patients were not randomized into groups because this was deemed irrelevant to this study. Written informed consent according to the Declaration of Helsinki was provided by all patients and healthy donors. Collection and use of the samples were approved for research purposes by the ethics committee of the University Hospital of Cologne (Cologne, Germany; #12-146, #19-1085, and #19-1089). Individual demographics and detailed information on clinical characteristics, cytogenetics, immunophenotypes, and follow-up for all 56 patients are presented in Supplementary Table S2).

Association of AGO2 protein with clinical data and with miR/mRNA alterations

For all patients of this 56-case set, triplicate immunoblot studies for AGO2 protein expression were performed following standard protocols (see Supplementary Materials and Methods; AGO2 antibody clone 11A9, gift of G. Meister, University of Regensburg, Regensburg, Germany). To assess for clinical associations with AGO2 expression, patients were divided in tertiles based on their AGO2 protein levels. Overlap of all profiling data (Supplementary Fig. S1A) allowed associations of AGO2 protein with *AGO2* mRNA and with *AGO2* copy number (CN) status in 46 of these 56 patients.

Moreover, we previously performed transcriptome and small RNA sequencing in a cohort of 46 T-PLL (10). Details on RNA isolation, sequencing, and data processing are given in (10). As part of this study, we obtained AGO2 protein expression data in 41 of those 46 patients with T-PLL. Differentially expressed genes and miRs between the high AGO2 protein tertile ($n = 14$) versus low AGO2 tertile ($n = 14$) were calculated (FDR < 0.05). Gene set enrichment analyses (GSEA) were performed on differentially expressed mRNAs as well as on sorted lists of protein-coding genes, based on Spearman correlation coefficients for each differentially expressed miR. Hallmark gene sets were applied (13). The Mann–Whitney–Wilcoxon (MWW) test was performed for systematic comparison of continuous data and the Fisher exact test for categorical data. A P value <0.05 was considered statistically significant.

Cell cultures

Primary T-PLL cells were cultured in suspension at concentrations of 2×10^6 cells/mL in RPMI1640 (Gibco, catalog no. 21875-034), supplemented with 10% FBS (Gibco, catalog no. 10270-106) and penicillin/streptomycin at 100 U/L (Gibco, catalog no. 15140-122). The T-cell leukemia/lymphoma cell lines Jurkat (male-derived, ATCC, catalog no. TIB-152, RRID:CVCL_0367) and the male-derived Hut78 (ATCC, catalog no. TIB-161, RRID:CVCL_0337) were used

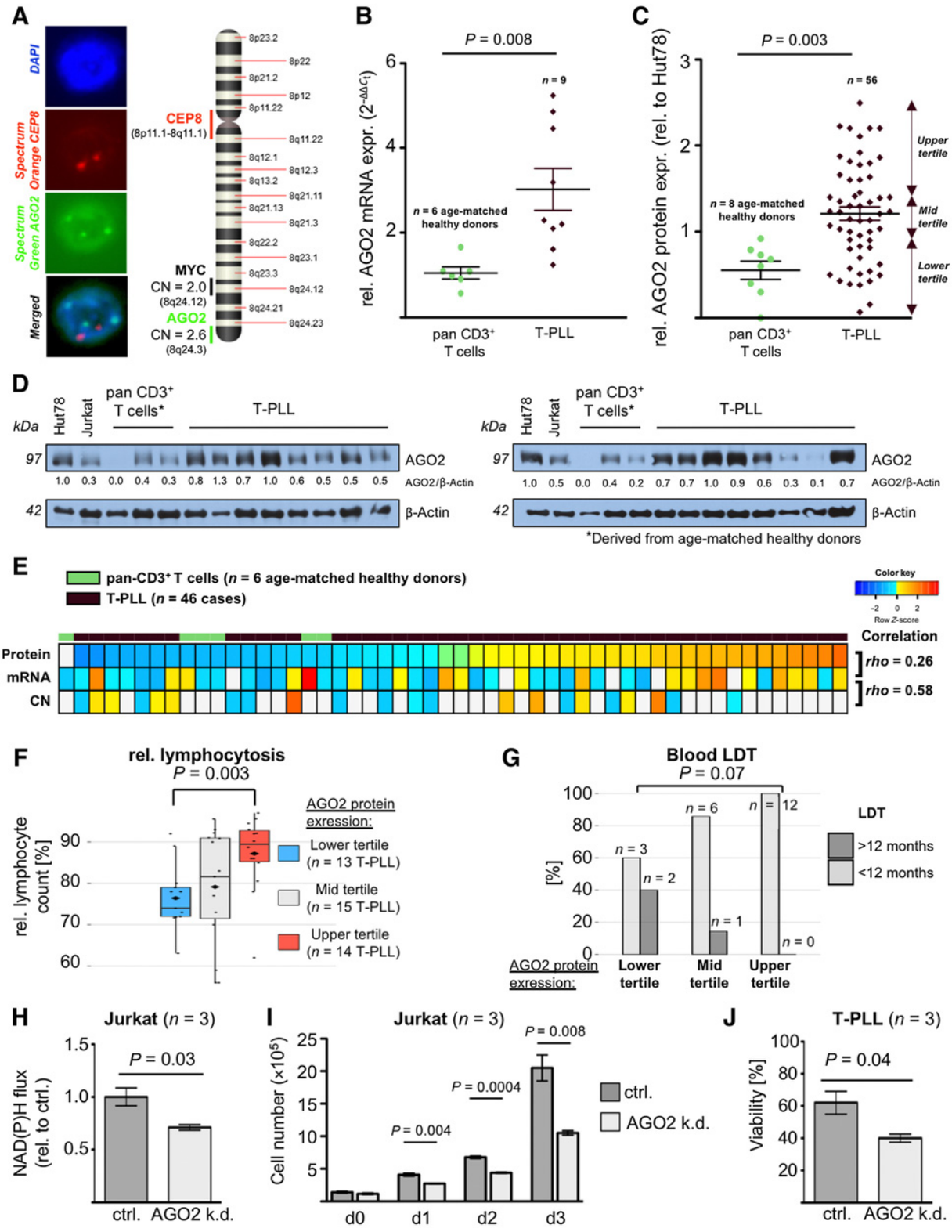

for *in-vitro* experiments. The identity of all cell lines was recently authenticated by short tandem repeat analysis. Presence of *Mycoplasma* was periodically tested by PCR. Their suspensions ($0.5–1.0 \times 10^6$ cells/mL) were maintained in RPMI1640 with 10% FBS. Details on transient AGO2 knockdowns, TCR stimulation, induction of DNA damage, and on assessment of cell viability, proliferation, and survival are presented in the Supplementary Materials and Methods. FISH, qRT-PCR, and immunoblots were performed according to standard procedures (8) and described in the Supplementary Materials and Methods.

Phosphokinase arrays

Phosphorylation of 43 human protein kinases in relation to two reference proteins was measured by an immunoblot-based human phosphokinase array (R&D Systems, catalog no. ARY003B). Details are given in the Supplementary Materials and Methods.

Immunoprecipitation and mass spectrometry

Detailed protocols on the analysis of the composition of immunoisolated protein complexes are provided in the Supplementary Materials and Methods. Generally, precleared protein lysates of three technical replicates each were incubated with bead-bound protein G–coupled AGO2 antibodies (Abcam, catalog no. ab186733, RRID: AB_2713978) or IgG isotype control (Cell Signaling Technology, catalog no. 2975, RRID:AB_10699151). Proteins eluted from the beads were denatured and electrophoretically separated. After trypsin and endoproteinase Lys-C based in-gel digestion and extraction, resulting peptides were subjected to high-resolution mass spectrometry (MS) in the CECAD Proteomics facility (for protocols, equipment, and raw data processing algorithms see Supplementary Materials and Methods).

Immunofluorescence stainings, proximity ligation assay, and confocal microscopy

Jurkat or primary T-PLL cells, untreated or pretreated with 10 μmol/L of the LCK inhibitor CAS 213743-31-8 (Sigma-Aldrich, catalog no. 428205-M), or with 10 μmol/L dasatinib (MedChemEx, HY-10181, CAS 302962-49-8) for 24 hours where indicated, were stimulated on anti-CD3 (BioLegend, catalog no. 317348 clone OKT3, RRID:AB_2571995)-coated coverslips for indicated times and fixed with paraformaldehyde. After blocking of the cross-linking antibody by incubation with IRDye800 anti-mouse antibody (LI-COR Biosciences, catalog no. 926-32212, RRID:AB_621847) for 1 hour at room temperature and additional paraformaldehyde fixation for 10 minutes, cells were permeabilized by 0.5% Triton X-100 in PBS for 5 minutes. Unspecific antibody binding was blocked for 15 minutes by 1% BSA in PBS, before samples were incubated with primary antibodies against ZAP70 (Cell Signaling Technology, catalog no. 3165, RRID: AB_2218656, 1:100) and AGO2 (Santa Cruz Biotechnology, catalog no. sc-53521, RRID: AB_628697, 1:50) for 1 hour at room temperature in 1% BSA in PBS.

For confocal microscopy, samples were incubated with anti-mouse Cy3 (Jackson ImmunoResearch, catalog no. 715-165-150, RRID: AB_2340813) and anti-rabbit alexa488 (Jackson ImmunoResearch, catalog no. 711-545-152, RRID:AB_2313584) secondary antibodies for 1 hour at room temperature. For proximity ligation assays (PLA), the Duolink In Situ Red Starter Kit Mouse/Rabbit (Sigma-Aldrich, catalog no. DUO92101) was applied according to manufacturer's instructions starting with the secondary antibodies. Nuclei were visualized using DAPI (Sigma, catalog no. D9542). Images were acquired on a Leica SP8X with white laser and HyD detector using a 63× objective and standard settings for sequential imaging. For data analyses, the FIJI/imageJ software was used to quantify PLA spots. For each condition, 50–100 cells were analyzed. Statistical significance was determined by a Mann–Whitney rank-sum test.

In silico modeling of AGO2–ZAP70 complexes

Singular models: Experimentally determined structures were integrated with predicted models (14) to gain highest possible accuracy of the implicated interactions. Recompiled information on the phosphorylation states of active forms was taken from UniProt (15) to amend the models accordingly.

Complexes of AGO2 with ZAP70 and ZAP70 with LCK: Searches of productive interactions by *in silico* docking with ambiguous interaction restraints defined around putative targets [relied on comparative alignments and data accessible on the PhosphositePlus (16)] were completed using the program Haddock (17) on the experimentally determined structures of the considered domains. The resulting models, in which the targeted tyrosine was too far away

Figure 1.

T-PLL cells exhibit elevated AGO2 protein expression levels associated with unfavorable clinical parameters and T-cell proliferation *in vitro*. **A,** Exemplary FISH (scale bar, 5 μm) presenting an *AGO2* amplification in a patient with T-PLL with preserved biallelic *MYC* (note: a rare case with normal karyogram of otherwise chromosome 8q–affected cases). **B,** *AGO2* mRNA was significantly upregulated in T-PLL ($P = 0.008$, Student *t* test) as analyzed by qRT-PCR (nine T-PLL samples; dark-brown) relative to mean values of healthy donor–derived pan-CD3$^+$ T cells (6 age-matched donors; green) by the $2^{-\Delta\Delta C_T}$ method. **C,** Expression of AGO2 protein was upregulated in T-PLL as compared with healthy donor–derived pan-CD3$^+$ T cells ($P = 0.004$, Student *t* test) as determined by immunoblots and subsequent densitometric quantification relative to Hut78 cells ($n = 56$ T-PLL, 8 age-matched healthy donors). AGO2 protein expression was determined by evaluating on average three independent immunoblots for each case. T-PLL cases were divided into three tertiles based on their AGO2 protein levels relative to the Hut78 control cell line (red, upper tertile, 1.4-fold to 2.5-fold expression; blue, lower tertile, 0.1-fold to 0.9-fold expression). **D,** Exemplary immunoblot from **C** showing upregulated AGO2 protein expression in T-PLL as compared with healthy donor–derived pan-CD3$^+$ T cells. **E,** CN gains of *AGO2* significantly correlated with elevated mRNA levels ($P = 0.02$, $R^2 = 0.58$ Spearman correlation) and *AGO2* mRNA levels were associated with AGO2 protein levels ($P = 0.08$, $R^2 = 0.26$ Spearman correlation). Heatmap presenting the *AGO2* CN status [as defined by SNP arrays (8)], *AGO2* mRNA levels [as defined by mRNA-seq (10)], and AGO2 protein levels (as defined by immunoblots) for 46 T-PLL cases each. Color codes represent z-scores based on means of the respective data dimension. Correlations are depicted in Supplementary Fig. S1. **F** and **G,** High AGO2 protein expression was associated with a higher relative lymphocytosis (mean: 87.2% vs. 76.4%, $P = 0.003$, MWW test) in blood at the time of sample acquisition and a shorter lymphocyte doubling time (LDT; $n = 12/12$ AGO2-high cases presenting a LDT <12 months vs. $n = 3/5$ cases in the low-AGO2 expressing tertile; $P = 0.07$, Fisher exact test). T-PLL cases were divided into three tertiles according to **Fig. 1C**. See Supplementary Table S3 for a summary of clinical data and Supplementary Fig. S2 for correlations and for additional data on platelet counts and serum LDH levels. **H** and **I,** Jurkat cells showed a reduced metabolic activity (measured by MTS assay; $P = 0.03$, Student *t* test; **H**) and a diminished proliferation (by cell counts at indicated time points; Student *t* test; **I**) upon siRNA-mediated AGO2 downregulation. Bar charts presenting metabolic activity and cell growth after transient AGO2 downregulation (ctrl, nontargeting siRNA pool, dark gray; AGO2 k.d., AGO2-targeting siPool, light gray). **J,** T-PLL cells showed reduced viability upon transient siRNA-mediated AGO2 downregulation ($P = 0.04$, Student *t* test) as detected via trypan blue staining aided cell counting 48 hours after siRNA nucleofection. Verification of AGO2 downregulation in Jurkat and primary T-PLL cell systems via immunoblot is presented in Supplementary Fig. S3.

from the gamma phosphate of ATP, were considered unlikely based on the assumption that the interaction is to result in tyrosine phosphorylation. Each chain of retained models was fused back into its relative structure and the whole complex was further challenged in a 60 ns molecular dynamics run in a water box.

Functional model TCR:LCK:ZAP70:AGO-2: The conjectural model was based on the motif analyses and SH2 and SH3 domain specificities. The placement of each protagonist was deduced from accessibilities and executed "by hand" in a PyMOL session. The whole system including a POPC membrane was built-up using the Membrane Builder module from CHARMM-GUI (18).

Short molecular dynamics or minimizations: The complex models were used to build systems in all-atoms molecular dynamics in explicit water at 150 mmol/L KCl with CHARMM-GUI (18). GROMACS (19) was used for these tasks. The Zap70:AGO-2 complex was challenged for 60 ns in a system of 464,189 atoms, while the conjectural model embedded in a membrane and consisting in a system of 1,778,446 atoms was simulated for a 10 ns, both remaining steady in the intervals. Simulations were executed by keeping the temperature at 310.15 K and pressure at 1 atm. Standard CHARMM-GUI output protocols were used.

Data availability

MS-based proteomics data are deposited at the ProteomeXchange Consortium via the PRIDE (20) partner repository with the dataset identifier PXD028170. Details on data processing and data availability of total and small RNA expression data used in this study are given in ref. 10. Further information and requests for resources and reagents should be directed to and will be fulfilled by the corresponding author.

Results

Elevated AGO2 protein expression in T-PLL is associated with unfavorable clinical parameters and enhanced T-cell proliferation *in vitro*

Central piece of this study was an integrated multilevel dataset derived from a cohort of 46 well-annotated T-PLL cases. Their primary PB-derived T-PLL cells were analyzed for CNAs, miR-ome profiles, and transcriptome signatures (Supplementary Fig. S1A). AGO2 protein expression was analyzed in 41 of those and in 15 additional cases (Supplementary Table S2). At the outset, we recapitulated our SNP-array based observation that genetic amplification of *AGO2* was involved in all of those T-PLL cases that harbored a minimally amplified region (MAR) on chromosome 8q (8). Here, all cases harboring this MAR showed a gain of *AGO2* ($n = 12/12$, average CN = 2.4; Supplementary Table S1), while the neighbouring *MYC* locus was only involved in approximately 80% of cases ($n = 10/12$, average CN = 2.3). **Figure 1A** illustrates biallelic *MYC* adjacent to an *AGO2* CN gain. Genomic losses of *AGO2* were not discovered here, neither were they reported previously (8, 21). Corresponding with this overrepresentation of *AGO2*, we observed elevated expression of *AGO2* mRNA in eight of nine isolates from primary T-PLL samples (by qRT-PCR) and of AGO2 protein (immunoblot-based levels) in cells from 41 of 56 analyzed cases as compared with healthy donor–derived pan-$CD3^+$ T cells [fold-change (fc) >1.5; **Fig. 1B–D**; Supplementary Tables S1 and S2]. While *AGO2* mRNA expression significantly correlated with the corresponding protein expression, there was no significant correlation between *AGO2* CN and protein expression, indicating additional ways of AGO2 upregulation beyond the genomic gains (**Fig. 1E**; Supplementary Fig. S1B and S1C). T-PLL with high AGO2 protein expression had a mean *AGO2* CN of 2.43 (vs. mean *AGO2* CN of 2.27 in those with low AGO2 protein expression).

We next associated AGO2 expression with clinical characteristics. Higher AGO2 protein levels were predominantly found in cases with more aggressive features, as represented by higher blood lymphocytosis, a shorter lymphocyte doubling time, more reduced platelet counts, and higher serum lactate dehydrogenase (LDH) levels (**Fig. 1F** and **G**; Supplementary Fig. S2A–S2D; Supplementary Table S3). Subsequent AGO2 knockdown experiments in Jurkat T cells and in primary T-PLL samples underlined the proactive tumor-promoting role of AGO2. Induced reduction of AGO2 negatively affected cellular metabolic activity [as measured by NAD(P)H flux], viability, and proliferative capacity (**Fig. 1H–J**; Supplementary Fig. S3A and S3B). Negative CERES dependency scores in hematopoietic and T-cell leukemia/lymphoma lines indicated that AGO2 is essential for most represented lines (depmap portal; Supplementary Fig. S3C).

miR-omes and transcriptomes in high AGO2 protein–expressing T-PLL reveal prominent signatures of enhanced survival signaling, augmented cell-cycle transition, and impaired DNA damage responses

To dissect how AGO2 might mediate this proleukemic effect, we followed two distinct strategies: (i) to evaluate global miR-mediated protumorigenic functions of AGO2 by analyzing miR/mRNA expression profiles associated with high AGO2 levels and (ii) to define immediate, potentially miR-independent, effects of high-level AGO2 on T-PLL–intrinsic oncogenic pathways through identification of direct AGO2–protein interactions.

Thus, we first analyzed in an integrated fashion the transcriptomes and miR-omes of primary T-PLL (generated as part of ref. 10) in association with stratified AGO2 protein expression. Using upper and lower tertiles, we compared $n = 14$ "*AGO2-high*" versus $n = 14$ "*AGO2-low*" cases (see Materials and Methods and Supplementary Table S2 for definition) with respect to AGO2-associated miR/mRNA deregulations (**Fig. 2A** and **B**). We identified an overall higher number of downregulated mRNAs ($n = 209$ vs. $n = 30$) and miRs ($n = 62$ vs. $n = 5$) in AGO2-high cases, suggesting a globally enhanced miR-mediated mRNA degradation (Supplementary Fig. S4A and S4B; Supplementary Table S4). This is in line with AGO2's established central function in RISC-mediated gene silencing.

miR-mediated regulation of cellular processes is based on the induction of low-level changes of mRNA abundances affecting a larger cohort of genes rather than one single factor (10). Thus, we refrained from analyzing specific single genes in detail but conducted GSEAs using the complete list of AGO2-associated mRNAs and miRs (Supplementary Table S4). As GSEA can only be performed on mRNA expression data (not miRs), we performed the latter analyses on mRNAs predicted to be regulated (and thus differentially expressed) by the identified AGO2-associated miRs.

Particularly mRNAs and miRs associated with the GSEA-based Hallmark pathways of survival signaling (e.g., "IL2/STAT5 signaling"), cell-cycle control (e.g., "E2F targets" or "G_2–M Checkpoint"), and DNA damage responses (e.g., "DNA repair" or "p53 Pathway") were significantly affected (T-PLL with high vs. low AGO2 protein; **Fig. 2C**; Supplementary Fig. S4C; Supplementary Table S4). Similar associations of AGO2 expression with gene expression profiles were found in cell line systems of short hairpin RNA–mediated AGO2 knockdown (Supplementary Fig. S5A and S5B; ref. 22), pointing toward a potential regulatory involvement of AGO2 in these processes.

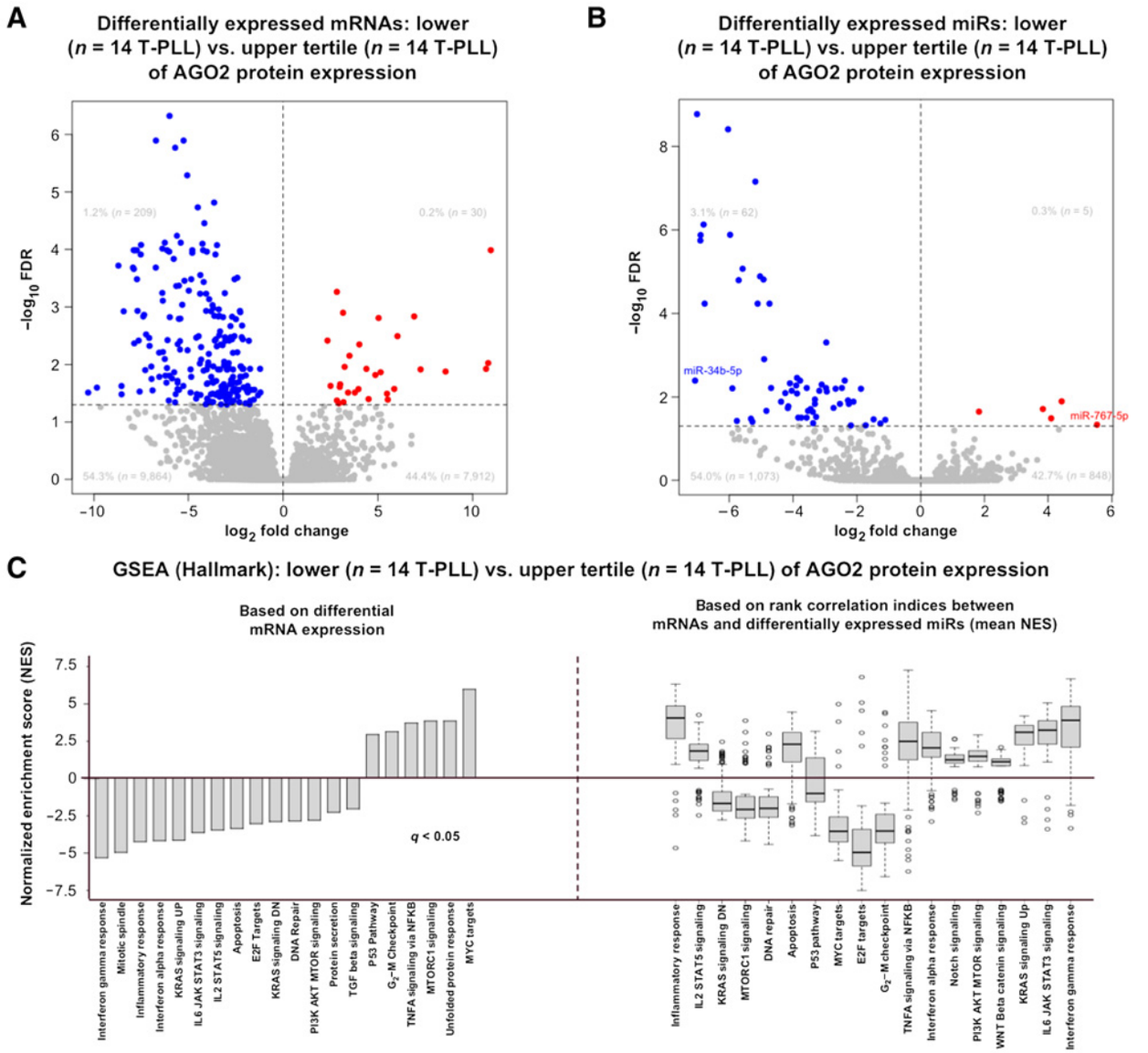

Figure 2.

Higher AGO2 protein expression associates with T-PLL miR-omes and transcriptomes of enhanced survival signaling, pronounced cell-cycle transition, and impaired DNA damage responses. Primary T-PLL cells (41 cases) were divided into three tertiles based on their AGO2 protein expression (see Supplementary Table S2). **A** and **B,** Volcano plots show fcs and FDRs of all expressed mRNAs [$n = 18{,}015$; polyA-RNA sequencing (10); **A**] and miRs [$n = 1{,}988$; small RNA sequencing (10); **B**]. Differentially expressed mRNAs/miRs comparing high versus low AGO2 protein–expressing T-PLL are highlighted in blue (down-regulation) and red (upregulation); see Supplementary Fig. S4A and S4B, and Supplementary Table S4 for heatmaps and gene lists. Given percentages indicate relative proportions based on all identified mRNAs. High AGO2 protein–expressing T-PLL showed a generally downregulated transcriptome and miR-ome. **C,** GSEA was performed for all differentially expressed mRNAs/miRs. mRNAs: Selected significantly enriched Hallmark pathways are displayed in the bar chart ($q < 0.05$, Kolmogorov–Smirnov test). An overview of all Hallmark pathways is given in Supplementary Table S4. miRs: GSEAs were conducted for all significantly deregulated miRs between the upper and lower tertile ($n = 67$ miRs) using ranked correlation indices between mRNA and miR expression in 41 T-PLL and 6 healthy donor–derived T-cell samples. Selected Hallmark pathways were summarized by calculating the mean normalized enrichment score of all 67 analyzed miRs and are displayed as box-whisker plots. See Supplementary Fig. S4C for heatmap showing all identified pathways. See **Fig. 5** for validation of selected Hallmark pathways in K-562 cells.

As a noncanonical function, AGO2 protein enhances leukemic TCR signaling

Besides its role in global miR/mRNA network regulation, AGO2 has been described to also directly interact with and to impact factors involved in pro-oncogenic pathways, for example, RAD51 in DNA damage responses (23). Moreover, given the central role of the TCR pathway in growth and survival of the T-PLL cell (6, 7) and to assess for nonconventional functions of AGO2, that is, in regulating intermediates of the TCR cascade, we interrogated the impact of modulated AGO2 on TCR signaling. First, using antibody-based phosphokinase

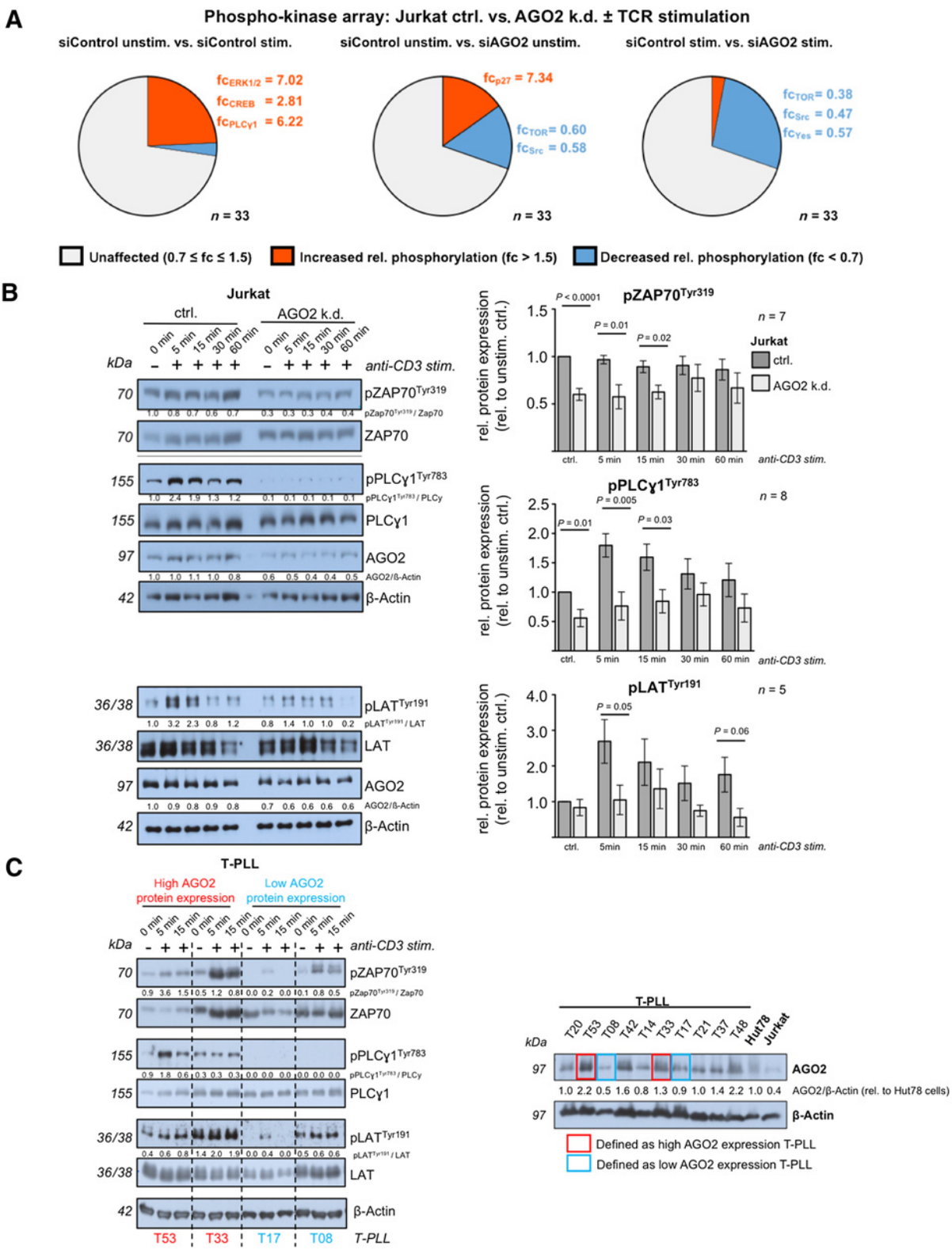

arrays, we observed diminished TCR-induced responses (anti-CD3 cross-linking) subsequent to siRNA-mediated AGO2 knockdowns in Jurkat T cells (selected kinases in **Fig. 3A**, examples in Supplementary Fig. S6A–S6C, for example, TOR, fc = 0.38; Src, fc = 0.47). While AGO2 knockdown cells presented a strong upregulation of p27 in the unstimulated condition (fc = 7.34), we showed downregulation of TCR-associated kinases in both conditions upon AGO2 downregulation (e.g., unstimulated condition: TOR, fc = 0.60; Src, fc = 0.58; stimulated condition: TOR, fc = 0.38; Src, fc = 0.47). Next, the positive effect of AGO2 on TCR-triggered kinase activation was specifically validated for pZAP70, pPLCγ1, and pLAT in separate AGO2 knockdown experiments in Jurkat cells (**Fig. 3B**; Supplementary Fig. S7A). Notably, we did not observe an altered expression or signal-induced phosphorylation of the proximal TCR kinase LCK upon AGO2 knockdown (Supplementary Fig. S7B). We further validated the enhancing effect of AGO2 upregulation on the TCR signaling cascade downstream of LCK in the Hut78 T-cell leukemia line (Supplementary Fig. S7C) as well as in AGO2-level stratified primary T-PLL samples (**Fig. 3C**). As for AGO2 protein expression itself, we observed elevated levels upon TCR stimulation in pan-$CD3^+$ T cells of one out of healthy donor samples and in 1 patient with T-PLL, with a stronger basal and longer-lasting upregulation of AGO2 in the T-PLL case (Supplementary Fig. S8).

To control for the possibility of TCR-induced signaling responses being altered merely due to an impaired miR processing machinery, we experimentally modified DICER expression levels in Jurkat cell systems to induce a global reduction of RISC complex function (Supplementary Fig. S9A–S9C; ref. 24). Detecting phosphorylation of LAT, ZAP70, and PLCγ1 upon TCR activation via anti-CD3 cross-linking and using immunoblots, we did not identify alterations in TCR pathway responses in DICER knockdown conditions.

These AGO2 knockdown systems also allowed us to validate the role of AGO2 in regulating its "conventional" effectors, such as the tumor suppressor p27. AGO2-depleted Jurkat T cells showed a strong upregulation of p27 in the TCR-unstimulated baseline condition (Supplementary Fig. S6C, fc = 7.34). According to p27's cell cycle and survival-regulating functions, this was associated with a reduced apoptotic resistance in response to irradiation-induced DNA damage (Supplementary Fig. S10).

Membrane-bound AGO2-ZAP70 protein complexes are formed upon TCR stimulation

To interrogate the TCR-enhancing impact of AGO2 as RNA-independent effects of the AGO2 protein in more detail, that is, to identify the underlying molecular mediators, we conducted immunoprecipitation experiments of endogeneous AGO2 in TCR-unstimulated versus TCR-activated Jurkat T cells (naturally TCL1A negative; **Fig. 4A**). Short-time TCR stimulation of 5 minutes was chosen to minimize miR-based and transcriptional effects on the interactome of AGO2. Subsequent MS analysis of AGO2-immune complexes identified 698 AGO2-interacting proteins common to both experimental conditions (**Fig. 4B–D**; Supplementary Fig. S11A and S11B; Supplementary Table S5), while 44 proteins were specifically enriched in the TCR-activated condition (Supplementary Fig. S11C). A functional network analysis of significantly enriched Reactome pathways ($P \leq 0.001$) showed a dominant association of AGO2 interactors with pathways of "RNA metabolism" (**Fig. 4E**; e.g., survival of motor neuron SMN1). This also identified coprecipitated proteins to be involved in regulation of "gene expression" (e.g., RISC-loading complex subunit TARBP2, histone deacetylase HDAC1), "DNA repair" (e.g., PARP1, an ADP-ribosylating enzyme essential for initiating various forms of DNA repair), and "cell-cycle control" (e.g., the cyclin-dependent kinase CDK1).

Importantly, the analysis of AGO2-antibody enriched proteins additionally identified LCK and ZAP70, both central kinases of the TCR signal cascade, as AGO2 protein complex constituents. We validated the interaction of AGO2 with ZAP70 and with phospho-$ZAP70^{Tyr319}$ in Western blot analyses of AGO2 immunoprecipitations in Jurkat T cells (**Fig. 4F**) and in primary T-PLL cells ($n = 3$, **Fig. 4G**). Of note, these protein interactions were predominantly detected under TCR-stimulated conditions.

To validate and to further interrogate the TCR-induced AGO2-ZAP70 complex formation, we applied confocal microscopy and PLAs in Jurkat cell line systems and primary T-PLL cells (**Fig. 5**; Supplementary Fig. S12). The amount of induced cytoplasmic membrane–associated AGO2-ZAP70 overlap peaked at 10 minutes subsequent to anti–CD3-mediated TCR activation as detected by AGO2 (green) and ZAP70 (red) fluorescence signals (**Fig. 5A**) and by PLA-assessed spots per cell (Supplementary Fig. S12A). TCR-signal dependence of AGO2-ZAP70 complexes was further underlined by inhibition of LCK through pretreatment of cells with CAS213743-31-8 or dasatinib (**Fig. 5B** and **C**; Supplementary Fig. S12B and S12C). Such blocking of LCK-mediated signal transduction in anti–CD3-stimulated Jurkat cells significantly reduced AGO2-ZAP70 complex formation to levels that were similar to those of unstimulated conditions (**Fig. 5B**). These observations could be recapitulated in primary T-PLL cells of two independent cases (**Fig. 5C**; Supplementary Fig. S12D).

In silico modeling predicts sequestration of AGO2 in a complex including CD3ζ, LCK, and ZAP70

To resolve and model the organization of the AGO2-ZAP70 complexes, we undertook a series of dockings with Haddock (targeting

Figure 3.

The enhancing impact of AGO2 protein expression on TCR signaling in Jurkat cells and primary T-PLL cells. **A,** Membrane-based antibody array (43 kinases) evaluating phosphorylation of human protein kinases upon TCR activation (anti-CD3 cross-link for 5 minutes) in Jurkat cells 48 hours after siRNA-mediated AGO2 knockdown (siControl, nontargeting siPool; siAGO2, AGO2-targeting siRNA-Pool; see Supplementary Fig. S5A for verification of stimulation and AGO2 downregulation and Supplementary Fig. S5B for full membranes of the array). Pie charts displaying unaffected (fc = 0.7–1.5; light gray), upregulated (fc > 1.5; red), and downregulated (fc < 0.7; blue) phosphokinases between siControl unstimulated and siControl stimulated (left); siControl unstimulated and siAGO2 unstimulated (middle); and siControl stimulated and siAGO2 stimulated (right) conditions. Exemplary kinases are presented within the pie chart (see Supplementary Fig. S5C for quantification of selected kinases). **B,** Basal and TCR-triggered (cross-linking anti-CD3 antibody) phosphorylation levels of TCR pathway–associated kinases ZAP70, PLCγ1, and LAT were significantly reduced 48 hours after siRNA-mediated AGO2 downregulation in Jurkat cells [exemplary immunoblots and summarizing bar charts; siControl pool (dark gray) or an siAGO2 pool (light gray)]. Quantification of kinase phosphorylation was performed relative to the unstimulated condition based on the expression of the total protein. Verification of AGO2 downregulation is shown in Supplementary Fig. S6A. Dependency of TCR-mediated kinase activation on AGO2 levels in the Hut78 cell line is shown in Supplementary Fig. S6B. **C,** Phosphorylation of TCR kinases PLCγ1 and LAT (relative to pan-protein) was higher in T-PLL cases with elevated AGO2 protein expression. Left, immunoblot showing phosphorylation of TCR kinases upon anti-CD3/CD28 stimulation in T-PLL cases with high ($n = 2$) and low ($n = 2$) AGO2 protein expression. Right, immunoblot showing AGO2 protein expression of 10 T-PLL cases. Selected cases for detection of TCR-mediated kinase activation: T08 and T17 (blue, low AGO2 protein–expressing cases); T33 and T53 (red, high AGO2 protein–expressing cases). Quantification of AGO2 protein expression was calculated relative to β-actin and normalized to AGO2 protein expression of Hut78 cells. See Supplementary Fig. S8 for basal and TCR-induced AGO2 protein levels in T cells derived from one T-PLL case and one healthy donor.

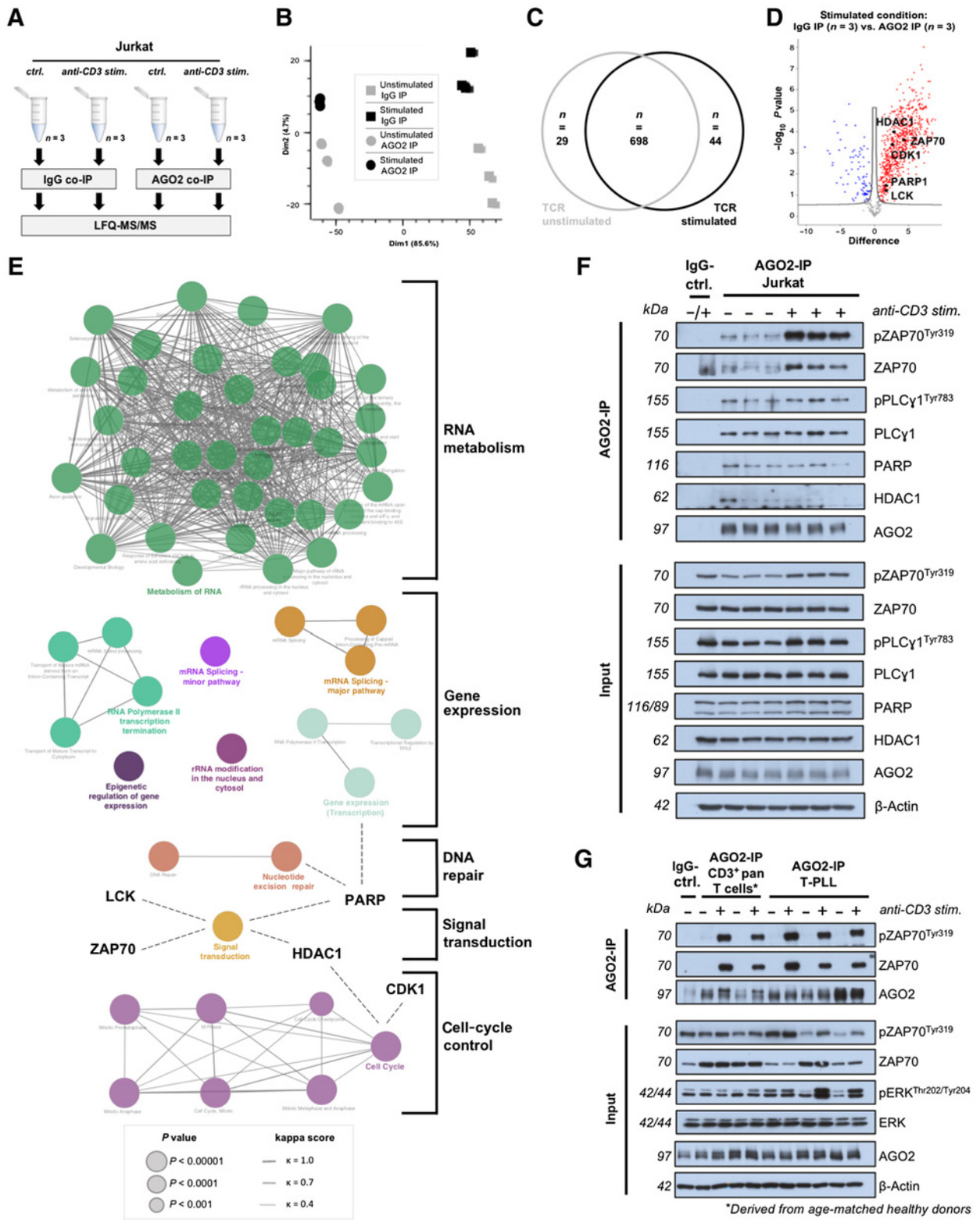

different tyrosines likely to undergo this modification) using ambiguous constraints around the target and involving the kinase mouth. A conclusive result for tyrosine 529 phosphorylation was retained [HADDOCK score—45.2 ± 11.0 (17)] (**Fig. 6A–C**; ZAP70, yellow; AGO2, pink) and placed in the structural architecture of the two partners further modeled in full-length versions. The full-length model (Supplementary Fig. S13A and S13B) was relaxed by a 40 ns molecular dynamics run [with GROMACS (19) in an all atoms system prepared with CHARMM-GUI (18) and typed with CHARMM36 m force field (25)]. This constitutes per se a possible modification model of a yet characterized phosphorylation site for AGO2 that supports ZAP70 to be a direct modulator of AGO2 activity. The results from our coimmunoprecipitation screening (**Fig. 4**) and functional colocalization assays (**Fig. 5**) point toward involvement of the TCR-central kinase LCK in the AGO2-ZAP70 complex formation. To contextualize this more and given suggested additional specific interactions at *a priori* complementary elements of structure and guided by existing similar complexes, we undertook the arrangement of a putative interaction of LCK with AGO2-ZAP70 at ITAMs of the TCR-associated CD3ζ chain (**Fig. 6D**; Supplementary Fig. S14A). **Figure 6D** shows a full view of the complex highlighting different interactors and key points for interrecognition. The presented model favors an LCK-mediated preactivation of ZAP70 by phosphorylation of its Y319 (Supplementary Fig. S14B) followed by phosphorylation of Y529 of AGO2 by ZAP70 (Supplementary Fig. S14C). Overall, our model suggests enhanced stability of LCK-AGO2-ZAP70 complexes through predicted protein–protein interactions, potentially explaining the TCR signal–enhancing effect of high AGO2 levels.

Overall, we describe that the frequent AGO2 overrepresentations at the genomic level underlie, but do not entirely explain, a general AGO2 protein overexpression in T-PLL. Higher AGO2 levels seem to promote T-cell leukemia growth. Besides AGO2-associated global impacts on miR and transcriptome profiles with expected implications in cell survival, cell-cycle control, and DNA damage responses, we also discover noncanonical AGO2 protein–mediated effects beyond RNA metabolism. Particularly the activating interaction of AGO2 with TCR kinases indicates that the strength of protumorigenic TCR signals can be determined by AGO2 levels.

Discussion

The mechanisms of AGO2 in small-RNA guided gene silencing are diverse and up to now not fully understood (12). On the basis of our findings of *AGO2* gene amplifications and protein overexpressions in T-PLL, we pursued the potential oncogenic role(s) of AGO2 in the pathogenesis of this T-cell malignancy. We characterized global AGO2-shaped miR-omes and transcriptomes in T-PLL and highlight that especially pathways of survival signaling, cell-cycle control, and DNA damage responses are affected in a proleukemic fashion by higher AGO2 levels.

In malignant B cells, miRs interconnect damage signals upstream of p53 and B-cell receptor signal strength, for example, through FOXP1 or phosphatase levels (26). Importantly, we describe for the first time a functional link of elevated AGO2 protein with enhanced TCR signaling activity at the level of kinase enhancements. Generally, regulatory impacts of several miR species on TCR signaling in T-cell physiology have been described. AGO2 itself can be subject to TCR-triggered proteasomal degradation (27, 28). Interestingly, we noted increased AGO2 protein levels upon TCR stimulation in pan-CD3$^+$ T cells of one healthy donor and 1 patient with T-PLL. Although we observed an association of *AGO2* CN with mRNA expression in T-PLL cells, AGO2 protein expression levels appeared less correlated with *AGO2* CN. This indicates further modes of AGO2 upregulation in T-PLL beyond genomic aberrations, which have been observed already in other cell systems, for example, regulation of AGO2 protein stability by miR availability (29).

In addition to miR-mediated transcriptome modifications, direct protein–protein interactions with specific signaling intermediates as well as posttranslational modifications of AGO2 induced by upstream kinases have been shown to contribute to AGO2's oncogenic function (12, 30). The study presented here, demonstrates a previously undisclosed relationship of AGO2 with TCR signaling, showing that (i) AGO2 augments TCR signal strength through protein–protein interactions and that (ii) TCR activation influences the AGO2 interactome, both eventually additionally affecting miR/transcriptome profiles.

With data on RNA-mediated and noncanonical direct protein-related effects of AGO2 in TCR signaling, our study adds to the understanding of AGO2's likely wide spectrum of functions, generally

Figure 4.

AGO2 interacts with proteins involved in regulation of gene expression, cell-cycle transition, DNA damage repair, and survival signaling. **A,** Experimental setup. Jurkat T cells were either stimulated with an anti-CD3 antibody for 5 minutes ($n = 3$) or left unstimulated ($n = 3$). Subsequent to AGO2/IgG coimmunoprecipitation (co-IP), interacting proteins were identified by label-free tandem-mass spectrometry (LFQ-MS/MS). See **Fig. 4F** for validation of stimulatory effect. **B,** Separate clustering of IgG coimmunoprecipitation and AGO2 coimmunoprecipitation samples in a PCA based on $\log_2$ LFQ values of all detected proteins ($n = 873$; Supplementary Table S5) validates the specificity of the predicted AGO2-interacting proteins. Light gray squares, unstimulated IgG coimmunoprecipitation; light gray circles, unstimulated AGO2 coimmunoprecipitation; dark gray squares, stimulated IgG coimmunoprecipitation; dark gray circles, stimulated AGO2 coimmunoprecipitation (each $n = 3$). **C,** Venn diagram presenting AGO2-interacting proteins detected in the unstimulated condition ($n = 29$), the anti–CD3-stimulated condition ($n = 44$), or common to both experimental conditions ($n = 698$). AGO2 interactors were defined as proteins (i) only detected in all three AGO2 coimmunoprecipitation conditions and/or (ii) significantly enriched in the AGO2 coimmunoprecipitation conditions (*t* test; FDR *q*-value ≤ 0.05). **D,** Volcano plots showing differences ($\log_2$ LFQ values; IgG coimmunoprecipitation vs. AGO2 coimmunoprecipitation; $n = 3$ experimental replicates each) and FDR values of all detected peptides in the TCR-stimulated condition. Exemplary proteins are displayed. See Supplementary Fig. S11 for unstimulated condition and for comparison between AGO2 coimmunoprecipitation of unstimulated versus TCR-stimulated cells. **E,** AGO2 interactors were significantly enriched in pathways of gene expression, cell cycle, DNA damage responses, and survival signaling. A functional network of significantly enriched Reactome pathways ($P \leq 0.001$) within the AGO2 interactome was created via the Cytoscape plugin Cluego (http://apps.cytoscape.org/apps/cluego). *P* values are reflected by circle sizes. Shared proteins between pathways were evaluated using the kappa (κ) statistics. Nodes with a κ score of 0.4 or higher were connected with edges. Thickness of the edges indicates the κ score. Terms with the highest significance are colored (leading terms). Exemplary proteins are highlighted. **F,** Immunoblot-based validation of AGO2 interactors in Jurkat cells ($n = 3$) with/without anti-CD3 cross-linking for 5 minutes ($n = 3$). IgG control, pooled lysate of unstimulated and stimulated conditions (equal parts) pulled down with IgG antibody. AGO2 interacts with proteins of DNA damage response pathways (PARP), epigenetic gene regulation (HDAC1), and TCR signaling (PLCγ1, ZAP70). TCR activation via anti-CD3 stimulation leads to a strong increase in the interaction with (phosphorylated) ZAP70. **G,** In primary T-PLL cells, the interaction of AGO2 with pZAP70^{Y319} and pan-ZAP70 was demonstrated. Upon TCR stimulation, ZAP70 (phosphorylated) strongly interacted with AGO2. No differential interaction of AGO2 and the TCR kinases between healthy donor–derived pan-T cells and T-PLL cells was observed. AGO2 coimmunoprecipitation in pan-T-cell lysates derived from age-matched healthy donors ($n = 2$) and T-PLL cell lysates ($n = 3$); cells were either left unstimulated or were TCR-stimulated with cross-linking anti-CD3 antibodies. Phosphorylation of ZAP70^{Tyr319} and ERK$^{T202/Y204}$ served as controls for TCR activation (input). One of the three T-PLL cases presenting basal phosphorylation of TCR kinases was used for IgG coimmunoprecipitation control.

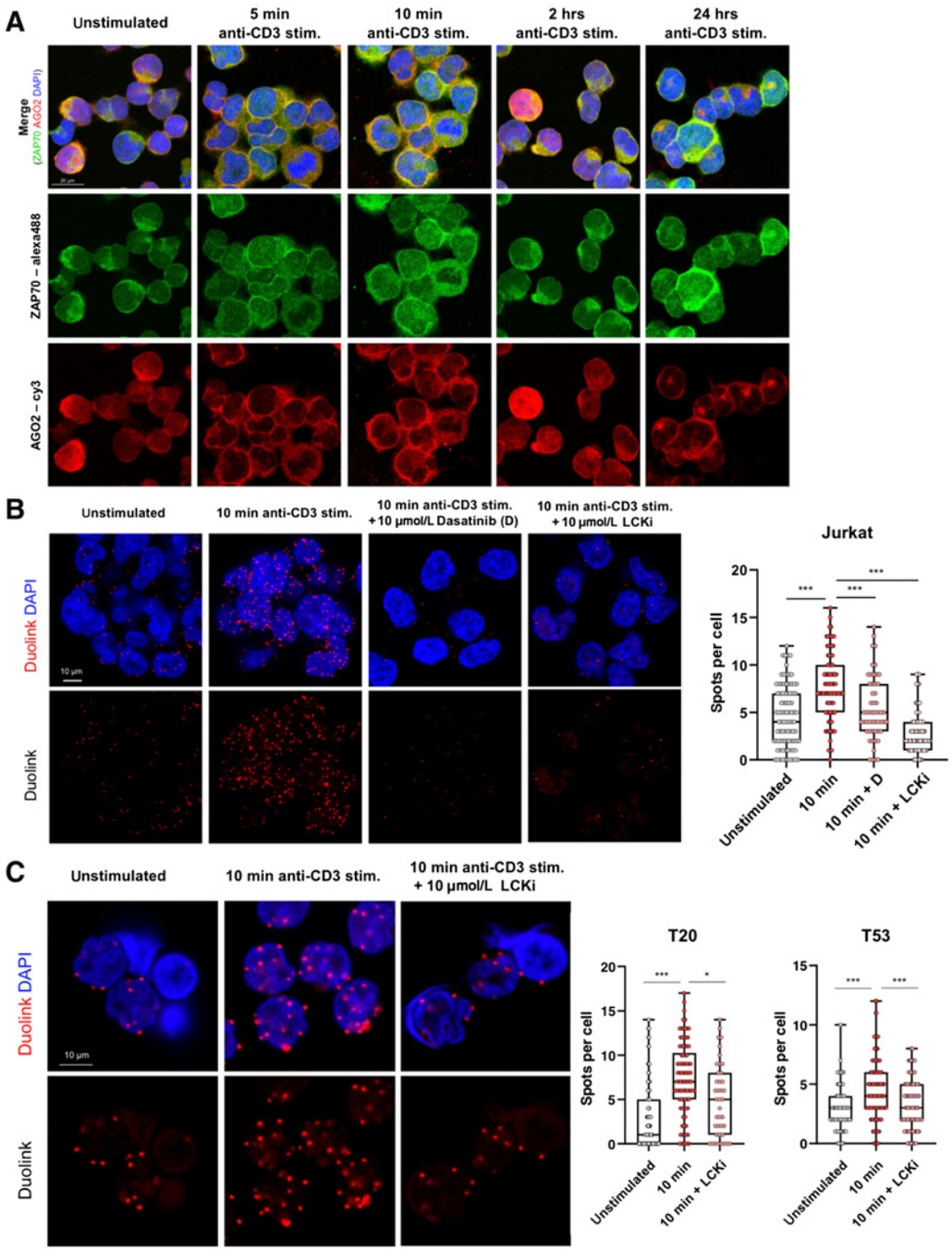

Figure 5.

TCR signal–dependent AGO2-ZAP70 complexes in Jurkat and T-PLL cells. **A,** Confocal microscopy showing membrane-associated AGO2-ZAP70 complexes in Jurkat cells subsequent to anti–CD3-mediated TCR activation; fluorescence signals from detected AGO2 (green), ZAP70 (red), and DAPI (blue). Jurkat cells were stimulated for the indicated times by anti-CD3 cross-linking. Induced AGO2-ZAP70 complexes peaked at 10 minutes of TCR activation. Representative images were selected. See Supplementary Fig. S12A for validation of the AGO2-ZAP70 interaction by PLAs. **B,** PLAs. Significantly reduced AGO2-ZAP70 complex formation in Jurkat cells upon inhibition of the proximal TCR kinase LCK via pretreatment with CAS 213743-31-8 and dasatinib (each 10 µmol/L; 24 hours). Left, representative images (DAPI, blue; Duolink, red). Right, quantification of Duolink spots per cell (***, $P < 0.001$). See Supplementary Fig. S12B (immunoblots) for validation of diminished TCR signaling upon LCK inhibition and Supplementary Fig. S12C for toxicity assessment of treatment with 10 µmol/L of LCK inhibitors for 24 hours. **C,** Confirmatory experiments in primary T-PLL cells (two independent cases). Formation of AGO2-ZAP70 complexes upon TCR stimulation is reduced upon inhibition of LCK (inhibitor pretreatment for 24 hours), as shown by PLA. AGO2 protein levels of T20 were in the mid tertile of the cohort; those of T53 were in the upper third. Left, representative images (DAPI, blue; Duolink, red). Right, quantification of Duolink spots per cell (*, $P < 0.05$; ***, $P < 0.001$). See Supplementary Fig. S12D for confocal microscopy of AGO2 and ZAP70 in primary T-PLL cells.

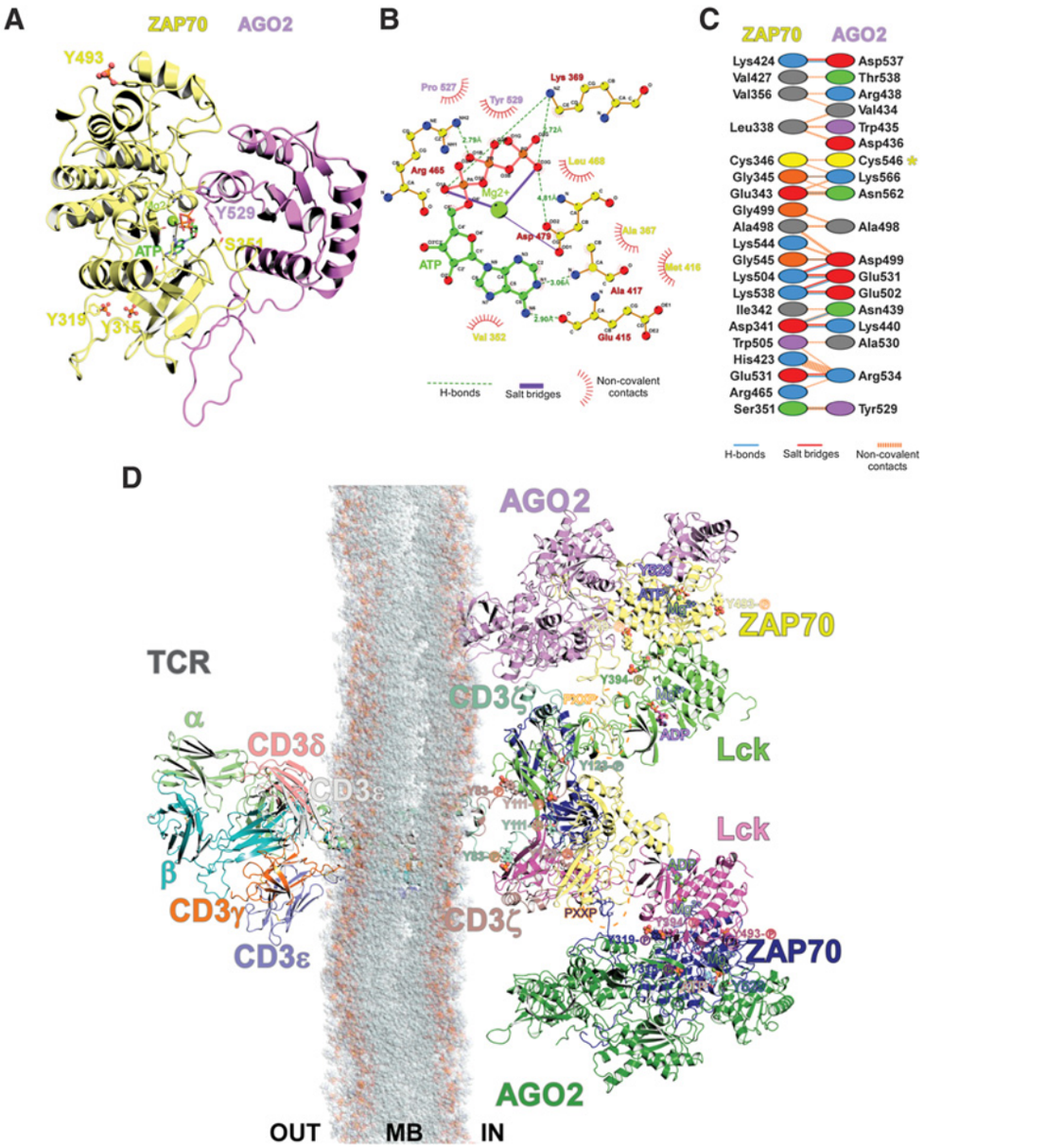

Figure 6.

Functional model involving sequestration of AGO2 at the cytoplasmic membrane in a complex including the TCR, LCK, and ZAP70. **A,** Schematic representation of the three-dimensional structure of a predicted AGO2-ZAP70 complex (illustrated with PyMOL). Yellow, ZAP70 kinase domain (ZAP70); lilac, AGO2 2 MID domain (AGO2). Balls and sticks represent previously described phosphorylation sites of ZAP70 (Y315, Y319, Y493; involved in full activation upon TCR stimulation) and AGO2 (Y529). Positions of the active site of the ZAP70 enzymatic domain are materialized in sticks around cofactor Mg^{2+} (green sphere) and ATP (sticks). The model suggests the AGO2 side chain of the targeted Y529 being held in close vicinity of the donor group of ATP (gamma phosphate). **B,** Interaction diagram of ATP and Mg^{2+} with the catalytic site of ZAP70 produced with Ligplot+ based on the refined model. Positions of AGO2's P527 and Y529 are displayed in pink. **C,** Interface interaction network predicted by Haddock. Residue colors: blue, positive (His, Lys, Arg); red, negative (Asp, Glu); green, neutral (Ser, Thr, Asn, Gln); gray, aliphatic (Ala, Val, Leu, Ile, Met); pink, aromatic (Phe, Tyr, Trp); orange (Pro, Gly); yellow Cys. The interaction implicates two areas of 1,100 $Å^2$, each stabilized by seven salt bridges, 12 H-bonds, and 81 noncovalent contacts. Yellow asterisk, potential disulfide bridge formed between ZAP70 and AGO2 conveying complex stability. **D,** Functional model of plasmalemmal sequestration of AGO2 involving CD3ζ, LCK, ZAP70, and AGO2. OUT, extracellular space; MB, membrane; IN, intracellular space. Potentially interacting amino acid residues and cofactors are highlighted. The presented model favors LCK-mediated preactivation of ZAP70 by phosphorylation of its Y319 residue, followed by phosphorylation of AGO2 at its Y529 residue mediated by ZAP70.

and in the context of T-cell tumorigenesis. Antibody-based phosphokinase arrays implicated further functions of AGO2 besides its involvement in TCR signaling (e.g., p27 deregulation), which should be task of future research.

The biochemical specifics of the interactions of the AGO2 protein with LCK and ZAP70 require more detailed analyses. We conclude that T-PLL cells are equipped with a miR and transcriptional network that is shaped by a cooperative impact of TCR signals and those by

AGO2, which enhance each other at the protein level. The observations we made here entail the future challenge of distinguishing the context specifics between (conventional) "indirect" miR-mediated versus (noncanonical) "direct" RNAi-independent pro-oncogenic effects of AGO2. The immediate nature of its recruitment to protein complexes within minutes subsequent to TCR activation, argues in favor of a miR-independent involvement of AGO2 in the regulation of TCR signals. However, to assess miR-mediated long-term effects (additionally) shaping enhanced TCR-derived signals, the basal miR processing machinery has to be modified in an experimental setting. This would cause an intrinsically altered artificial cell that is not comparable with our system of interest (31). Further studies also need to address the predicted impact of TCR kinases (i.e., ZAP70) on AGO2 activity (see model in **Fig. 6D**). Phosphorylation of AGO2 at its residue Y529, predicted to be essential for the binding of ZAP70, was shown to be associated with strongly reduced small RNA binding, further pointing toward a noncanonical function of AGO2, when phosphorylated at Y529 (32).

Overall, our findings unravel a nonconventional mode of action of AGO2, namely via protein–protein interactions in the context of TCR signals, in addition to its classical miR/mRNA-mediated effects. This also further underlines the central role of TCR signaling in T-PLL's pathophysiology. Besides TCL1A as a catalytic enhancer of TCR kinases (i.e., ERK and AKT; refs. 6–8) and besides loss of negative regulators of T-cell activation (i.e., CTLA4 and other coreceptors; refs. 6, 8), the activating effects of the AGO2 protein on ZAP70, PLCγ1, and LAT described here, represent a new mode of promoting a TCR-hyperactivated phenotype of the T-PLL cell or its precursor. This emphasizes TCR signaling intermediates as candidates for targeted therapeutic approaches in T-PLL, for example, as pursued by first generations of IL2-inducible T-cell kinase inhibitors (33).

Authors' Disclosures

No disclosures were reported.

Authors' Contributions

T. Braun: Conceptualization, resources, data curation, formal analysis, validation, investigation, methodology, writing–original draft. **J. Stachelscheid:** Conceptualization, data curation, formal analysis, investigation, methodology, sample acquisition. **N. Bley:** Data curation, formal analysis, investigation, methodology. **S. Oberbeck:** Data curation, formal analysis, investigation. **M. Otte:** Data curation, formal analysis, investigation. **T.A. Müller:** Data curation, formal analysis, investigation, methodology. **L. Wahnschaffe:** Data curation, formal analysis, methodology. **M. Glaß:** Data curation, formal analysis, methodology. **K. Ommer:** Resources, data curation, sample acquisition. **M. Franitza:** Resources, data curation, supervision. **B. Gathof:** Resources, data curation, supervision. **J. Altmüller:** Resources, data curation, supervision. **M. Hallek:** Resources, data curation, supervision, project administration, writing–review and editing. **D. Auguin:** Resources, data curation, supervision, funding acquisition, writing–original draft, project administration, *in silico* modeling. **S. Hüttelmaier:** Resources, supervision, funding acquisition, project administration, writing–review and editing. **A. Schrader:** Resources, formal analysis, supervision, funding acquisition, investigation, methodology, writing–original draft, project administration. **M. Herling:** Resources, supervision, funding acquisition, project administration, writing–review and editing.

Acknowledgments

This research was funded by the DFG Research Unit FOR1961 (Control-T; HE3553/4-2), the Köln Fortune program, and the Fritz Thyssen Foundation (10.15.2.034MN). This work was also funded by the EU Transcan-2 consortium "ERANET-PLL" and by the ERAPerMed Consortium "JAKSTAT-TARGET." A. Schrader was supported by a scholarship of the German José Carreras Leukemia Foundation (DJCLS 03 F/2016). MS analyses were conducted at the CECAD proteomics facility. The authors gratefully acknowledge their help during data acquisition and data analysis. Furthermore, the authors thank the ENCODE Consortium and the Brenton Gravely Lab for making AGO2 knockdown data available. Finally, they thank all patients with their families for their invaluable contributions.

The costs of publication of this article were defrayed in part by the payment of page charges. This article must therefore be hereby marked *advertisement* in accordance with 18 U.S.C. Section 1734 solely to indicate this fact.

Received June 16, 2021; revised January 23, 2022; accepted March 4, 2022; published first March 8, 2022.

References

1. Braun T, von Jan J, Wahnschaffe L, Herling M. Advances and perspectives in the treatment of T-PLL. Curr Hematol Malig Rep 2020;15:113–24.
2. Staber PB, Herling M, Bellido M, Jacobsen ED, Davids MS, Kadia TM, et al. Consensus criteria for diagnosis, staging, and treatment response assessment of T-cell prolymphocytic leukemia. Blood 2019;134:1132–43.
3. Herling M, Khoury JD, Washington LT, Duvic M, Keating MJ, Jones D. A systematic approach to diagnosis of mature T-cell leukemias reveals heterogeneity among WHO categories. Blood 2004;104:328–35.
4. Dearden C. How I treat prolymphocytic leukemia. Blood 2012;120:538–51.
5. Matutes E, Brito-Babapulle V, Swansbury J, Ellis J, Morilla R, Dearden C, et al. Clinical and laboratory features of 78 cases of T-prolymphocytic leukemia. Blood 1991;78:3269–74.
6. Oberbeck S, Schrader A, Warner K, Jungherz D, Crispatzu G, von Jan J, et al. Non-canonical effector functions of the T-memory-like T-PLL cell are shaped by cooperative TCL1A and TCR signaling. Blood 2020;136:2786–802.
7. Herling M, Patel KA, Teitell MA, Konopleva M, Ravandi F, Kobayashi R, et al. High TCL1 expression and intact T-cell receptor signaling define a hyperproliferative subset of T-cell prolymphocytic leukemia. Blood 2008;111:328–37.
8. Schrader A, Crispatzu G, Oberbeck S, Mayer P, Pützer S, von Jan J, et al. Actionable perturbations of damage responses by TCL1/ATM and epigenetic lesions form the basis of T-PLL. Nat Commun 2018;9:697.
9. Wahnschaffe L, Braun T, Timonen S, Giri AK, Schrader A, Wagle P, et al. JAK/STAT-activating genomic alterations are a hallmark of T-PLL. Cancers 2019;11:1833.
10. Braun T, Glass M, Wahnschaffe L, Otte M, Mayer P, Franitza M, et al. MicroRNA networks in T-cell prolymphocytic leukemia reflect T-cell activation and shape DNA damage response and survival pathways. Haematologica 2020;107:187–200.
11. Meister G, Landthaler M, Patkaniowska A, Dorsett Y, Teng G, Tuschl T. Human Argonaute2 mediates RNA cleavage targeted by miRNAs and siRNAs. Mol Cell 2004;15:185–97.
12. Müller M, Fazi F, Ciaudo C. Argonaute proteins: from structure to function in development and pathological cell fate determination. Front Cell Dev Biol 2020;7:360.
13. Liberzon A, Birger C, Thorvaldsdóttir H, Ghandi M, Mesirov JP, Tamayo P. The molecular signatures database hallmark gene set collection. Cell Syst 2015;1:417–25.
14. Jumper J, Evans R, Pritzel A, Green T, Figurnov M, Ronneberger O, et al. Highly accurate protein structure prediction with AlphaFold. Nature 2021;596:583–9.
15. The UniProt Consortium. UniProt: the universal protein knowledgebase. Nucleic Acids Res 2017;45:D158–69.
16. Hornbeck PV, Zhang B, Murray B, Kornhauser JM, Latham V, Skrzypek E. PhosphoSitePlus, 2014: mutations, PTMs and recalibrations. Nucleic Acids Res 2015;43:D512–20.
17. van Zundert GCP, Rodrigues JPGLM, Trellet M, Schmitz C, Kastritis PL, Karaca E, et al. The HADDOCK2.2 web server: user-friendly integrative modeling of biomolecular complexes. J Mol Biol 2016;428:720–5.
18. Lee J, Patel DS, Ståhle J, Park S-J, Kern NR, Kim S, et al. CHARMM-GUI membrane builder for complex biological membrane simulations with glycolipids and lipoglycans. J Chem Theory Comput 2019;15:775–86.

19. Hess B, Kutzner C, van der Spoel D, Lindahl E. GROMACS 4: algorithms for highly efficient, load-balanced, and scalable molecular simulation. J Chem Theory Comput 2008;4:435–47.
20. Perez-Riverol Y, Csordas A, Bai J, Bernal-Llinares M, Hewapathirana S, Kundu DJ, et al. The PRIDE database and related tools and resources in 2019: improving support for quantification data. Nucleic Acids Res 2019;47:D442–50.
21. Johansson P, Klein-Hitpass L, Choidas A, Habenberger P, Mahboubi B, Kim B, et al. SAMHD1 is recurrently mutated in T-cell prolymphocytic leukemia. Blood Cancer J 2018;8:11.
22. ENCODE Project Consortium. An integrated encyclopedia of DNA elements in the human genome. Nature 2012;489:57–74.
23. Gao M, Wei W, Li MM, Wu YS, Ba Z, Jin KX, et al. Ago2 facilitates Rad51 recruitment and DNA double-strand break repair by homologous recombination. Cell Res 2014;24:532–41.
24. Min-Sun Song JJR. The effect of Dicer knockout on RNA interference using various Dicer substrate interfering RNA structures. bioRxiv 2020.
25. Huang J, Rauscher S, Nawrocki G, Ran T, Feig M, de Groot BL, et al. CHARMM36m: an improved force field for folded and intrinsically disordered proteins. Nat Methods 2017;14:71–3.
26. Cerna K, Oppelt J, Chochola V, Musilova K, Seda V, Pavlasova G, et al. MicroRNA miR-34a downregulates FOXP1 during DNA damage response to limit BCR signalling in chronic lymphocytic leukaemia B cells. Leukemia 2019; 33:403–14.
27. Bronevetsky Y, Villarino AV, Eisley CJ, Barbeau R, Barczak AJ, Heinz GA, et al. T cell activation induces proteasomal degradation of Argonaute and rapid remodeling of the microRNA repertoire. J Exp Med 2013;210: 417–32.
28. Grewers Z, Krueger A. MicroRNA miR-181-A rheostat for TCR signaling in thymic selection and peripheral T-cell function. Int J Mol Sci 2020;21: 6200.
29. Smibert P, Yang J-S, Azzam G, Liu J-L, Lai EC. Homeostatic control of Argonaute stability by microRNA availability. Nat Struct Mol Biol 2013;20:789–95.
30. Ye Z, Jin H, Qian Q. Argonaute 2: a novel rising star in cancer research. J Cancer 2015;6:877–82.
31. Yang J-S, Lai EC. Alternative miRNA biogenesis pathways and the interpretation of core miRNA pathway mutants. Mol Cell 2011;43:892–903.
32. Rüdel S, Wang Y, Lenobel R, Körner R, Hsiao H-H, Urlaub H, et al. Phosphorylation of human Argonaute proteins affects small RNA binding. Nucleic Acids Res 2011;39:2330–43.
33. Dondorf S, Schrader A, Herling M. Interleukin-2-inducible T-cell kinase (ITK) targeting by BMS-509744 does not affect cell viability in T-cell prolymphocytic leukemia (T-PLL). J Biol Chem 2015;290:10568–9.

ARTICLE

Micro-RNA networks in T-cell prolymphocytic leukemia reflect T-cell activation and shape DNA damage response and survival pathways

Till Braun,[1*] Markus Glaß,[2*] Linus Wahnschaffe,[1*] Moritz Otte,[1] Petra Mayer,[1] Marek Franitza,[3] Janine Altmüller,[3] Michael Hallek,[1] Stefan Hüttelmaier,[2#] Alexandra Schrader,[1#] and Marco Herling[1#]

[1]Department I of Internal Medicine, Center for Integrated Oncology (CIO), Aachen-Bonn-Cologne-Duesseldorf, Excellence Cluster for Cellular Stress Response and Aging-Associated Diseases (CECAD), Center for Molecular Medicine Cologne (CMMC), University of Cologne (UoC), Cologne; [2]Institute of Molecular Medicine, Section for Molecular Cell Biology, Faculty of Medicine, Martin Luther University Halle-Wittenberg, Charles Tanford Protein Center, Halle, and [3]Cologne Center for Genomics, Center for Molecular Medicine Cologne (CMMC), University of Cologne, Cologne, Germany

**TB, MG and LW contributed equally as co-first authors.*

#SH, AS and MH contributed equally as co-senior authors.

Ferrata Storti Foundation

Haematologica 2022
Volume 107(1):187-200

ABSTRACT

T-cell prolymphocytic leukemia (T-PLL) is a poor-prognostic mature T-cell malignancy. It typically presents with exponentially rising lymphocyte counts, splenomegaly, and bone marrow infiltration. Effective treatment options are scarce and a better understanding of T-PLL's pathogenesis is desirable. Activation of the *TCL1* proto-oncogene and loss-of-function perturbations of the tumor suppressor *ATM* are T-PLL's genomic hallmarks. The leukemic cell reveals a phenotype of active T-cell receptor (TCR) signaling and aberrant DNA damage responses. Regulatory networks based on the profile of microRNA (miR) have not been described for T-PLL. In a combined approach of small-RNA and transcriptome sequencing in 46 clinically and moleculary well-characterized T-PLL, we identified a global T-PLL-specific miR expression profile that involves 34 significantly deregulated miR species. This pattern strikingly resembled miR-ome signatures of TCR-activated T cells. By integrating these T-PLL miR profiles with transcriptome data, we uncovered regulatory networks associated with cell survival signaling and DNA damage response pathways. Despite a miR-ome that discerned leukemic from normal T cells, there were also robust subsets of T-PLL defined by a small set of specific miR. Most prominently, miR-141 and the miR-200c-cluster separated cases into two major subgroups. Furthermore, increased expression of miR-223-3p as well as reduced expression of miR-21 and the miR-29 cluster were associated with more activated T-cell phenotypes and more aggressive disease presentations. Based on the implicated pathobiological role of these miR deregulations, targeting strategies around their effectors appear worth pursuing. We also established a combinatorial miR-based overall survival score for T-PLL (miROS-T-PLL), that might improve current clinical stratifications.

Introduction

T-cell prolymphocytic leukemia (T-PLL) is a neoplasm of post-thymic T cells.[1] It represents the most frequent mature T-cell leukemia in Western countries, however, with an incidence of 2 per million per year, it is still classified as an orphan disease.[2] T-PLL patients typically present at a median age of about 65 years, with exponentially rising lymphocytosis, marked bone marrow infiltration, and splenomegaly.[3] Phenotypically, T-PLL cells resemble mature, antigen-experienced T cells.[4,5] The aggressive growth of T-PLL cells is paralleled by a refractory behavior towards most conventional chemotherapies.[6] The current

Correspondence:

MARCO HERLING
Marco.Herling@medizin.uni-leipzig.de

Received: July 20, 2020.

Accepted: November 6, 2020.

Pre-published: November 19, 2020.

https://doi.org/10.3324/haematol.2020.267500

treatment of choice, the CD52-antibody alemtuzumab, is efficient in inducing initial responses, but nearly all patients relapse within 12-24 months thereafter.[7,8] Second-line options are even less efficient and the median overall survival (OS) of T-PLL patients is <2 years.[1,3,9,10]

Activating translocation of the T-cell leukemia/lymphoma 1 (*TCL1*) proto-oncogene is the most prevalent genetic aberration in T-PLL.[11] In addition, loss-of-function perturbations of the tumor suppressor ataxia telangiectasia mutated (*ATM*) are reported for >80% of T-PLL patients.[1] Both alterations contribute towards a phenotype of enhanced T-cell receptor signaling (TCR) and an aberrant DNA damage response, including resistance to p53-mediated cell death, deregulated cell cycle control, and deficient DNA repair mechanisms.[1,11] Activating lesions in janus kinase (*JAK*) and signal transducer and activator of transcription (*STAT*) molecules as well as epigenetic aberrations have emerged as further hallmarks of T-PLL pathology, resulting in a sustained survival signaling and pro-oncogenic cell cycle deregulation.[1,12–15] Despite these recent advances, a better understanding of T-PLL's pathobiology is of importance in order to identify novel treatment options.

MicroRNA (miR) have increasingly been recognized as relevant in the pathogenesis of hematopoetic and solid tumors. They are small non-coding RNA with an average length of 22 nucleotides. By targeting specific mRNA, miR function as posttranscriptional repressors.[16] Importantly, most miR regulate a large set of genes, often resulting in a cooperative effect on a given cellular pathway, rather than a specific effect on a single gene. Both onco miR and tumor-suppressive miR have been causally implicated in mature B- and T-lymphoid malignancies.[17–19] As a prominent example, chronic lymphocytic leukemia (CLL) harbors an unique miR expression signature with miR-181b downregulation as the best investigated miR deregulation.[20] When overexpressing miR-181b in the *Eμ-TCL1A* CLL mouse model, leukemic expansion is decelerated.[21] Moreover, miR-181b as well as the miR-29 and miR-34b/c were shown to target the proto-oncogene *TCL1A*, reflected by an association of their downregulation with oncogenic TCL1A overexpression in CLL.[22] Likewise, specific miR have been identified to be involved in the pathogenesis of mature T-cell tumors such as cutaneous T-cell lymphoma (CTCL) (e.g., deregulation of miR-29 and miR-200)[17,23] or NK/T-cell lymphoma (downregulated miR-150).[24] In T-PLL, frequent genomic aberrations of argonaute RISC catalytic component 2 (*AGO2*), a master regulator of miR processing,[25] provide first hints for altered miR activity and miR expression signatures (miR-omes).[1] However, global miR deregulations, likely involved in T-PLL's pathophysiology, have not been reported.

In the presented study, we performed small-RNA sequencing to investigate the spectrum of differential miR expression in T-PLL. We identify global, T-PLL-specific miR alterations associated with gene signatures affiliated to functional categories of survival signaling and DNA damage response pathways. In addition, we show that the miR-omes of T-PLL cells and of activated T cells are remarkably similar. Finally, we identify associations of miR alterations with cellular activation, clinical tumor burden, and patient outcome, all underlining the impact of miR deregulations in T-PLL.

Methods

Patient cohort

Primary isolates of 48 well-annotated T-PLL patients and of T cells from six age-matched healthy donors were studied (banked 2009-2019; patient characteristics in Table 1). The diagnosis of T-PLL was confirmed according to World Health Organization criteria[26] and consensus guidelines.[2] All patients (median age 68 years) provided informed consent according to the Declaration of Helsinki. Collection and use of the samples have been approved for research purposes by the ethics committee of the University Hospital of Cologne (#11–319). Most samples (82.6%) were collected prior to any first-line treatment (n=38 of 46).

Sequencing and data processing

RNA from peripheral blood mononuclear cells (PBMC) of T-PLL patients (median purity 95.4%) and $CD3^+$ pan-T cells of six age-matched healthy controls (median purity 90.2%) was subjected to library preparation and sequenced on the NovaSeq 6000 (n=48 T-PLL) and the HiSeq4000 platform (n=46 T-PLL, Illumina, San Diego, USA) according to the manufacturer's instructions for polyA-RNA and small-RNA sequencing, respectively. Details on cell isolation, stimulation, RNA isolation, library preparation, sequencing, and data processing are given in the *Online Supplementary Methods*.

Gene set enrichment analysis

Gene set enrichment analysis (GSEA) were performed on pre-ranked lists using the GSEA-software (v3.0)[27] and MSigDB (v7.0)[28] HALLMARK gene sets. For each considered miR, Spearman correlation coefficients for this miR and all protein-coding genes were determined by comparing the respective gene's count per million (CPM) and fragments per kilobase of million (FPKM) mapped reads. Sorted lists of correlation coefficients were then used as input for the GSEA.

MiR target prediction

In order to obtain putative mRNA targets for each miR, predicted miR bindings were first determined using the R-package multiMiR (v1.6.0, Database Version 2.3.0),[29] all of eight prediction databases (diana_microt, elmmo, microcosm, miranda, mirdb, pictar, pita, targetscan), and a 20% default prediction cutoff. All bindings predicted by <2 different databases were removed. From the remaining predicted genes, we chose those as putative miR targets that showed a negative Spearman correlation (rho<0; P<0.05; false discovery rate [FDR] <0.25) of their expression values with the expression of the respective miR.

Correlations with clinical data

In order to test for associations of miR-223-3p, miR-21, miR-29, and miR-200c/141 with clinical characteristics, cytogenetics, immunophenotypes, and outcome data, cases were divided into groups by the mean or tertiles as cutoffs according to the distribution of expression values within the patient cohort. Further details on statistics are provided in the *Online Supplementary Methods*.

Survival score

In order to develop a survival score, we (i) randomly divided our cohort into a training set (n=22) and a validation set (n=22). We then (ii) identified miR that were expressed in at least 80% of T-PLL samples and (iii) that were highly associated with OS in the training set (upper tertile of patients with highest *vs.* tertile with the lowest expression) using log-rank tests. Several other parameters that had been described to be prognostically relevant in T-PLL (e.g., leukocyte counts, TCL1 mRNA expression) were added to

Table 1. Clinical, cytogenetic and immunophenotypic characteristics of analyzed T-cell prolymphocytic leukemia (n=46 cases analyzed by small-RNA sequencing).

Patients' characteristics		
Median age, years (range)[1]	68 (32-88); n = 46	
Sex	Male = 25 Female = 21	
Median OS from diagnosis, months (range)[1]	17.1 (0.4-98.7); n = 44	
Clinical presentation	**At diagnosis**	**At sample**
Median WBC count, x10^9/L (range)[1]	91.4 (16.7-825.2); n = 38	114.1 (20.8-756.2); n = 43
Median hemoglobin, g/dL (range)[1]	12.6 (6.6-16.6); n = 34	12.6 (6.2-15.6); n = 36
Median platelet count, x10^9/L (range)[1]	129 (33-438); n = 34	118 (48-394); n = 36
Median LDH, U/L (range)[1]	567 (178-9423); n = 29	795 (226-8634); n = 36
Splenomegaly (%)[2]	n = 18/29 (62.07)	
Hepatomegaly (%)[2]	n = 5/27 (18.52)	
Lymphadenopathy (%)[2]	n = 15/26 (57.69)	
Cytogenetic features		
inv(14)(q11;q32) (%)[2]	n = 27/36; (75.00)	
t(14;14)(q11;q32) (%)[2]	n = 3/35; (8.57)	
t(X;14)(q28;q11) (%)[2]	n = 2/36; (5.56)	
TCR gene rearrangement[3] (%)[2]	n = 37/39; (94.87)	
MYC amplification[3] (%)[2]	n = 23/27; (85.19)	
ATM deletion[3] (%)[2]	n = 15/33; (45.45)	
Immunophenotype		
TCL1 (%)[2]	n = 35/38; (92.11)	
CD3$^+$ (%)[2]	n = 36/40; (90.00)	
CD5$^+$ (%)[2]	n = 40/40; (100.00)	
CD7$^+$ (%)[2]	n = 39/40; (97.50)	
CD4$^+$/CD8$^-$ (%)[2]	n = 27/39; (69.23)	
CD4/CD8$^+$ (%)[2]	n = 7/39; (17.95)	
CD4$^+$/CD8$^+$ (%)[2]	n = 5/39; (12.82)	

[1]Range reaches from lowest value to highest value in the cohort; [2]percentages are out of total cases with sufficient data; [3]evaluated by fluorescence *in situ* hybridization. OS: overall survival; TCR: T-cell receptor; WBC: white blood cell; LDH: serum lactate dehydrogenase.

the resulting miR with the strongest single OS associations (lowest *P*-values) towards a multi-parameter training model. Next, (iv) we subjected all parameters to a recursive partitioning algorithm using the rpart R package (v.4.1-15) to identify optimum individual cut-offs in our training set. Such deprioritizations finally retained the four factors miR-200a-3p, miR-223-3p, miR-424-5p, and TCL1A, for which optimum cutoffs best allowed discriminations of T-PLL patients with shorter *versus* longer OS. We then (v) built multivariate scores for all possible combinations of these four parameters, adding one point to the total score if the respective expression cutoff was passed, and calculated optimum thresholds for these scores. We (vi) selected the score which allowed best discrimination of OS in our training set and (vii) verified our score in the validation set as well as in the total cohort of 44 T-PLL patients.

Results

Global T-cell prolymphocytic leukemia-specific microRNA (miR) deregulations highlight differential expression of miR-200c and miR-141 clusters

In order to investigate the spectrum of cellular miR expressed in T-PLL, small-RNA sequencing was performed of peripheral blood (PB)-isolated tumor cells from 46 T-PLL patients and of pan-T cells of PB from six healthy donors. T-PLL patient characteristics are presented in Table 1 and sample purities in the *Online Supplementary Figure S1*. As T-PLL cases show a spectrum of (often nonconventional) memory T-cell phenotypes and of small naïve subsets,[5] we chose age-matched CD3$^+$ pan-T cells as controls (reflecting a representative mix of populations) in these global profiling analyses.

In total, we identified 2,094 miR, of which 37 miR displayed a differential expression in T-PLL *versus* healthy donor T cells (q<0.05, *Online Supplementary Table S1*). Of these, 14 miR sequences were upregulated (0.7% of all identified miR) and 23 were downregulated in T-PLL (1.1%, Figure 1A). While miR-6724-5p (fold change [fc]=0.18, q<0.0001) and miR-206 (fc=0.04, q<0.0001) showed the strongest downregulation, miR-5699-3p (fc=122, q=0.02), miR-200c-3p (fc=38.2, q=0.005), and miR-141-3p (fc=43.2, q=0.005) were the most upregulated. Considering all T-PLL cases, miR-141-3p and miR-21-5p showed the highest absolute abundance while miR-206, miR-651-3p and miR-6774-5p displayed the lowest absolute expression (*Online Supplementary Figure S2*). Among the 37 deregulated miR, miR-6724-5p was annotated four times due to its expression from four different genomic loci. The following analyses are, therefore, based on 34 miR, containing a sum

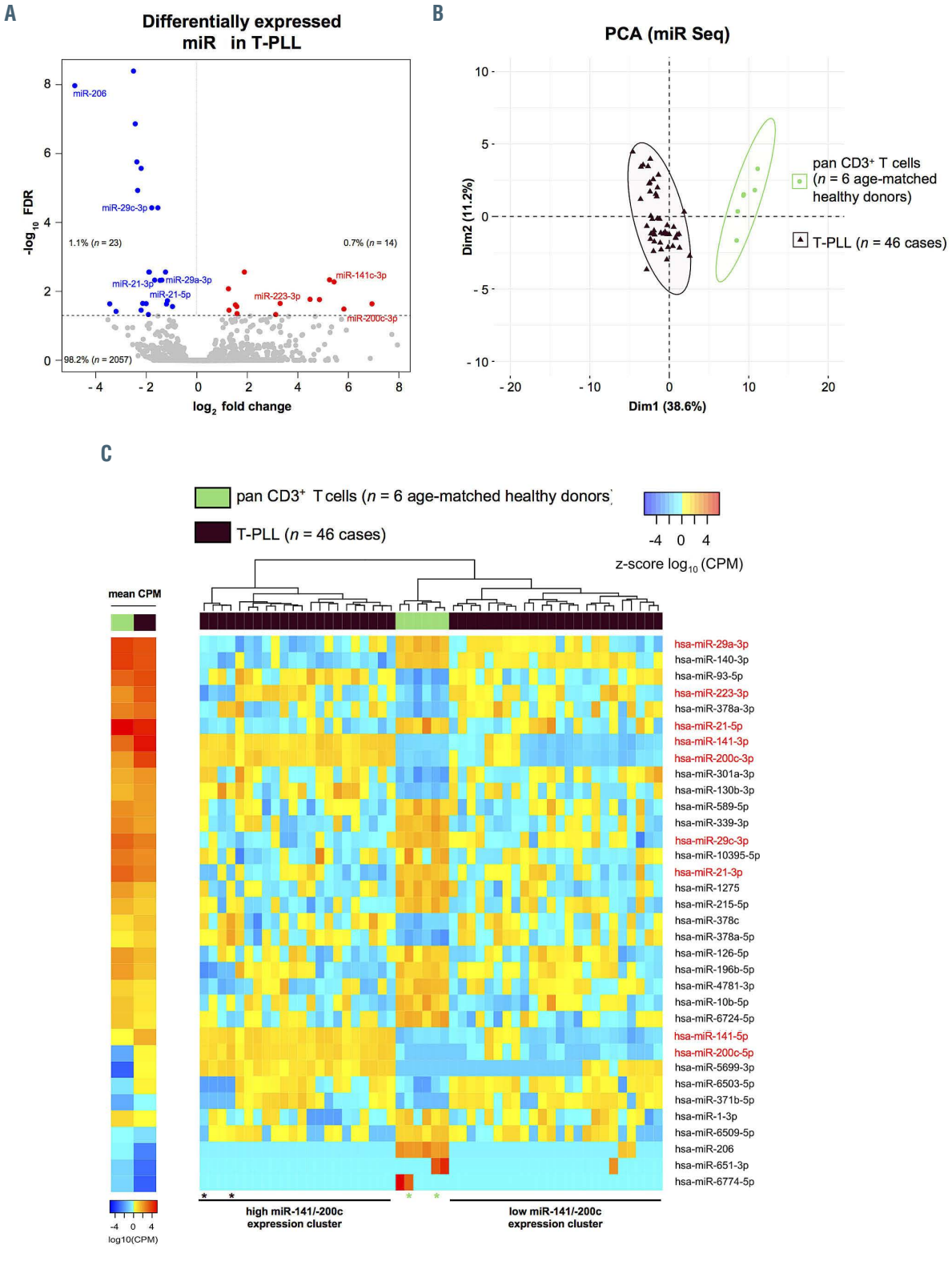

Figure 1. Global microRNA-deregulations highlight differential expression of miR-141 and miR-200c clusters in T-cell prolymphocytic leukemia. (A) MicroRNA (miR) profiles were evaluated using small-RNA sequencing of primary human peripheral blood-derived T-cell prolymphocytic leukemia (T-PLL) cells (n=46 cases) and CD3$^+$ healthy donor-derived pan-T cell controls (n=6 donors). Volcano plot showing fold changes (fc) and false discovery rates (FDR) of all identified miR (n=2,094). Differentially expressed miR (n=37, *Online Supplementary Table S1*) are highlighted in blue (downregulation) and red (upregulation). Relative proportions are based on all identified miR. (B) Principle component analysis (PCA) based on miR differentially expressed comparing T-PLL cases (n=46) to healthy donor controls (n=6). Separate clustering of cases and controls indicates global differences in miR expression profiles. (C) Heatmaps of differentially expressed miR (n=34; FDR<0.05) in T-PLL samples *vs.* CD3$^+$ pan-T cells of healthy donors. Left two-column heatmap: mean counts per million (CPM) values compared between healthy donor controls (n=6) and T-PLL (n=46; red=higher expression; blue=lower expression). Right heatmap: colors represent z-scores of respective CPM values calculated for each miR (red=higher z-score; blue=lower z-score). Control samples with slightly lower purities (77% and 85%) and T-PLL cases presenting a rather unique transcriptome, which clusters closer to control T cells (*Online Supplementary Figure S4C*), are indicated by asterixis (brown: T-PLL cases; green: control cases).

expression for miR-6724-5p. In order to validate our results from small-RNA sequencing, we performed quantitative real-time polymerase chain reaction (qRT-PCR) analyses of three highly deregulated miR (miR-223-3p, miR-200c-3p, miR-141-3p, *Online Supplementary Figure S3A* to *C*) in eight T-PLL and four healthy donor T-cell controls. A strong correlation between the results from small-RNA sequencing and qRT-PCR (r^2=0.84, *P*<0.0001, Pearson, *Online Supplementary Figure S3D*) confirmed differential (over)expression of these miR in T-PLL and underlines the robustness of the sequencing data. Using a previously published independent data set from single nucleotide polymorphism (SNP) arrays of 83 T-PLL[1] (overlap of 23 cases with the cohort presented here), we identified only small fractions of cases to carry genomic losses of significantly downregulated miR: miR-140-3p, miR-196b-5p (both CN<1.5 in 4.82% of cases), miR-339-3p, and miR-589-5p (both CN<1.5 in 8.43%, *Online Supplementary Table S2*).

Unsupervised clustering by principal component analysis (PCA) based on miR differentially expressed in T-PLL *versus* healthy donor T cells indicated a homogeneity across T-PLL samples and confirmed the global differences in the miR profiles between T-PLL and healthy controls (Figure 1B). Interestingly, unsupervised hierarchical clustering analysis of miR expression revealed two clusters of T-PLL cases, which were distinguished by expression of miR-200c and miR-141 family members (Figure 1C): 23 T-PLL cases showed low miR-141/-200c expression as compared to $CD3^+$ pan-T cell controls whereas 23 T-PLL samples had higher than normal T-cell expression of miR-141 and -200c. Besides higher serum lactate dehydrogenase (LDH) levels (*P*=0.03, Mann-Whitney-Wilcoxon test [MWW]) and a lower incidence of TP53 deletions (by fluorescence *in situ* hybridisation [FISH], *P*=0.02, Fisher's exact test) in the miR-141/-200c high-expressing cohort, we did not find other differences between these two subsets (*Online Supplementary Table S3*). Comparing the transcriptomes of cases allocated to these two separate clusters, we identified 356 genes to be differentially expressed (*Online Supplementary Table S4*). In line with GSEA based on miR141/200c-correlated genes (see following analyses), we identified the *HALLMARK* pathways *E2F TARGETS* (normalized enrichment score [NES]=4.38, q<0.0001) and *G2M CHECKPOINT* (NES=2.68, q<0.0001) as significantly altered between the two clusters of T-PLL. Furthermore, global miR-ome profiles were not associated with distinct cellular immunophenotypes, e.g., neither with CD45RA/RO expression (i.e., "memory-like" *vs.* "naïve-like" T-PLL) nor with CD4/8 expression (*Online Supplementary Figures S4A* and *B*).

MicroRNA-profiles of T-cell prolymphocytic leukemia resemble those of T-cell receptor signaling-activated T cells and form regulatory networks around nodes of DNA damage response and prosurvival signaling

In order to align the miR-ome data with those of global transcriptome alterations, polyA-RNA sequencing was performed on PB-isolated tumor cells from 41 miR-characterized T-PLL patients and seven additional T-PLL patients as well as on $CD3^+$ PB pan-T cells from six age-matched healthy donors. In total, we detected 948 protein-encoding mRNA to be differentially expressed (q<0.05, *Online Supplementary Figure S5A*; *Online Supplementary Table S5*). Using this set of deregulated genes, PCA corroborated homogeneity among T-PLL cases and a clear distinction to normal T-cell controls (*Online Supplementary Figure S5B*). In accordance with published data, *TCL1A* (fc=1843, q<0.0001) and CTLA4 (fc=0.06, q<0.0001) were among the most differentially expressed genes in T-PLL *versus* T-cell controls (*Online Supplementary Figure S5C*). In their transcriptome profiles two T-PLL clustered closer to control T cells than the bulk of cases. However, their miR expression signature (Figure 1C) and clinical presentation did not differ from the overall cohort.

GSEA (*HALLMARK* gene sets[27]) determined 34 gene sets as upregulated in T-PLL when compared to T-cell controls, of which 19 gene sets were significantly enriched at a FDR of <5%. Sixteen gene sets were downregulated in T-PLL (11 with FDR <0.05, *Online Supplementary Table S6*). The identified significantly altered pathways associated with cancer and/or immunology are presented in Figure 2A. These included several *HALLMARK* gene sets reflecting dysregulations in DNA damage response pathways (e.g., DNA REPAIR: NES=-2.18, q=0.005; *E2F TAGETS*: NES=2.05, q=0.01) and prosurvival signaling (e.g., *INFLAMMATORY RESPONSE*, NES=3.12, q<0.0001; *TNFA SIGNALING VIA NFKB*, NES=2.44, q=0.001), in line with previously published data.[1]

As T-PLL cells generally display a mature, T-cell activated phenotype,[1,11] we investigated whether T-PLL cell miR-omes resemble those of TCR-activated healthy donor-derived T cells. For that, PBMC (to avoid direct manipulation of T cells) of four healthy donors were cultured for 72 hours with and without stimulation by anti-CD3/CD28 crosslinking, followed by miR sequencing of $CD3^+$-enriched cells. Sample purities and experimental controls are shown in the *Online Supplementary Figure S6*. We identified 56 miR which are differentially expressed in response to TCR activation (q<0.05, *Online Supplementary Figure S7A*; *Online Supplementary Table S7*). PCA indicated homogeneity within both groups (T-PLL and normal PBMC) as well as global differences between their TCR-induced miR profiles (*Online Supplementary Figure S7B*). We identified miR known to be affected by TCR activation (e.g., miR-150-5p)[31] as well as previously unreported miR (e.g., miR-18a-5p; *Online Supplementary Figure S7C*). Integrative PCA based on differentially expressed miR in T-PLL *versus* healthy controls (Figure 1C) showed that the stimulated (over unstimulated) T cells clustered closer to T-PLL (Figure 2B). Fittingly, unsupervised clustering comparing TCR-stimulated T cells to unstimulated controls confirmed that the miR profiles of T-PLL cells resemble the miR-ome of TCR-activated healthy donor-derived T cells (Figure 2C).

We next assessed implicated functional relationships by predicted mRNA targets for each deregulated miR in T-PLL. For that, we (i) ranked mRNA based on their degree of correlation with a specific miR and (ii) performed *HALLMARK* set GSEA on these ranked mRNA. Pathways reflecting dysregulations of DNA damage response and prosurvival signaling emerged as predominantly associated with the alterations of miR expression. Exemplary *HALLMARK* pathways are shown in Figure 3A, a full list of gene sets is displayed in *Online Supplementary Figure S8*. For example, we obtained highly significant NES for the *E2F TARGET* and the *IL2 STAT5 SIGNALING HALLMARK* gene sets for (i) the transcriptome of T-PLL as compared to the one of healthy controls (*E2F TARGETS*: NES=1.92, q=0.02; *IL2 STAT5 SIGNALING*: NES=-2.86, q<0.0001, *Online Supplementary Table S6*) and (ii) for most of the miR differentially expressed in T-PLL (Figure 3A).

Overall, there was a striking similarity of the miR pro-

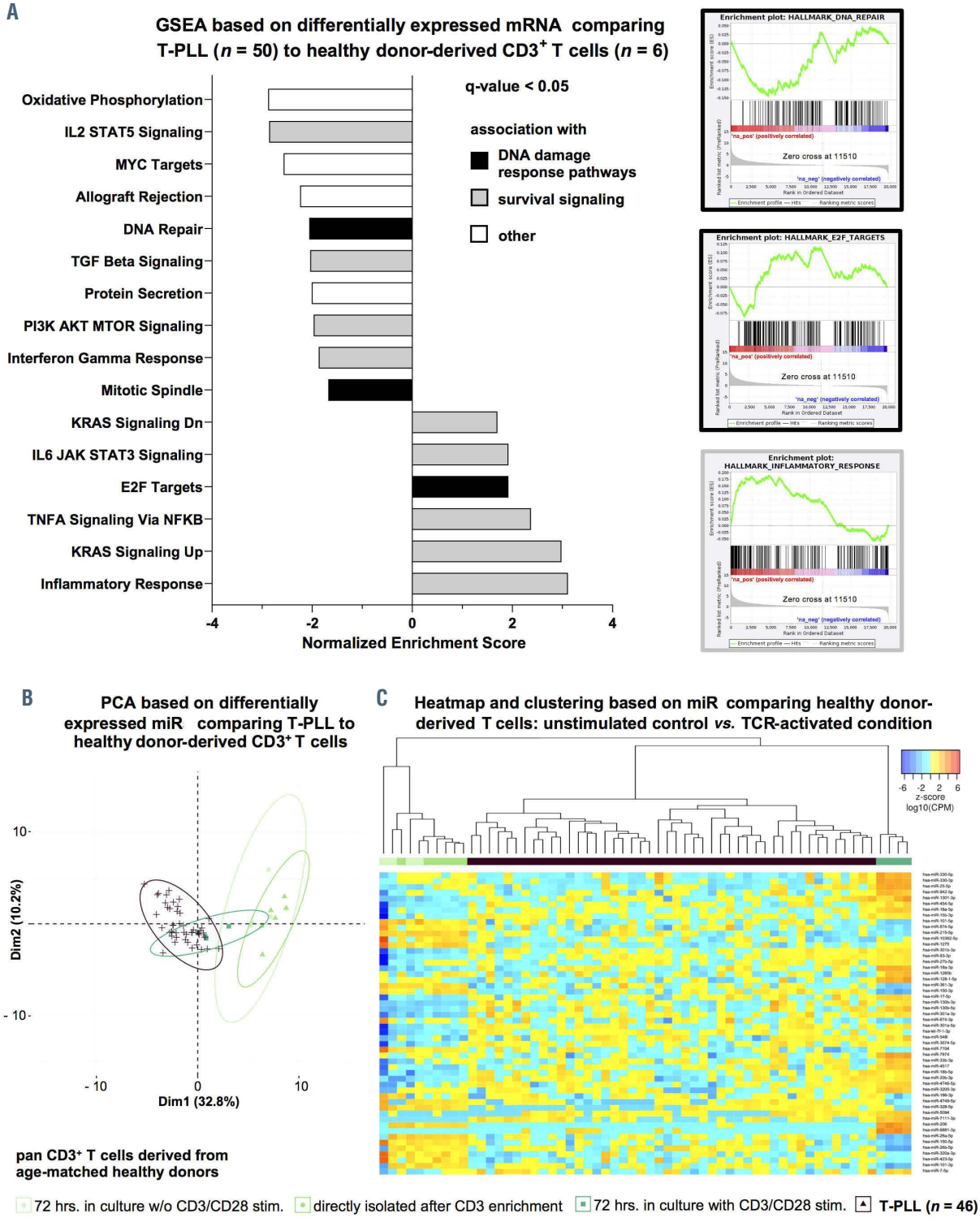

Figure 2. Global alterations of T-cell prolymphocytic leukemia microRNA expression signatures/ transcriptome networks resemble those of T-cell receptor-activated T cells. (A) Gene set enrichment analysis (GSEA) of differentially expressed mRNA in T-cell prolymphocytic leukemia (T-PLL) using *HALLMARK* gene sets (n=948 genes, *Online Supplementary Table S6*; *Online Supplementary Figure S5*; total n=48 gene sets). Gene expression profiles were assessed using global mRNA sequencing of primary T-PLL cells (n=48 cases) and healthy donor-derived CD3+ pan-T cells (n=6 donors). Color code represents assignment to dysregulation to either altered DNA damage response pathways (black) or prosurvival signaling (grey). Exemplary GSEA plots are presented (*DNA REPAIR*: normalized enrichment score [NES]=-2.18, q=0.008, *E2F TARGETS*: NES=2.05, q=0.01, *INFLAMMATORY RESPONSE*: NES=3.12, q<0.0001). (B and C) T-PLL miR-omes resembled those of activated healthy donor T cells: age-matched healthy donor-derived peripheral blood mononuclear cells (PBMC) were isolated via density gradient centrifugation. T-cell activation was achieved via antibody-mediated CD3/CD28 crosslinking. After 72 hours (hrs), CD3+ primary T cells were isolated by magnetic-activated cell sorting (MACS) (negative selection; see Method section for details; cell purities are given in *Online Supplementary Figure S6A*, see *Online Supplementary Figure S6B* and *C* for control experiments on stimulation). MiR profiles were generated using small-RNA sequencing. Unstimulated cultured controls clustered together with directly isolated control samples, indicating that there was a negligible cell culture effect on miR expression profiles. Color code: T-PLL in brown, controls in green colors (light green: CD3+ T cells cultured *in vitro* for 72 hrs. without stimulation; green: CD3+ T cells submitted to miR-ome sequencing directly after enrichment; dark-green: CD3+ T-cell cultures at 72 hrs. subsequent to T-cell receptor [TCR] activation). (B) PCA based on differentially expressed miR comparing T-PLL to healthy donor-derived T cells (n=37 miR, *Online Supplementary Table S1*). TCR-activated healthy donor-derived T cells clustered with T-PLL cases. (C) Heatmap and clustering based on differentially expressed miR comparing healthy donor-derived T cells: unstimulated controls *versus* TCR-activated condition (n=56 miR, FDR<0.05). Colors represent z-scores of CPM values calculated for each miR (blue=lower z-score; red=higher z-score).

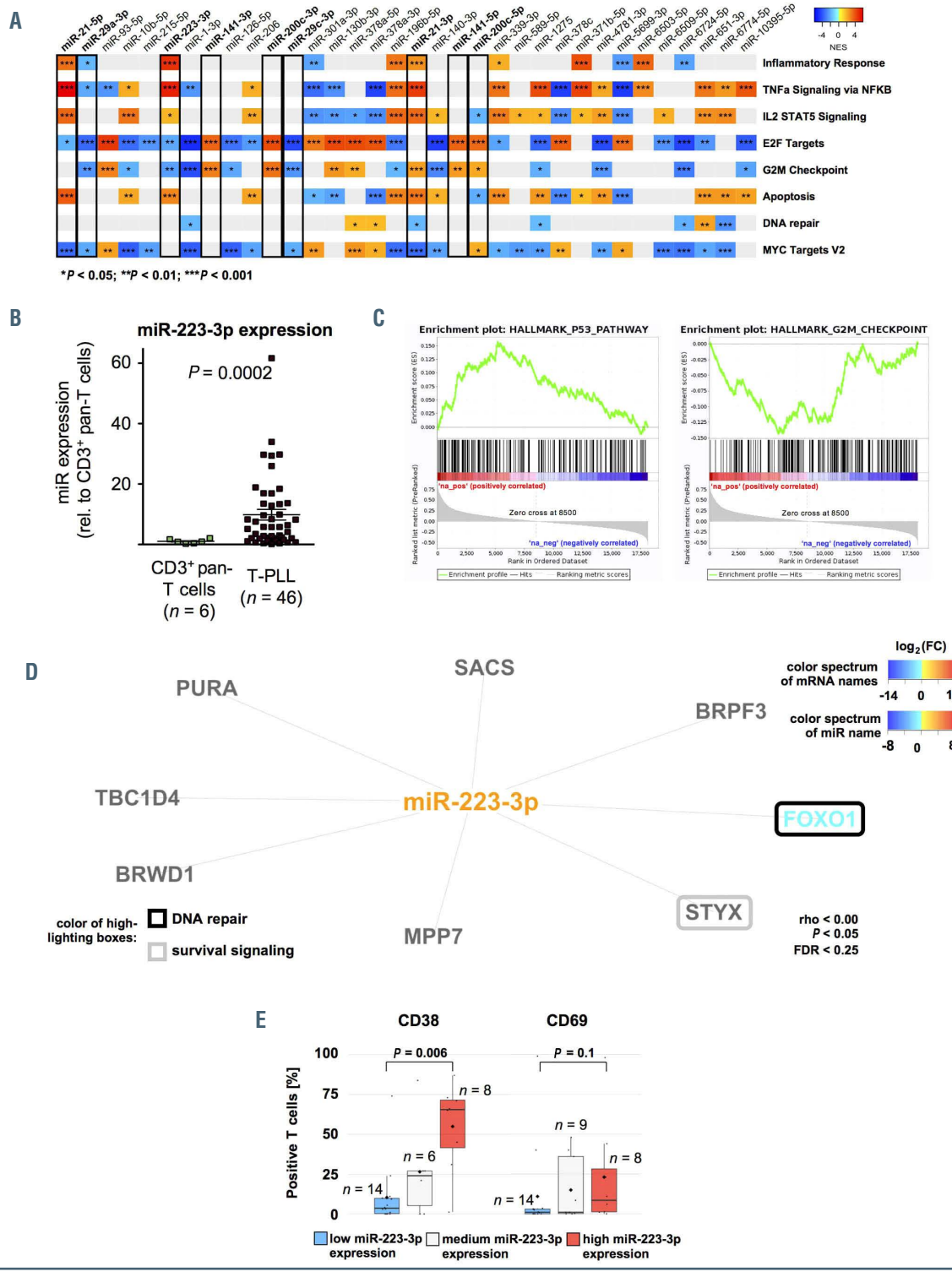

Figure 3. Functional affiliations of predicted microRNA-targets reflect associations with processes of altered DNA damage response and prosurvival signaling. (A) Gene set enrichment analysis (GSEA) heatmap based on microRNA (miR) associated mRNA. GSEA were conducted for all significantly deregulated miR (n=34 miR; *Online Supplementary Table S1*) using ranked correlation indices between mRNA and miR expression in 41 T-PLL and six healthy donor-derived T-cell samples. Exemplary HALLMARK pathways are displayed. Full figure is displayed in *Online Supplementary Figure S8*. Color code summarizes normalized enrichment scores (NES, blue=negative NES; red=positive NES). Statistical significance is summarized via asterisks (*P<0.05; **P<0.01 ; ***P<0.001 ; Kolmogorov-Smirnov-test). (B) Differential expression of miR-223-3p as analyzed by small-RNA sequencing shows significant upregulation in T-PLL (n=46) over normal T-cell controls (n=6); (fc=9.85; P=0.0002). (C) Exemplary GSEA plots of miR-223-3p correlated mRNA: *P53 PATHWAY*: NES=2.59, q<0.0001, *G2M CHECKPOINT*: NES=-2.34, q=0.003). (D) Predicted targets (by seed sequences, see Methods section for details) that correlated negatively with miR-223-3p expression in all analyzed cases and controls represent regulatory networks involved in DNA damage response and prosurvival signaling. Font color represents differential expression of mRNA comparing T-PLL cells (n=48 cases) and healthy donor-derived CD3$^+$ pan-T cells (n=6 donors; for description of global mRNA sequencing results refer to *Online Supplementary Figure S5* and *Online Supplementary Table S5*, blue= lower expression; red= higher expression). Color of highlighted boxes represents assignment of genes to functional groups of DNA damage response pathways (black) and prosurvival signaling (grey). (E) Groups of low and high miR-233-3p expression were assigned by results of small-RNA sequencing *via* comparison of the lower *versus* upper tertile of cases. Primary T-PLL cases were evaluated for CD38 and CD69 surface expression using flow cytometry (see *Online Supplementary Table S8* for the comprehensive dataset). T-PLL with high miR-223-3p expression levels presented with a more activated T-cell phenotype (median CD38 expression: 65.5% *vs.* 3.6%, P=0.006; median CD69 expression: 8.5% *vs.* 1.0%, P=0.1; Mann–Whitney–Wilcoxon [MWW] test).

files of T-PLL cells with those of TCR-activated T cells. By integrating T-PLL's miR profiles with transciptome data via GSEA (based on differentially expressed mRNA and on mRNA ordered by their correlation to the respective miR), we uncovered prominent regulatory networks around DNA damage response and prosurvival pathways in T-PLL.

Increased miR-223-3p expression is linked to activated T-cell phenotypes and associates with signatures of altered DNA damage response and cell cycle deregulation

We next focused on phenotypic and clinical associations of miR (i) differentially expressed in our cohort and (ii) already linked to B- and / or T-cell leukemogenesis. In our sequencing analysis of small-RNA, miR-223-3p was significantly upregulated in T-PLL over $CD3^+$ pan-T cells from age-matched healthy donors (fc=9.85, *P*=0.0002, Figure 3B). GSEA based on mRNA ranked by their correlation to miR-223-3p expression revealed an association of miR-223-3p with signatures of altered DNA damage responses (e.g., *P53 PATHWAY*: NES=2.59, q<0.0001) and deregulated cell-cycle mediators (e.g., *G2M CHECKPOINT*: NES=-2.34, q=0.003, Figure 3C). We further evaluated potential miR-223-3p target mRNA, by combining target prediction databases and miR-ome – transcriptome correlations. Defining criteria of mRNA as putative miR targets in T-PLL are outlined in the Methods section. In total, we identified eight putative targets of miR-223-3p in T-PLL (Figure 3D). Notably, FOXO1 (rho=-0.41, *P*=0.005) was identified as one of them and was significantly downregulated in T-PLL (n=32 of 48 cases with fc<0.5 compared to normal T-cell controls). Tumor suppressive FOXO1 is a prominent regulator of redox balances and DNA insult-mediated cell death.[32]

When T-PLL cases were divided into three subgroups based on miR-223-3p expression (high, medium, low), we found that miR-223-3p expression correlated significantly with surface expression levels of the TCR activation markers CD38 (mean surface expression: 65.5% *vs*. 3.6%, *P*=0.006, MWW) and CD69 (mean 8.5% *vs.* 1.0%, *P*=0.1, MWW, Figure 3E, *Online Supplementary Table S8* with summary of clinical data).

Increased levels of miR-200c and miR-141 species are associated with deregulated cell cycle molecules, activated phenotypes, and more aggressive presentations

Another miR family, miR-200c/-141, was significantly upregulated in a subset of 23 T-PLL cases (Figures 4A and 1C). Upregulation for miR-141-3p was 43.2-fold (*P*<0.0001), for miR-141-5p 29.0-fold (*P*=0.0001), for miR-200c-3p 38.2-fold (*P*<0.0001), and for miR-200c-5p 56.6-fold (*P*=0.003) over all cases. MiR-141-3p showed the highest absolute CPM values among all deregulated miR in the entire cohort of T-PLL (mean $CPM^{miR\text{-}141\text{-}3p}$ =26,561; mean CPM of all significantly deregulated miR in T-PLL =1,440, fc=18.4; *Online Supplementary Figure S2*). GSEA based on mRNA ranked by their correlation to miR-200c/-141 family members revealed significant enrichments of the *HALLMARK E2F TARGET* (NES=3.64, q<0.0001) and *HALLMARK G2M CHECKPOINT* gene sets (NES=3.05, q<0.0001, both based on miR-141-3p correlated mRNA, Figure 4B). Additionally, we identified 93 mRNA as potential targets of miR-200c/-141 (Figure 4C) in T-PLL. While nine mRNA showed an overlap between miR-141-3p and miR-200c-3p target mRNA, we found only a small set of putative targets which were shared between either miR-141-3p or miR-200c-3p and miR-141-5p. Exemplarily, KAT2B, a known tumor suppressor affecting DNA damage and cell cycle regulation,[33] emerged as a potential target of miR-200c-3p (rho=-0.41, *P*=0.005, Spearman). Surface expression of the T-cell activation marker CD40L was elevated in cases with high miR-141-3p (mean 16.5% *vs*. 0.05%, *P*=0.03, MWW), high miR-200c-3p (mean 16.5% *vs*. 0.05%, *P*=0.03, MWW), and high miR-200c-5p expression (mean 20.0% *vs*. 0.0%, *P*=0.009, MWW, Figure 4D). Serum LDH levels at the time of sample correlated with increased miR-141-3p (mean 898 U/L *vs*. 509 U/l, *P*=0.03, MWW, Figure 4E) and elevated miR-200c-3p expression (mean 917 U/L *vs*. 509 U/L, *P*=0.02, MWW, *Online Supplementary Table S9* with summary of clinical data).

Reduced miR-21 expression is linked to features of advanced or aggressive disease

The small-RNA sequencing analysis also revealed a 3.7-fold reduction of miR-21-3p expression (fc=0.27, *P*<0.0001) and a 3.2-fold reduction of miR-21-5p expression (fc=0.31, *P*<0.0001) in T-PLL (*Online Supplementary Figure S9A*). Interestingly, absolute expression (CPM) values of miR-21-5p were the second most altered among all deregulated miR in T-PLL (mean CPM of all significantly deregulated miR in T-PLL of 1440 *vs*. mean $CPM^{miR\text{-}21\text{-}5p}$ of 15,526, fc=10.8, *Online Supplementary Figure S2*), suggesting a highly T-PLL-specific loss of expression. GSEA of miR-21-associated mRNA implicated relevance of this miR in apoptosis and cell cycle regulation, as gene sets like *HALLMARK P53 PATHWAY* and *G2M CHECKPOINT* were significantly deregulated (NES of *APOPTOSIS PATHWAY* considering miR-21-5p-associated mRNA=3.89, q<0.0001; NES of G2M CHECKPOINT considering miR-21-3p-associated mRNA=2.39, q=0.001, *Online Supplementary Figure S9B*). Furthermore, we assessed potential target mRNA of miR-21-3p and miR-21-5p as described above (n=42, e.g., MAP3K1 as a putative target of both miR-21-3p and miR-21-5p, *Online Supplementary Figure S9C*). In contrast to the current concept of miR-21 being a potent suppressor of cell cycle arrest and apoptosis induction, we did not find negative correlations with mRNA mediating these published effects (e.g., PDCD4: rho=0.04, *P*=0.79; BTG2: rho=0.28, *P*=0.05; correlations based on miR-21-5p expression, Spearman).[34] Dichotomized by mean miR-21-5p expression, T-PLL with low miR-21-5p levels revealed higher white blood cell (WBC) counts (mean 154 G/L *vs*. 90.0 G/l, *P*=0.02, MWW) and lower platelet counts (mean 110 G/L *vs*. 153 G/L, P=0.03, MWW, *Online Supplementary Figure S9D*) at the time of sampling, indicating a more active growth behavior of T-PLL with low miR-21 expression. Fittingly, serum levels of LDH (mean 933 U/L *vs.* 522 U/L, *P*=0.02, MWW, *Online Supplementary Figure S9E*) were elevated in patients with low cellular miR-21-5p expression (*Online Supplementary Table S10* with summary of clinical data).

Reduced expression of miR-29 clusters is associated with alterations of survival signaling and cell cycle regulators reflected in features of a more active disease

As analyzed by small-RNA sequencing, the miR-29 family members miR-29a-3p (fc=0.29, *P*<0.0001), miR-29b-1-5p (fc=0.47, *P*=0.001), and miR-29c-3p (fc=0.29, *P*<0.0001) showed a homogenous downregulation in T-PLL over

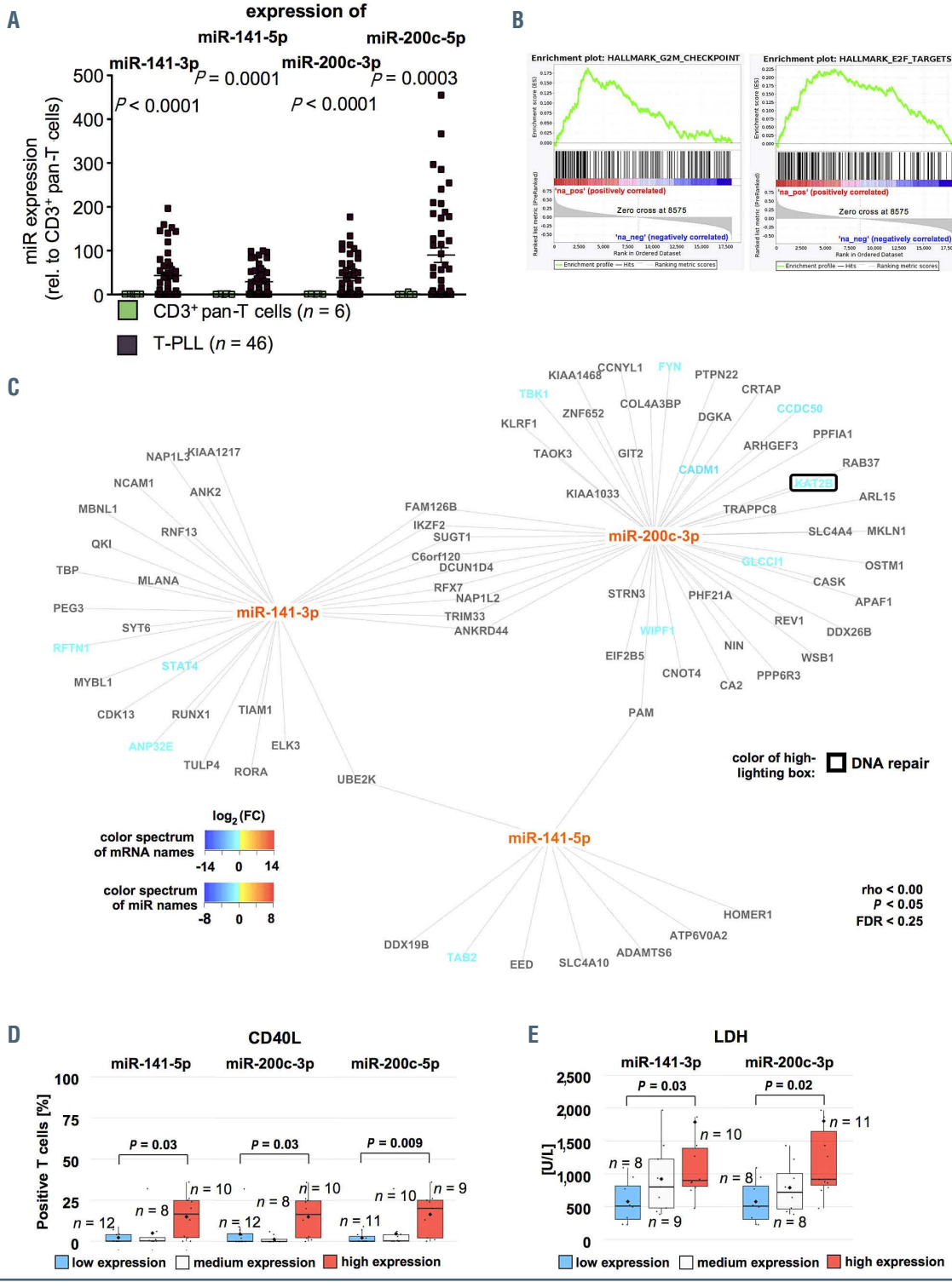

Figure 4. Increased expression of miR-200c and miR-141 clusters is associated with deregulation of cell cycle regulators reflected in more activated phenotypes and more aggressive disease course. (A) Differential expression of miR-141 and miR-200 family members as analyzed by small-RNA sequencing showed significant upregulation of miR-141-3p (fold change [fc]=43.2; *P*<0.0001), miR-141-5p (fc=29.0; *P*=0.0001), miR-200c-3p (fc=38.2; *P*<0.0001) and miR-200c-5p (fc=56.6; P=0.003, n=46 T-cell prolymphocytic leukemia [T-PLL], n=6 controls). (B) Exemplary gene set enrichment analysis (GSEA) plots of miR-200/-miR-141 correlated mRNA: *E2F TARGETS*: NES=3.64, q<0.0001, *G2M CHECKPOINT*: NES=3.05, q<0.0001 (both based on miR-141-3p correlated mRNA). (C) Predicted targets (by seed sequences, see Methods section for details) correlating negatively with miR-141/-miR-200 expression in all analyzed cases and controls showed regulatory networks involved in DNA damage response and prosurvival signaling. Font color represents differential expression of mRNA comparing T-PLL cells (n=48 cases) and healthy donor-derived CD3+ pan-T cells (n=6 donors; for description of global mRNA sequencing results refer to *Online Supplementary Figure S5* and *Online Supplementary Table S5*, blue= lower expression; red= higher expression). Color of highlighting boxes represents assignment of genes to functional groups of DNA damage response pathways (black) and prosurvival signaling (grey). (D) Groups of low and high miR-141/-200 expression were assigned by results of small-RNA sequencing: after division into three tertiles, cases of the lower were compared to those of the upper tertile. Cases were evaluated for CD40L surface expression using flow cytometry. T-PLL with higher miR-141-5p, miR-200c-3p, and miR-200c-5p expression presented with a more activated T-cell phenotype (median CD40L expression: 16.5% *vs.* 0.05%, *P*=0.03; 16.5% *vs.* 0.05%, *P*=0.03, 20.0% *vs.* 0.0%, *P*=0.009; MWW). (E) Higher serum LDH levels (see *Online Supplementary Table S9* for a summary of clinical data) were associated with high expression of miR-141-3p and miR-200c-3p (median 898 U/L *vs.* 509 U/L; *P*=0.03; median 917 G/L *vs.* 509 G/L; *P*=0.02; MWW). Groups were divided into three tertiles and the lower was compared against the upper tertile.

healthy donor T cells (*Online Supplementary Figure S10A*). GSEA of associated mRNA showed an enrichment of genes of the *HALLMARK E2F TARGET* (NES=-3.52, q<0.0001) and of the *TNFA SIGNALING VIA NFKB* gene sets (NES=-2.08, q=0.01, both miR-29a-3p-correlated mRNA) in low miR-29 expressing T-PLL *(Online Supplementary Figure S10B*). Furthermore, we identified 79 putative-target mRNA of the miR-29a-3p / miR-29b-1-5p / miR-29c-3p cluster in T-PLL by the above described strategy (*Online Supplementary Figure S10C*). Indicating an association of reduced miR-29 species with aberrant survival signaling, surface TCR activation markers were elevated in T-PLL with low miR-29a-3p (*Online Supplementary Figure S10D*), namely CD38 (mean expression 43.1% *vs*. 12.9%, *P*=0.02, MWW) and CD69 (mean 27.9% *vs*. 0.89%, *P*=0.02, MWW). A more active disease state as indicated by lower platelet counts (mean 110 G/L *vs*. 186 G/L, *P*=0.15, MWW) and higher LDH serum levels (mean 1,850 U/L *vs.* 708 U/l, *P*=0.06, MWW) at sampling was linked to low miR-29b-1-5p expression (*Online Supplementary Figure S10E* and *F*). Lower miR-29c expression tended to be associated with a higher incidence of effusions (six of 12 over one of ten with high miR-29c-3p-expression; *P*=0.07, Fisher's exact test, *Online Supplementary Figure S11A*). In addition, genomic *ATM* deletions were more frequent in cases with low miR-29b-1-5p expression (nine of 11 *vs.* one of 11 with high miR-29b-1-5p; *P*=0.002, Fisher's exact test, *Online Supplementary Figure S11B, Online Supplementary Table S11* with summary of clinical data).

A combinatorial miR-based overall survival score for T-cell prolymphocytic leukemia

Based on the observed correlation of miR expression with clinical parameters, we aimed to establish a prognostic score that stratifies T-PLL patients according to miR expression levels. In order to identify best candidates in an unbiased fashion, we first associated miR expression levels with OS for all miR detected in at least 80% of T-PLL samples (n>36 cases) and compared T-PLL patients with highest expression levels (upper tertile) to those with lowest expression of the respective miR (lower tertile; *Online Supplementary Table S12* with summary of clinical data). In this analysis, miR-98-3p (median OS in high *vs*. low expression: 16.3 months *vs*. 29.4 months, *P*=0.0008, log-rank, Figure 5A), miR-200a-3p (52.7 months *vs*. 19.1 months, *P*=0.001, log-rank, Figure 5B), miR-223-3p (14.9 months *vs*. 26.0 months, *P*=0.001, log-rank, Figure 5C), and miR-424-5p (14.4 months *vs*. 26.0 months, *P*=0.0007, log-rank, Figure 5D) were most significantly correlated with OS. We subjected a training model composed of these four miR (miR-98-3p, miR-200a-3p, miR-223-3p, miR-424-5p) and of selected factors that had shown to be of prognostic relevance in T-PLL (e.g., WBC counts, TCL1A mRNA level)[1,11,30] to parameter shaving by recursive partitioning. This algorithm identified optimum individual thresholds stratifying OS in the randomly created 22-case training set. Using these cutoffs, three miR (200a-3p, miR-223-3p, miR-424-5p) and TCL1A expression remained as most significant discriminators for OS. Multiple combinatorial scores of these four parameters were built and for these scores optimum thresholds for discrimination of OS were calculated (recursive partitioning, see Methods). Best separation was obtained using a miR-exclusive 3-tier score: miR-200a-3p fc<2.21, miR-223-3p fc≥9.8, miR-424-5p fc≥0.91; relative to healthy donor T cells) with a cutoff of ≥2 sum points (Table 2). Finally, we verified the miROS-T-PLL score in the 22-case validation set (*P*=0.0004, log-rank) and in the total cohort of 44 T-PLL (median OS high *vs*. low miROS-T-PLL: 14.4 months *vs*. 29.4 months, *P*<0.0001, log-rank, Figure 5E).

In order to identify variables underlying (as potential confounders) the miR-based prognostic separation, we associated the expression of miR, which we used for the score, as well as the miROS-T-PLL score itself, with genomic, mRNA expression, immunophenotypic, and clinical data (*Online Supplementary Tables S13* and *S14*). We did not detect significant differences in the distribution of these parameters between the groups determined by expression of the three miR or by the miROS-T-PLL score, further validating the newly established score.

Discussion

Here, we report a pilot analysis of cellular miR expression in a cohort of 46 T-PLL patients. We identified 34 miR to be significantly deregulated in comparison to PB-derived T cells from age-matched healthy donors. These miR included those which had already been reported as altered in T-cell acute lymphoblastic leukemia (T-ALL, e.g., miR-223-3p)[35] and in CTCL (e.g., miR-29 and miR-200).[17,23] They also contained miR that had not been described in the neoplastic context (e.g., miR-10395-5p). The global profiles of deregulated miR in T-PLL showed a rather uniform pattern across the analyzed cases. Together with the integrated information from transcriptome sequencing, this set of data allows for the first time insights into miR-based regulatory networks in T-PLL.

It is important to mention, that four of the 34 differentially expressed miR presented with low CPM values (<1), either being unspecific background in the sequencing technology or representing biological relevant miR expressed at low levels. In addition, for two of the small-RNA identified to be differentially expressed in T-PLL (miR-6724-5p, miR-5699-3p), miR-base[36] assigned questionable confidence in their annotation, although their expression was previously reported in other entities (e.g., bladder cancer).[37]

In line with T-PLL's phenotype of augmented TCR activation,[1,5,11] our comparative profiling revealed a resemblance of T-PLL's miR-ome to the one of TCR-activated healthy donor-derived T cells. A specific remodeling of the miR repertoire upon TCR activation had been shown,[38] however, analysis of full spectrum miR expression by small RNA sequencing upon TCR activation in healthy donor-derived pan-T cells had not been reported before. We identified here previously unknown miR (e.g., upregulation of miR-18a-5p) to be altered upon TCR activation in addition to those that had been described (miR-17-5p or miR-150-5p).[31,39] We conclude that constitutive TCR activation shapes the characteristic miR-ome of T-PLL cells.

As hallmarks of T-PLL's miR-ome, we identified miR-223-3p, miR-21, the miR-29 family, and the miR-200c/-141 cluster as significantly deregulated. These miR have previously emerged as either onco miR or tumor-suppressive miR in other T- or B-cell malignancies.[23,40–43] We further identified putative target signatures, potentially mediating the postulated effects of prosurvival signaling and aberrant DNA damage responses (e.g., downregulation of FOXO1 upon miR-223 upregulation). Limiting, the postulated target genes are, although predicted through multiple robust algorithms, based on associations without proven biological

effects, which has to be addressed in future experiments. Deregulation of these hallmark miR in T-PLL was further associated with either a pronounced cellular activation phenotype or more aggressive clinical presentations.

MiR-21 stood out as one of the most abundant miR in T-PLL. In contrast to the current concept of miR-21 being an onco miR,[44] we detected significantly downregulated miR-21 levels in T-PLL samples as compared to healthy donor T cells. Our integrative correlations further revealed an association of low miR-21 expression with more aggressive disease presentations. We identified SKP2 and MAP3K1 as predicted targets of miR-21 in T-PLL, potentially mediating these features. Notably, we did not find significant negative correlations of miR-21 with those mRNA that were previously described to mediate the effect of this miR as a potent suppressor of cell cycle inhibition and apoptosis.[34] This indicates a T-cell specific and context-dependent function of miR-21.

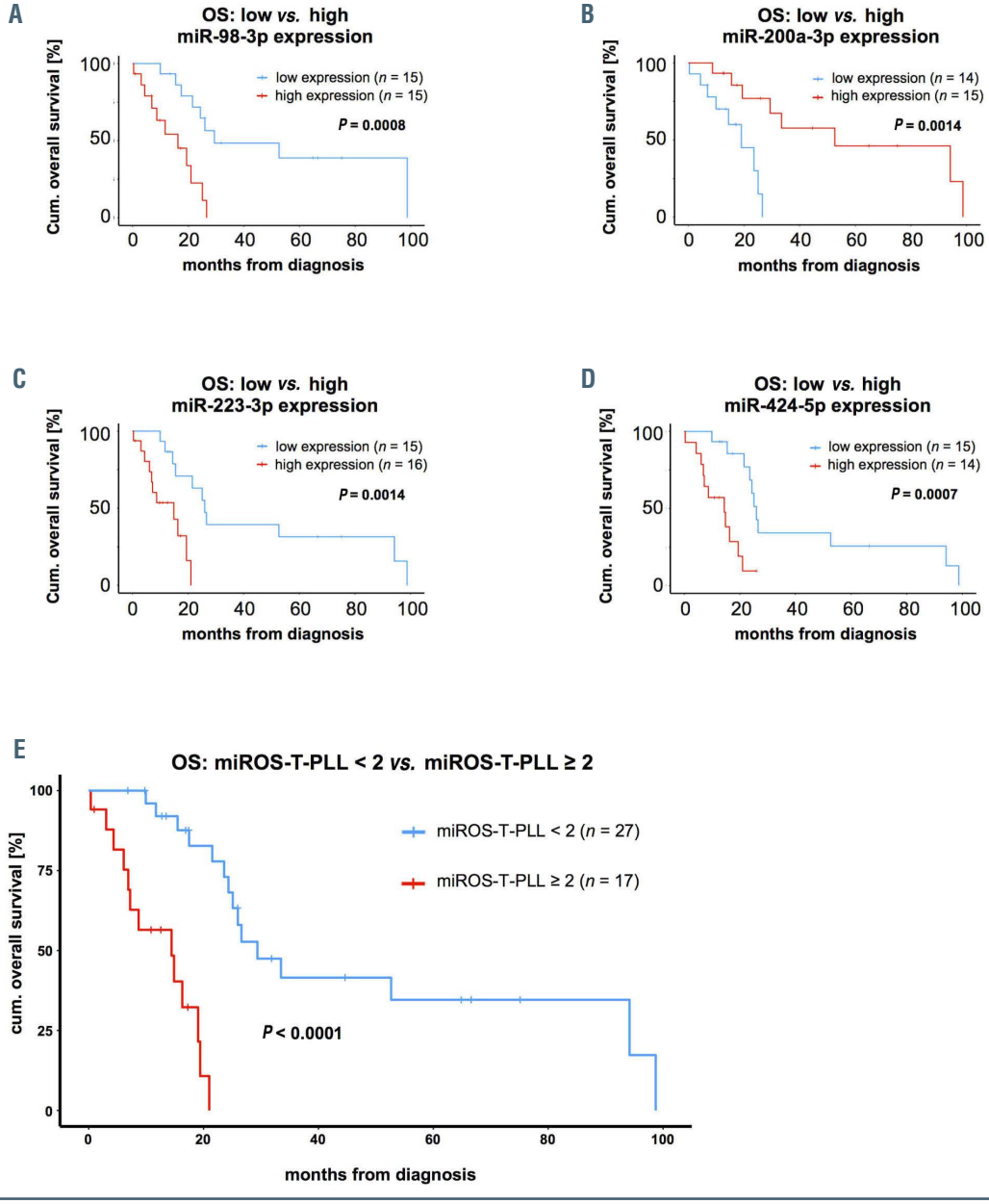

Figure 5. miR-based overall survival score for T-cell prolymphocytic leukemia (miROS-T-PLL) stratifies patients based on miR-200a-3p, miR-223-3p, and miR-424-5p expression. (A to D) Associations of microRNA (miR) expression with overall survival (OS) from diagnosis (see *Online Supplementary Table S12* for the comprehensive dataset). (A) miR-98-3p (median OS high *vs.* low expression: 16.3 months *vs.* 29.4 months, *P*=0.0008, log-rank test); (B) miR-200a-3p (median OS high *vs.* low expression: 52.7 months *vs.* 19.1 months, *P*=0.001, log-rank test); (C) miR-223-3p (median OS high *vs.* low expression: 14.9 months *vs.* 26.0 months, *P*=0.001, log-rank test), and (D) miR-424-5p (median OS high *vs.* low expression: 14.4 months *vs.* 26 months, *P*=0.0007, log-rank test) were most significantly associated with OS, when comparing the tertile of T-PLL patients with the highest expression to the tertile with the lowest expression of the respective miR. (E) Analysis via training (n=22) and validation data sets (n=22): optimum thresholds were calculated by recursive partitioning for all possible combinations of miR-200a-3p, miR-223-3p, and miR-424-5p expression levels, adding one point to the total score if the respective expression cutoff was passed. Best results were obtained using the following thresholds: miR-200a-3b: fold change (fc)<2.21, miR-223-3p: fc ≥9.8, miR-424-5p: fc≥0.91 (fc relative to $CD3^+$ pan-T cells derived from healthy donors) and a cutoff of ≥2 points. A significant OS association was observed in the validation set (*P*=0.0004, log-rank test) as well as (E) in the total cohort of 44 T-PLL patients (median OS high *vs.* low expression: 14.4 months *vs.* 29.4 months, *P*<0.0001, log-rank test).

Our computational analyses of mRNA targeted by deregulated miR in T-PLL suggest a strong impact of altered miR clusters on activation, death resistance, and aberrant DNA damage responses. Abnormal activity of these pathways, triggered by TCL1A overexpression and damaging *ATM* aberrations, has emerged as a hallmark of T-PLL pathobiology.[1,11] We propose that protumorigenic miR networks in their function as posttranscriptional regulators may further enhance the effects of these key genomic lesions, contributing substantially to the pathogenesis of T-PLL. Similar cooperative miR-mRNA networks were postulated for T-ALL and CLL.[35,45] The causes of the miR deregulations we observed here, remain unknown and are, besides TCR activation, likely multifactorial. As T-PLL is characterized by a strong genomic instability and high burdens of reactive oxygen species,[1,46] mutations or copy number alterations of miR-encoding genes provide possible explanations, in addition to epigenetic mechanisms. Notably, incidences of genomic losses of the downregulated miR-140-3p, miR-196b-5p, miR-339-3p, and miR-589-5p were in the order of 4-9% of T-PLL cases in our cohort.

In summary, we identified a T-PLL-specific miR-ome, with 34 differentially deregulated miR, that appears instructed by TCR activation. By integrating altered miR expression with the information derived from transcriptome analyses, we postulate that the miR-ome of T-PLL shapes (dys)regulated networks towards apoptotic resistance, cell cycle abrogation, and defective DNA damage repair (Figure 6). Highlighting the pathobiological impact of the discovered miR deregulations, we developed the first

Table 2. Prognostic score (miROS-T-PLL) including miR-200a-3p, miR-223-3p, and miR-424-5p expression levels.

Parameter	0 Points	1 Point
miR-200a-3p expression[1] (FC, rel. to healthy CD3+ pan-T cells)	≥ 2.21	< 2.21
miR-223-3p expression[1] (FC, rel. to healthy CD3+ pan-T cells)	< 9.80	≥ 9.80
miR-424-5p expression[1] (FC, rel. to healthy CD3+ pan-T cells)	< 0.91	≥ 0.91
Prognostic Groups		
Lower Risk	0-1 points	
Higher Risk	2-3 points	

[1]evaluated by small-RNA sequencing and compared to the mean expression of CD3+ pan-T cells of six healthy donors: FC: fold change; miR: microRNA; T-PLL: T-cell prolymphocytic leukemia; miROS-T-PLL: miR-based overall survival score for T-PLL.

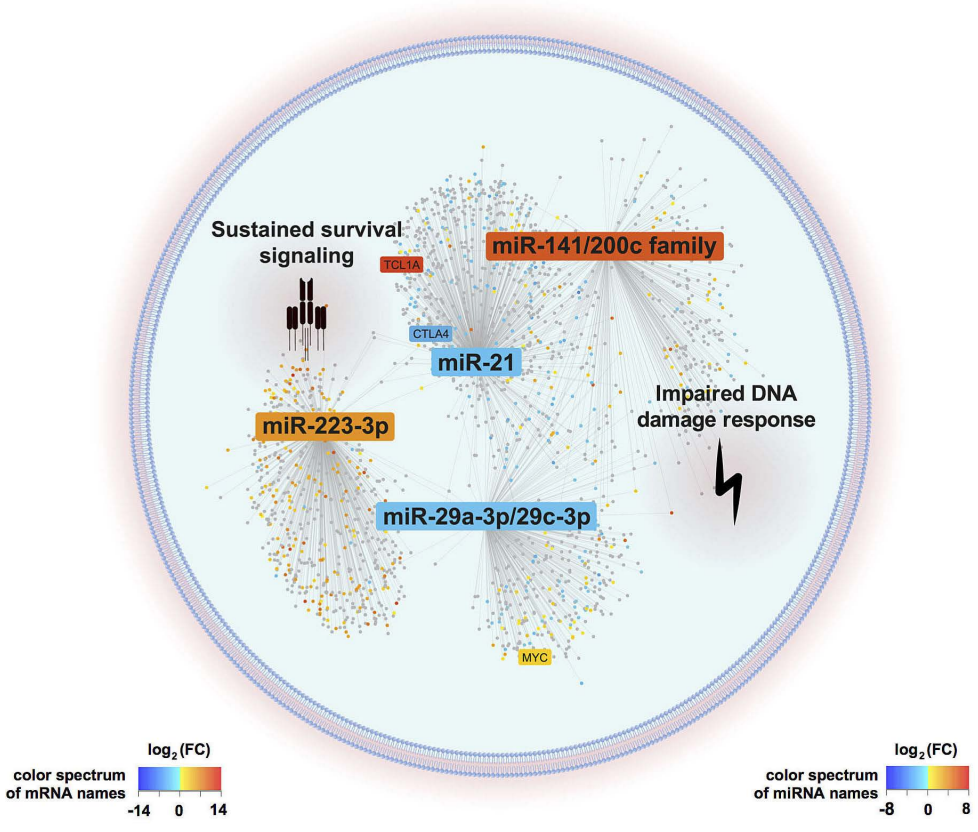

Figure 6. Graphical summary of postulated microRNA/mRNA-based deregulated networks in T-cell prolymphocytic leukemia. T-cell activity shaped microRNA expression signatures (miR-omes)/ transcriptome networks are displayed as identified by our combinatorial approach of small-RNA and transcriptome sequencing analyses in 41 clinically well characterized T-cell prolymphocytic leukemia (T-PLL) cases. MiR differentially expressed in T-PLL and mRNA associated with these miR (P<0.05) are presented. The background color of miR and mRNA (dots) indicates the fold changes of differential expression as compared to age-matched healthy donor-derived CD3$^+$ pan-T cells (blue=downregulation, red=upregulation). MiR-223-3p, the miR-21 family, the miR-29 family, and the miR-200c/141 family emerged as hallmarks of the T-PLL miR-ome, as they were (i) significantly deregulated among T-PLL cases, (ii) presented putative targets involved in oncogenic pathways of T-PLL's pathobiology, (iii) showed associations with prognostic parameters, and (iv) were already described in the leukemogenesis of other B- and T-cell malignancies. Deregulations of these four miR-families were associated with cooperative effects on DNA damage response pathways as well as on pro-proliferative and cell survival signaling (as revealed by gene set enrichment analysis based on correlated mRNA). Genes previously described as hallmarks of T-PLL (e.g., *TCL1A*, *CTLA4*, and *MYC*) were found within the network of the identified miR-associated mRNA.

clinical survival score that predicts T-PLL patients' outcomes, based on expression levels of miR-200a-3p, miR-223-3p, and miR-424-5p.

Clinical management of T-PLL remains challenging and current studies mainly focus on the development of targeted treatments directed against anti-apoptotic factors like BLC2[47] or sustained prosurvival signaling mediated via JAK/STAT pathways.[48,49] Our study suggests that developing a miR-directed targeting strategy could allow tackling a combination of those pathways and might therefore be a promising approach to successfully eradicate T-PLL cells. However, these concepts have to be tested in subsequent preclincal studies. Furthermore, the presented miROS-T-PLL survival score might help in better discriminating rather indolent *versus* aggressive T-PLL disease phases at the time of diagnosis.

Disclosures

No conflicts of interest to disclose.

Contributions

TB, AS, and MH developed the concept of the research; TB, PM, MF, MH and JA acquired the data; TB, MG, LW and MO performed the formal analysis; MG and LW acquired and analyzed the data; TB, LW and AS prepared the original draft and wrote the manuscript; SH and MH wrote, reviewed and edited the mansucript; AS, SH, MH and MHa supervised the work; TB and MO did the project administration. All authors reviewed and approved the final version of the manuscript.

Funding

This research was funded by the DFG Research Unit FOR1961 (Control-T; HE3553/4-2), the Köln Fortune program, and the Fritz Thyssen Foundation (10.15.2.034MN). This work was also funded by the EU Transcan-2 consortium 'ERANET-PLL' and by the ERAPerMed consortium 'JAKSTAT-TARGET'. A.S. was supported by a scholarship of the German José Carreras Leukemia Foundation (DJCLS 03F/2016). We gratefully acknowledge patients with their families for their invaluable contributions.

References

1. Schrader A, Crispatzu G, Oberbeck S, et al. Actionable perturbations of damage responses by TCL1/ATM and epigenetic lesions form the basis of T-PLL. Nat Commun. 2018;9(1):697.
2. Staber PB, Herling M, Bellido M, et al. Consensus criteria for diagnosis, staging, and treatment response assessment of T-cell prolymphocytic leukemia. Blood. 2019;134(14):1132-1143.
3. Braun T, von Jan J, Wahnschaffe L, Herling M. Advances and perspectives in the treatment of T-PLL. Curr Hematol Malig Rep. 2020;15(2):113-124.
4. Matutes E, Brito-Babapulle V, Swansbury J, et al. Clinical and laboratory features of 78 cases of T-prolymphocytic leukemia. Blood. 1991;78(12):3269-3274.
5. Oberbeck S, Schrader A, Warner K, et al. Non-canonical effector functions of the T-memory-like T-PLL cell are shaped by cooperative TCL1A and TCR signaling. Blood. 2020 Dec 10;136(24):2786-2802.
6. Hopfinger G, Busch R, Pflug N, et al. Sequential chemoimmunotherapy of fludarabine, mitoxantrone, and cyclophosphamide induction followed by alemtuzumab consolidation is effective in T-cell prolymphocytic leukemia. Cancer. 2013;119(12):2258-2267.
7. Cross M, Dearden C. B and T cell prolymphocytic leukaemia. Best Pract Res Clin Haematol. 2019;32(3):217-228.
8. Dearden CE, Khot A, Else M, et al. Alemtuzumab therapy in T-cell prolymphocytic leukemia: comparing efficacy in a series treated intravenously and a study piloting the subcutaneous route. Blood. 2011;118(22):5799-802.
9. Dearden C. How I treat prolymphocytic leukemia? Blood. 2012;120(3):538-551.
10. Pflug N, Cramer P, Robrecht S, et al. New lessons learned in T-PLL: results from a prospective phase-II trial with fludarabine–mitoxantrone–cyclophosphamide–alemtuzumab induction followed by alemtuzumab maintenance. Leuk Lymphoma. 2019;60(3):649-657.
11. Herling M, Patel KA, Teitell MA, et al. High TCL1 expression and intact T-cell receptor signaling define a hyperproliferative subset of T-cell prolymphocytic leukemia. Blood. 2008;111(1):328-337.
12. Wahnschaffe L, Braun T, Timonen S, et al. JAK/STAT-activating genomic alterations are a hallmark of T-PLL. Cancers (Basel). 2019;11(12):1833.
13. Bellanger D, Jacquemin V, Chopin M, et al. Recurrent JAK1 and JAK3 somatic mutations in T-cell prolymphocytic leukemia. Leukemia. 2014;28(2):417-419.
14. Kiel MJ, Velusamy T, Rolland D, et al. Integrated genomic sequencing reveals mutational landscape of T-cell prolymphocytic leukemia. Blood. 2014;124(9):1460-1472.
15. Stengel A, Kern W, Zenger M, et al. Genetic characterization of T-PLL reveals two major biologic subgroups and JAK3 mutations as prognostic marker. Genes Chromosomes Cancer. 2016;55(1):82-94.
16. Jonas S, Izaurralde E. Towards a molecular understanding of microRNA-mediated gene silencing. Nat Rev Genet. 2015;16(7):421-433.
17. Kohnken R, Wen J, Mundy-Bosse B, et al. Diminished microRNA-29b level is associated with BRD4-mediated activation of oncogenes in cutaneous T-cell lymphoma. Blood. 2018;131(7):771-781.
18. Zenz T, Mohr J, Eldering E, et al. miR-34a as part of the resistance network in chronic lymphocytic leukemia. Blood. 2009;113(16):3801-3808.
19. Wallaert A, Van Loocke W, Hernandez L, Taghon T, Speleman F, Van Vlierberghe P. Comprehensive miRNA expression profiling in human T-cell acute lymphoblastic leukemia by small RNA-sequencing. Sci Rep. 2017;7(1):7901.
20. Calin GA, Ferracin M, Cimmino A, et al. A microRNA signature associated with prognosis and progression in chronic lymphocytic leukemia. N Engl J Med. 2005;353(17):1793-1801.
21. Bresin A, Callegari E, D'Abundo L, et al. miR-181b as a therapeutic agent for chronic lymphocytic leukemia in the Eμ-TCL1 mouse model. Oncotarget. 2015;6(23):19807-19818.
22. Pekarsky Y, Santanam U, Cimmino A, et al. Tcl1 Expression in chronic lymphocytic leukemia is regulated by miR-29 and miR-181. Cancer Res. 2006;66(24):11590-11593.
23. Shen X, Wang B, Li K, et al. microRNA signatures in diagnosis and prognosis of cutaneous T cell lymphoma. J Invest Dermatol. 2018;138(9):202.
24. Wu SJ, Chen J, Wu B, Wang YJ, Guo KY. MicroRNA-150 enhances radiosensitivity by inhibiting the AKT pathway in NK/T cell lymphoma. J Exp Clin Cancer Res. 2018;37(1):18.
25. Ye Z, Jin H, Qian Q. Argonaute 2: a novel rising star in cancer research. J Cancer. 2015;6(9):877-882.
26. Herling M, Khoury JD, Washington LT, Duvic M, Keating MJ, Jones D. A systematic approach to diagnosis of mature T-cell leukemias reveals heterogeneity among WHO categories. Blood. 2004;104(2):328-335.
27. Subramanian A, Tamayo P, Mootha VK, et al. Gene set enrichment analysis: a knowledge-based approach for interpreting genome-wide expression profiles. Proc Natl Acad Sci. 2005;102(43):15545-15550.
28. Liberzon A, Birger C, Thorvaldsdóttir H, Ghandi M, Mesirov JP, Tamayo P. The Molecular Signatures Database hallmark gene set collection. Cell Syst. 2015;1(6):417-425.
29. Ru Y, Kechris KJ, Tabakoff B, et al. The multiMiR R package and database: integration of microRNA–target interactions along with their disease and drug associations. Nucleic Acids Res. 2014;42(17):e133.
30. Jain P, Aoki E, Keating M, et al. Characteristics, outcomes, prognostic factors and treatment of patients with T-cell prolymphocytic leukemia (T-PLL). Ann Oncol. 2017;28(7):1554-1559.
31. Rodríguez-Galán A, Fernández-Messina L, Sánchez-Madrid F. Control of immunoregulatory molecules by miRNAs in T cell activation. Front Immunol. 2018;9:2148.
32. Dansen TB, Burgering BMT. Unravelling the tumor-suppressive functions of FOXO proteins. Trends Cell Biol. 2008;18(9):421-429.
33. Zhu C, Qin Y-R, Xie D, et al. Characterization of tumor suppressive function of P300/CBP-associated factor at frequently deleted region 3p24 in esophageal squamous cell carcinoma. Oncogene. 2009;28(31):2821-2828.
34. Buscaglia LEB, Li Y. Apoptosis and the target genes of microRNA-21. Chin J Cancer. 2011;30(6):371-380.
35. Mavrakis KJ, Van Der Meulen J, Wolfe AL,

et al. A cooperative microRNA-tumor suppressor gene network in acute T-cell lymphoblastic leukemia (T-ALL). Nat Genet. 2011;43(7):673-678.
36. Kozomara A, Griffiths-Jones S. miRBase: annotating high confidence microRNAs using deep sequencing data. Nucleic Acids Res. 2013;42(D1):D68-D73.
37. Usuba W, Urabe F, Yamamoto Y, et al. Circulating miRNA panels for specific and early detection in bladder cancer. Cancer Sci. 2019;110(1):408-419.
38. Bronevetsky Y, Villarino AV, Eisley CJ, et al. T cell activation induces proteasomal degradation of Argonaute and rapid remodeling of the microRNA repertoire. J Exp Med. 2013;210(2):417-432.
39. Sousa IG, do Almo MM, Simi KCR, et al. MicroRNA expression profiles in human CD3(+) T cells following stimulation with anti-human CD3 antibodies. BMC Res Notes. 2017;10(1):124.
40. Pomari E, Lovisa F, Carraro E, et al. Clinical impact of miR-223 expression in pediatric T-Cell lymphoblastic lymphoma. Oncotarget. 2017;8(64):107886-107898.
41. Kwon JJ, Factora TD, Dey S, Kota J. A systematic review of miR-29 in cancer. Mol Ther Oncolytics. 2018;12:173-194.
42. Humphries B, Yang C. The microRNA-200 family: small molecules with novel roles in cancer development, progression and therapy. Oncotarget. 2015;6(9):6472-6498.
43. Garzon R, Heaphy CEA, Havelange V, et al. MicroRNA 29b functions in acute myeloid leukemia. Blood. 2009;114(26):5331-5341.
44. Feng YH, Tsao CJ. Emerging role of microRNA-21 in cancer (Review). Biomed Rep. 2016;5(4):395-402.
45. Li J, Qin Y, Zhang H. Identification of key miRNA-gene pairs in chronic lymphocytic leukemia through integrated analysis of mRNA and miRNA microarray. Oncol Lett. 2018;15(1):361-367.
46. Prinz C, Vasyutina E, Lohmann G, et al. Organometallic nucleosides induce non-classical leukemic cell death that is mitochondrial-ROS dependent and facilitated by TCL1-oncogene burden. Mol Cancer. 2015;14:114.
47. Boidol B, Kornauth C, van der Kouwe E, et al. First-in-human response of BCL-2 inhibitor venetoclax in T-cell prolymphocytic leukemia. Blood. 2017;130(23):2499-2503.
48. Gomez-Arteaga A, Margolskee E, Wei MT, van Besien K, Inghirami G, Horwitz S. Combined use of tofacitinib (pan-JAK inhibitor) and ruxolitinib (a JAK1/2 inhibitor) for refractory T-cell prolymphocytic leukemia (T-PLL) with a JAK3 mutation. Leuk Lymphoma. 2019;60(7):1626-1631.
49. Bailey NG, Elenitoba-Johnson KSJ. What is new in mature T-cell leukemias? Semin Diagn Pathol. 2020;37(1):72-78.